Titre: Title:	Design and Development of a Lightweight Ankle Exoskeleton for Human Walking Augmentation
Auteur: Author:	Yacine Bougrinat
Date:	2018
Type:	Mémoire ou thèse / Dissertation or Thesis
Référence: Citation:	Bougrinat, Y. (2018). Design and Development of a Lightweight Ankle Exoskeleton for Human Walking Augmentation [Master's thesis, École Polytechnique de Montréal]. PolyPublie. https://publications.polymtl.ca/3076/

Document en libre accès dans PolyPublie
Open Access document in PolyPublie

URL de PolyPublie: PolyPublie URL:	https://publications.polymtl.ca/3076/
Directeurs de recherche: Advisors:	Sofiane Achiche, & Maxime Raison
Programme: Program:	Génie mécanique

UNIVERSITÉ DE MONTRÉAL

DESIGN AND DEVELOPMENT OF A LIGHTWEIGHT ANKLE EXOSKELETON FOR
HUMAN WALKING AUGMENTATION

YACINE BOUGRINAT

DÉPARTEMENT DE GÉNIE MÉCANIQUE

ÉCOLE POLYTECHNIQUE DE MONTRÉAL

MÉMOIRE PRÉSENTÉ EN VUE DE L'OBTENTION

DU DIPLÔME DE MAÎTRISE ÈS SCIENCES APPLIQUÉES

(GÉNIE MÉCANIQUE)

AVRIL 2018

UNIVERSITÉ DE MONTRÉAL

ÉCOLE POLYTECHNIQUE DE MONTRÉAL

Ce mémoire intitulé :

DESIGN AND DEVELOPMENT OF A LIGHTWEIGHT ANKLE EXOSKELETON FOR
HUMAN WALKING AUGMENTATION

présenté par : BOUGRINAT Yacine

en vue de l'obtention du diplôme de : Maîtrise ès sciences appliquées

a été dûment accepté par le jury d'examen constitué de :

M. STIKOV Nikola, Ph. D., président

M. ACHICHE Sofiane, Ph. D., membre et directeur de recherche

M. RAISON Maxime, Doctorat, membre et codirecteur de recherche

M. LAMOUREUX Étienne, B.Ing., membre

ACKNOWLEDGEMENTS

Any achievement, particularly in studies and research, is not only the result of our work but also the result of the support of many outstanding persons. In this regard, I would like to heartily thank my supervisors Professor Sofiane Achiche and Professor Maxime Raison who have been supportive during all my master studies. I would like to thank you for giving me the opportunity to work on such an interesting project which helped me develop different and many new skills. Thank you for inspiring me and pushing me to my limits. Thank you for all the support you have provided during my studies which was very important to successfully finish this amazing project. Apart from research, I am grateful to you for giving me the opportunity to have a remarkable teaching experience that has significantly enriched my experience at Polytechnique Montreal.

I also would like to thank Alvaro Ramirez who helped me in many occasions to find solutions to technical issues that I faced during the project. Alvaro has shared lots of his experience with me which was very helpful in pushing the project forward. Thank you, Alvaro.

Thank you, all the members of our research lab, (Conception de Systèmes Intelligents et Mécatroniques - COSIM) for making our workplace environment, friendly and collaborative.

Finally, I would like to express my profound gratitude towards my parents and family members who have been very supportive and encouraging during all my studies.

RESUMÉ

La plupart des exosquelettes motorisés de la cheville ont une masse distale considérable, ce qui limite leur capacité à réduire l'énergie dépensée par l'utilisateur durant la marche. L'objectif de notre travail est de développer un exosquelette de chevilles avec le minimum de masse distale ajoutée comparé aux exosquelettes motorisés de chevilles existants. Aussi, l'exosquelette doit fournir au moins 50 Nm de support au couple de flexion plantaire. L'exosquelette développé dans le cadre de ce mémoire utilise deux câbles Bowden pour transmettre la force mécanique de l'unité d'actionnement attachée à la taille aux deux tiges en fibre de Carbonne attachées à la botte de l'utilisateur. Quand les deux tiges sont tirées, ils génèrent un couple qui supporte le mouvement de flexion plantaire à la fin de la phase d'appui du cycle de marche. Une pièce conçue sur mesure et imprimé en plastique par prototypage rapide a été attachée au tibia pour ajuster la direction des câbles. Une étude d'optimisation a été effectuée pour minimiser la masse des tiges limitant ainsi la masse distale de l'exosquelette (attaché au tibia et pied) à seulement 348 g. Le résultat principal obtenu à partir des tests de marche est la réduction de l'activité des muscles soléaire et gastrocnémien du sujet par une moyenne de 37% et 44% respectivement lors de la marche avec l'exosquelette comparée à la marche normale. Cette réduction s'est produite quand l'exosquelette a fourni une puissance mécanique de 19 ± 2 W avec un actionnement qui a commencé à 38% du cycle de marche. Ce résultat démontre le potentiel de notre exosquelette à réduire le cout métabolique de marche et souligne l'importance de réduire la masse distale d'un exosquelette de marche.

ABSTRACT

Most of powered ankle exoskeletons add considerable distal mass to the user which limits their capacity to reduce the metabolic energy of walking. The objective of the work presented in this master thesis is to develop an ankle exoskeleton with a minimum added distal mass compared to existing autonomous powered ankle exoskeletons, while providing at least 50 Nm of assistive plantar flexion torque. The exoskeleton developed in this master thesis uses Bowden cables to transmit the mechanical force from the actuation unit attached to the waist to the carbon fiber struts fixed on the boot. As the struts are pulled, they create an assistive ankle plantar flexion torque. A 3D-printed brace was attached to the shin to adjust the direction of the cables. A design optimization study was performed to minimize the mass of the struts, thereby limiting the total added distal mass, attached to the shin and foot, to only 348 g. The main result obtained from walking tests was the reduction of the soleus and gastrocnemius muscles activity by an average of 37% and 44% respectively when walking with the exoskeleton compared to normal walking. This reduction occurred when the exoskeleton delivered a mechanical power of 19 ± 2 W with an actuation onset fixed at 38% of the gait cycle. This result shows the potential of the proposed exoskeleton to reduce the metabolic cost of walking and emphasizes the importance of minimizing the distal mass of ankle exoskeletons.

TABLE OF CONTENTS

LIST OF TABLES

LIST OF FIGURES

LIST OF SYMBOLS AND ABBREVIATIONS

EHPA   Exoskeletons for Human Performance Augmentation

DARPA   Defense Advanced Research Projects Agency

BLEEX   The Berkeley Lower Extremity Exoskeleton

DOF   Degree of freedom

HAL   Hybrid Assistive Leg

PID   Proportional Integrator Derivative

GUI   Graphical User Interface

IMU   Inertial Measurement Unit

FSR   Force Resistive Sensor

EMG   Electromyography

WAXO   Walking Augmentation Ankle Exoskeleton

BLDC   Brushless Direct Current

PC   Personal Computer

ROM   Range Of Motion

PAM   Pneumatic Artificial Muscle

SEA   Series Elastic Actuator

DC   Direct Current

AC   Alternating Current

BLDC   Brushless Direct Current

MR   Magneto-Rheological

pHR   physical Human-Robot

CAD   Computer Aided Design

LIST OF APPENDICES

CHAPTER 1   INTRODUCTION

Walking is one of the most frequent daily activities for humans [1]. It also requires more metabolic energy (i.e. energy from consumed food) compared to other daily activities [2]. Humans naturally consume a minimal energy during walking by selecting optimal parameters such as stride length and walking speed [3]. However, walking for long distances especially with heavy backpacks is required in many occupations. For example, soldiers often walk many kilometers while carrying heavy backpacks that could weigh more than 50% of their lean body mass [4]. Firefighters are also subject to wearing heavy personal protective equipment [5]. To help reduce these effects, many exoskeletons (also called wearable robots) were developed to reduce the metabolic cost of walking and amplify the human capabilities. One of the first lower limb exoskeletons for human locomotion augmentation was patented in 1890 [6]. With significant advancements in related engineering fields, plenty of other devices were developed over the years for human performance amplification and endurance [7-11]. Despite the huge efforts made in developing these devices, only few were able to demonstrate their ability to improve human locomotion efficiency [1, 12, 13].

The interest in augmenting human capabilities and reducing the metabolic cost of walking has increased since the launch of the Exoskeletons for Human Performance Augmentation (EHPA) program by the Defense Advanced Research Projects Agency (DARPA). The Berkeley Lower Extremity Exoskeleton (BLEEX) is one of the famous exoskeletons developed under this program [14]. The exoskeletons that were designed under the EHPA program had the same general mechanical structure that included a bilateral rigid frame with many joints in parallel to the three biological joints, hip, knee and ankle. However, the number of degrees of freedom as well as the actuation source were different [15]. These mechanical structures were in most cases bulky and heavy [15]. This was one of the main reasons why these exoskeletons increased the metabolic expenditure of the user [16].

To reduce the complexity of these wearable robots, researchers have developed single joint exoskeletons [12, 17-20]. In addition to reducing the weight of the exoskeleton, single joint augmentation robots are easier to control, therefore, they can help better understand how the human biological system reacts to these robots. In most cases, these single joint exoskeletons were either designed for hip or ankle joints because these joints, unlike the knee joint, have a positive average mechanical power over the gait cycle [15]. Ankle exoskeletons have particularly captured the

interest of many researchers as they have more potential in reducing the metabolic cost of walking [21]. The ankle joint produces the highest peak of power on the gait cycle compared to the other joints [22]. Using artificial actuators, exoskeletons can decrease the magnitude of the force required by the muscles to produce this power and therefore potentially reduce the metabolic cost of walking as well. The ankle joint power profile is also suitable for passive exoskeletons as it is characterized by a negative phase where the power can be stored in an elastic element followed by a positive power burst where the stored power can be released [23].

There are now some ankle exoskeletons that could reduce the metabolic cost of walking [1, 12, 13]. All of these exoskeletons have a lightweight structure either using only passive elements [1], soft fabric instead of rigid elements [13] or lightweight materials such as fiberglass [12]. However, as the ankle joint is located distal from the hip, the design of powered ankle exoskeletons becomes more challenging because adding a distal mass away from the hip joint has a higher effect on the metabolic expenditure [24]. Therefore, reducing the distal mass of an active ankle exoskeleton while keeping its mechanical power at a high level is an important optimization problem that can result in a reduction of the metabolic cost of walking for the user.

Our objective in this project is to develop an active ankle exoskeleton with the lowest added distal mass compared to existing exoskeletons delivering at least 50 Nm of assistive plantar flexion torque. Chapter 2 presents a background that is essential for understanding the rest of the master's thesis as well as a detailed literature review of the topic.

CHAPTER 2   LITERATURE REVIEW

2.1 Human Walking Biomechanics

As the exoskeletons function in harmony with the human movements, it is important to understand the biomechanics of human walking to properly design a lower limb exoskeleton. In particular, gait phases, joints kinematics and kinetics during walking are the main gait features that need to be considered during the design phase.

2.1.1 Gait Cycle Phases

Human gait is a cyclic movement that is characterized by two main phases: stance phase and swing phase [25]. The stance phase starts by the heel strike which represents the beginning of the gait cycle and ends when the toe leaves the ground at 60% of the gait cycle [26]. During this phase, the foot remains in contact with the ground. The swing phase starts at the end of the stance phase when the toe leaves the ground and ends on the heel strike which represents the end of one gait cycle and the beginning of another one. During the swing phase, the foot moves in the air without any contact with the ground. Figure 2-1 represents a typical gait cycle. It is important to note that the gait cycle is represented only in the sagittal plane as the movements during walking are predominantly in this plane and relatively negligible in the other anatomic planes (coronal and transverse planes). Figure 2-2 shows the anatomical body planes.
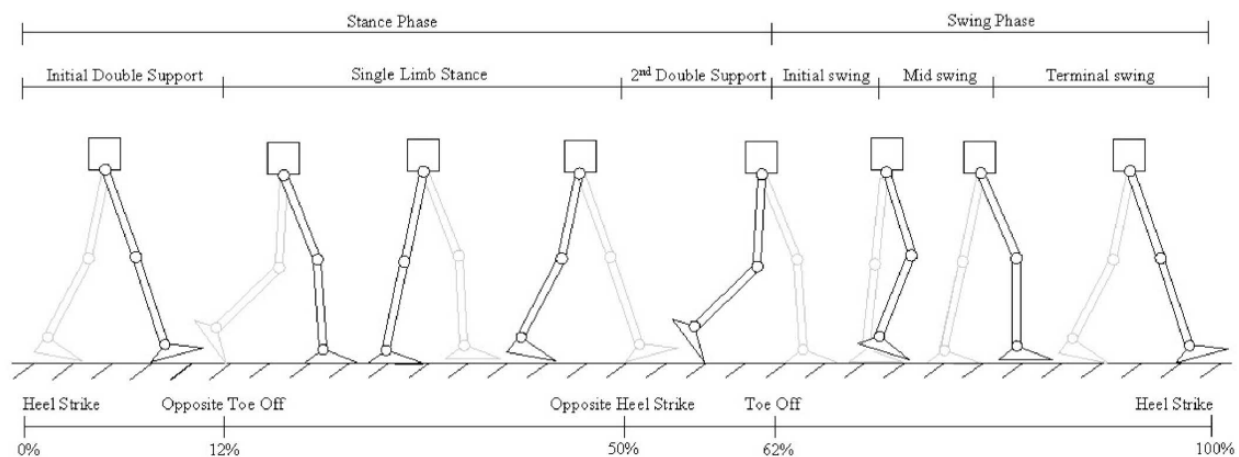
Figure 2-1: Gait cycle phases. Copyright © 2008 IEEE [15]
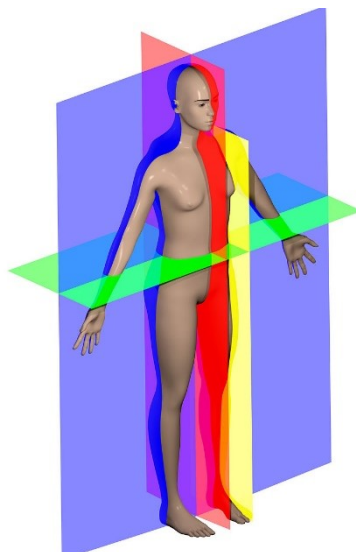
Figure 2-2: Anatomical body planes. Sagittal (red), median (green), and coronal (blue) [27]

2.1.2 Joints Kinematics and Dynamics

The human leg is usually modeled as a system of three rigid bodies with 7 degrees of freedom (DOF) that represent the movements of the three biological joints: hip, knee and ankle [15]. The hip and ankle joints have 3 DOF each, whereas the knee joint has 1 DOF. The movements in the sagittal plane are shown in figure 2-3. The range of motion (ROM), kinematics and kinetics of each DOF are different. Figure 2-4, 2-5 and 2-6 [22] show the angle, torque and power for each joint over the gait cycle for an adult during level walking with natural speed.
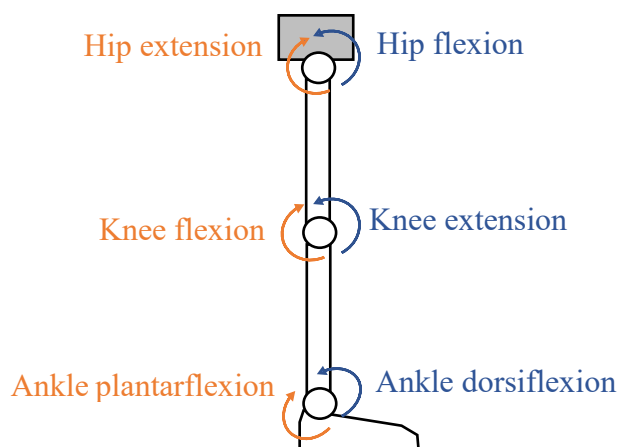
Figure 2-3: Lower limb movements in the sagittal plane

Hip, Knee and ankle joint angles over the gait cycle
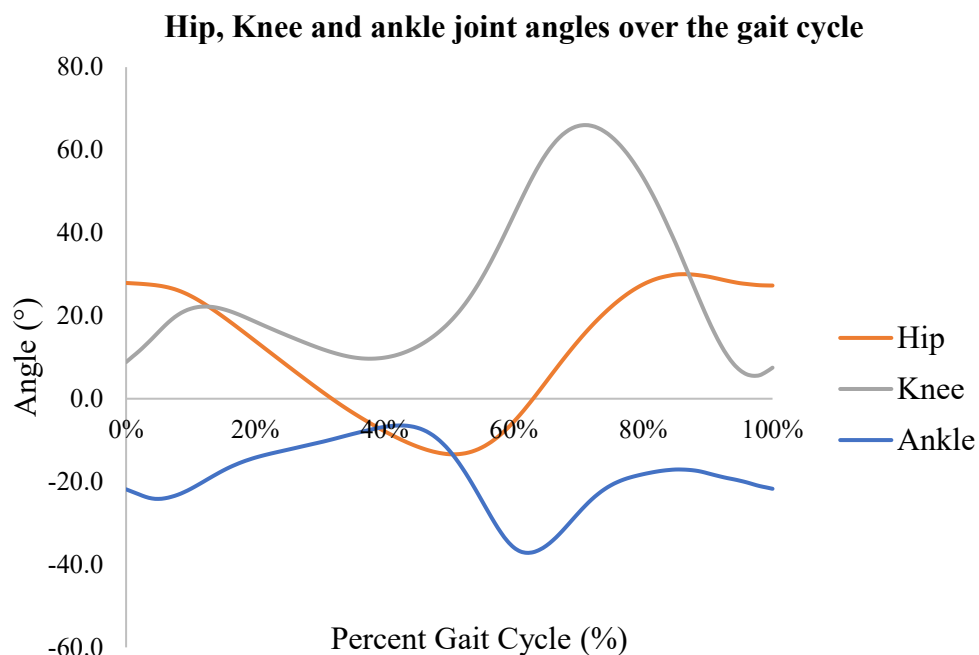
Figure 2-4: Joint angles over the gait cycle

Ankle, Kee and Hip Joint torques over the gait cycle
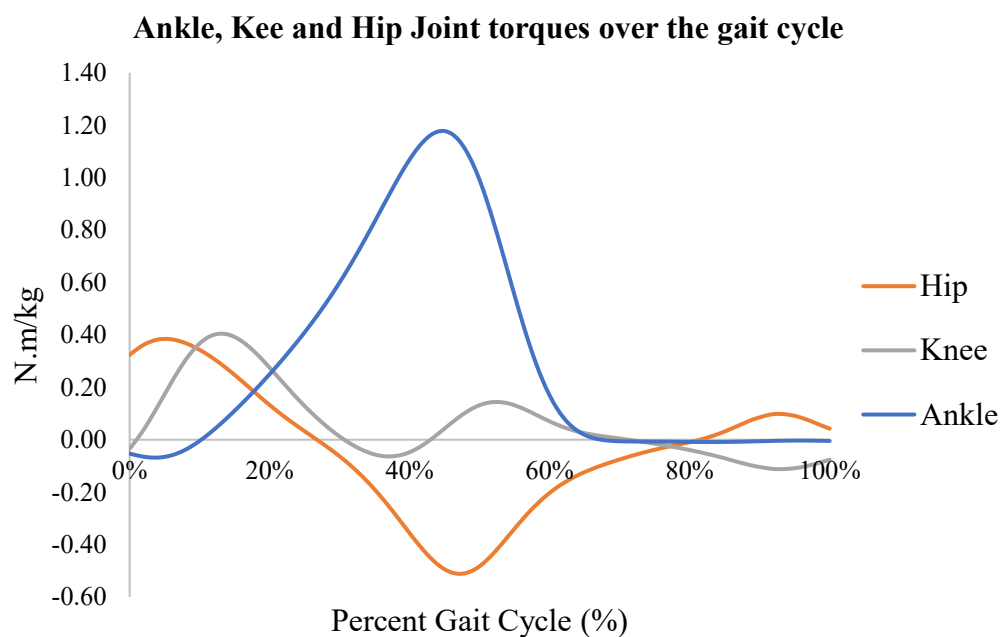
Figure 2-5: Joint torques over the gait cycle

Power on hip, knee and ankle joints over the gait cycle
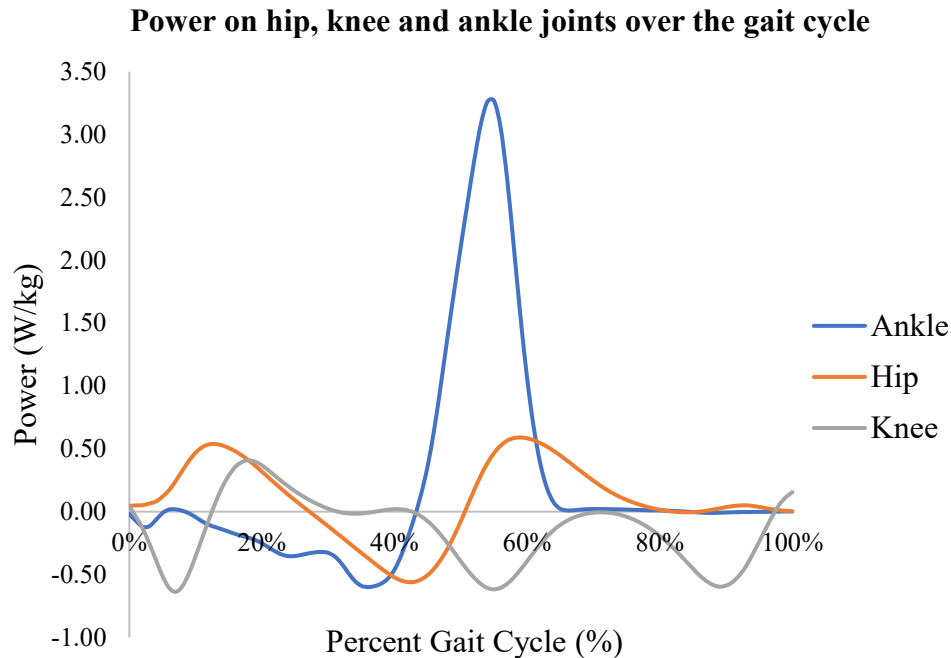
Figure 2-6: Joints power over the gait cycle

The power requirement for each joint is particularly important to understand for the design of active exoskeletons. For instance, as shown in figure 2-6, the hip joint has a positive average power, the knee power remains negative or null during most of the gait cycle and the power on the ankle is characterized by a sudden increase in the middle of the gait cycle to propel the body forward. This power burst is preceded by a negative power. The power distribution for each joint over the gait cycle is translated into design requirements and choices. For example, most exoskeletons add positive power on the hip and ankle and use dissipating elements on the knee [15].

2.1.3 Metabolic Cost of Walking

The metabolic cost of walking or metabolic rate expressed in Watts, defines the amount of energy (coming from food) consumed by the body per unit of time during walking. Although there is no established standard for assessing the performance of exoskeletons for human walking augmentation, the metabolic cost of walking is widely used as the main performance metric [16]. Precisely, the benefit of walking exoskeletons is examined by the amount of reduction in metabolic cost when walking with the device versus walking without it. Analysis of muscle electromyography (EMG) signals is also frequently used to assess the effect of wearing the exoskeleton on specific muscles during gait [1, 28, 29]. In general, reducing the EMG signals can result in a reduction in

the metabolic rate as the muscles are the major consumer of metabolic energy when performing physical activities [1].

2.2 Lower Limb Exoskeletons

2.2.1 Definition of an Exoskeleton

An exoskeleton is a wearable robotic device attached to the body to assist the human in performing physical activities such as walking, stair ascent and load bearing [15]. An exoskeleton is therefore a wearable robot that works in parallel with the human body as opposed to a prosthesis which replaces a limb in the body and works in series with the adjacent limb. The terms orthosis and exoskeleton are sometimes used interchangeably in the literature, however, an orthosis is an exoskeletal device that is designed to assist persons with a gait pathology, whereas, an exoskeleton is usually used to describe devices that augment and amplify the capabilities of typically developed persons [15].

2.2.2 Classification of Exoskeletons

The exoskeletons can be classified into different categories depending on the classification criteria such as the intended application, number of degrees of freedom, actuation type, etc. Broadly, exoskeletons can be separated into three groups: upper-limb, lower-limb and full-body exoskeletons. In this master thesis, we only focus on lower-limb exoskeletons. Among the classification criteria, distinction between exoskeletons by their intended application is crucial for the design, because each application usually has some specific requirements that are not relevant for the other applications. In terms of the application, exoskeletons can be classified into four groups: gait restoration, gait rehabilitation, industrial applications and human performance augmentation.

2.2.2.1 Gait Restoration Exoskeletons

The main objective of gait restoration exoskeletons is to allow persons with disabilities to walk independently and recover their capabilities to perform daily activities [30]. Therefore, the main performance measures for this type of exoskeleton are stability, safety, and ability to provide full support to the user to walk autonomously [16].

Several devices have been developed in this category [15, 16]. Depending on the intended population, these devices can be full-leg exoskeletons [31-33] or targeting selected joints of the lower limb such as active ankle foot orthoses [34-36] and active knee orthoses [37-39]. Currently, there are three commercial full-leg exoskeletons (ReWalk [40], Ekso [41], Indego [42]) approved by the US Food and Drug Administration to be used with patients suffering from a spinal cord injury [43]. The HAL (Hybrid Assistive Leg) is a product of the Japanese company Cyberdyne. It is the only commercial exoskeleton that uses surface electromyography (EMG) sensors to determine the user intent and apply a control signal accordingly [44]. Full-leg exoskeletons designed for gait assistance are typically bilateral and actuate the hip and knee joints in the flexion and extension movements. Kinematic and kinetics sensors are used by most of these exoskeletons to determine the user state [45-47].

Figure 2-7 shows some of the gait restauration exoskeletons.

Figure 2-7: HAL-5 Exoskeleton (left) © Nilsson et al.; licensee BioMed Central Ltd. 2014 [48], H2 Exoskeleton © Bortole et al. 2015 [49], Ekso Bionics Exoskeleton Copyright © IEEE 2012 [50]

2.2.2.2 Gait Rehabilitation Exoskeletons

Gait rehabilitation exoskeletons are used by clinicians for gait training of patients suffering from locomotor dysfunctions or joint injuries. They are used in clinics as an alternative to trainings that rely entirely on the physical efforts of the therapist [16]. Although many therapeutic robotic systems are stationary such as the LOKOMAT [51], LOPES [52] and GaitTrainer [53]. Mobile

exoskeletons are also being used to provide more flexibility in the training. For instance, most of the gait restoration exoskeletons discussed previously are being used for therapeutic applications as well, in addition, some mobile exoskeletons were developed only for this purpose [54] [55].

2.2.2.3   Industrial Exoskeletons

The exoskeletons in industry are primarily used to reduce the load on workers resulting from lifting and/or manipulating heavy objects, operating heavy tools, or standing for long hours [56]. These excessive loads result in poor health conditions for workers. For instance, each year, more than 40% of workers in the European Union report having back pain or neck and shoulder pain [57]. Over the last decade, many research teams have developed wearable exoskeletons for industrial use [56]. Specifically, those wearable devices support workers on shop floors for lifting loads [58, 59] and during still postures [60, 61]. The FORTIS exoskeleton from Martin Lockheed and ZeroG from Ekso Bionics are two commercially available industrial exoskeletons. They use a bilateral rigid frame to transfer the load of the tool being used to ground (see figure 2-8).

Figure 2-8: The FORTIS exoskeleton [62]

2.2.2.4   Human Performance Augmentation Exoskeletons

The exoskeletons for human performance augmentation are built with the main objective of extending human physical capabilities beyond those acquired naturally. For example, allowing the user of the exoskeleton to lift heavy loads or walk long distances while spending less metabolic energy compared to walking without the exoskeleton. In this thesis, we only focus on exoskeletons

that are designed for the specific objective of augmenting human walking capacity. In other words, these walking exoskeletons are designed to reduce the fatigue and the metabolic energy consumed by a human during walking. These exoskeletons could improve the working conditions of individuals whose occupations require carrying and walking with heavy backpacks and equipment [63], such as soldiers and wildland firefighters. Although industrial exoskeletons are also designed for human performance augmentation, in most cases, they are not engineered for distance walking. Human walking is a complex operation in which multiple joints and muscles are involved simultaneously [26]. Therefore, walking exoskeletons need to be carefully designed to operate in accordance with the biological system.

The earliest device reported in the literature designed for human walking enhancement was patented in 1890 by Yagn [6]. His idea consisted in attaching a leaf spring to each leg to assist the user during walking, running and jumping. Although, there were some few other devices during the 20th century [64, 65], it wasn't until the EHPA program was launched by DARPA that the field has witnessed extensive development. The scope of the DARPA initiative was to push the capabilities of soldiers beyond those of a normal human [66]. One of the most prominent devices developed under the DARPA program is the BLEEX [7]. Other featured devices from the same program include the MIT Exoskeleton [67] and Sarcos Exoskeleton [68]. Besides the DARPA program, there were many other lower limb exoskeletons developed in the U.S.A and worldwide [1, 9, 11, 20, 69]. This extensive and rapid progress over the last decade has resulted in a variety of designs that have been continuously optimized to achieve the best performance.

Reducing the metabolic cost of walking is a challenging task given that the body employs an optimal combination of parameters (step length, walking speed…etc.) to spend a minimum amount of energy [3]. Any change that alters one of these parameters, because of the use of an exoskeleton for example, is most likely going to increase the energy expenditure [1]. In fact, none of the exoskeletons developed under the EHPA program has demonstrated a reduction in metabolic cost for the user, usually it was an increase that was recorded [23] in spite of their technological sophistication [15]. Recently, with new innovative designs, locomotion exoskeletons started to bring an energetic benefit for the user [1, 12, 70].

2.2.3   Trends in the Design of Walking Augmentation Exoskeletons

There are many design trends and concepts of exoskeletons, each with its own advantages and limitations. The main design characteristics of an exoskeleton are:

- Actuation form: passive or active

- Number of degrees of freedom

- Physical interface: rigid or soft

In the remainder of this section, we explain each of these characteristics, mention their advantages and disadvantages, then, introduce examples of some walking exoskeletons having different combinations of these characteristics.

2.2.3.1   Passive Exoskeletons

The exoskeletons that use passive actuation systems do not have means of generating active positive power, instead, they only use a combination of passive elements such as springs and dampers to store and release energy at specific moments during the gait cycle [71-73]. Quasi-passive exoskeletons use passive exoskeletons whom parameters could be controlled using an electrical signal such as a variable damper [23]. Clutches are also used in some passive exoskeletons to control the store and release of energy [74, 75].

Passive actuation systems reduce considerably the weight of an exoskeleton and do not limit its autonomy as no battery is needed except for a quasi-passive exoskeleton. However, passive exoskeletons are limited in terms of power they can add to joints.

2.2.3.2   Active Exoskeletons

Active exoskeletons have at least one active joint where positive power is generated by an actuator. Given that an actuation system could be chosen for a desired performance, active exoskeletons can be designed to achieve biological torque levels, therefore, their support for human locomotion could have a greater impact than passive exoskeletons. The main limitation of using motors in autonomous exoskeletons is the added weight and inertia caused by the actuator and its accessories. Also, the exoskeleton in this case needs a battery for its functioning, thus, adding more weight and limiting the autonomy.

A variety of actuators have been used in wearable robots including traditional systems such as hydraulic, pneumatic and electrical actuators and other systems such as Series Elastic Actuators (SEAs) and Pneumatic Artificial Muscles (PAMs). Eventually, those actuation systems differ in terms of power, size, weight and efficiency [76]. In general, for exoskeleton design, the emphasis when selecting an appropriate actuation system is on the power to mass ratio (specific power). A higher specific ratio is desired to achieve high torque and speed with a limited added mass.

2.2.3.2.1 Hydraulic Actuators

Hydraulic actuators can provide very high forces with a higher power to mass ratio compared to pneumatic and electric motors. However, these advantages come at the expense of a bulky hydraulic power supply, usually as an off-board unit which hinders the portability of the robot. For this reason, these actuators are commonly used in heavy duty industrial robots [77] but rarely in autonomous lower limb exoskeletons except for some military devices [7] [8].

2.2.3.2.2 Pneumatic Actuators and Pneumatic Artificial Muscles

Pneumatic actuators provide rapid movements with fast response and high specific power at a relatively cheap price [78]. Nevertheless, it is difficult to achieve precise position control with a pneumatic cylinder due to the different nonlinearities such as air compressibility [79]. In most cases, pneumatic cylinders include a piston which slides over the cylinder under the air pressure. Instead, PAMs (also known as McKibben muscles) are made of a rubber bladder surrounded by a braided fiber in a helical manner (figure 2-9). When the air inside the bladder is pressurized, the muscle assembly increases its diameter and contracts [80]. McKibben actuators are lightweight, intrinsically compliant and can produce high force magnitudes. For this reason, they were used in several exoskeletons and orthotic devices [29, 81-84].

Despite the advantages of pneumatic actuators, their use for autonomous walking exoskeleton is very limited due to the need of an external air compressor. In most cases, they were used for rehabilitation devices meant to be used inside a laboratory.
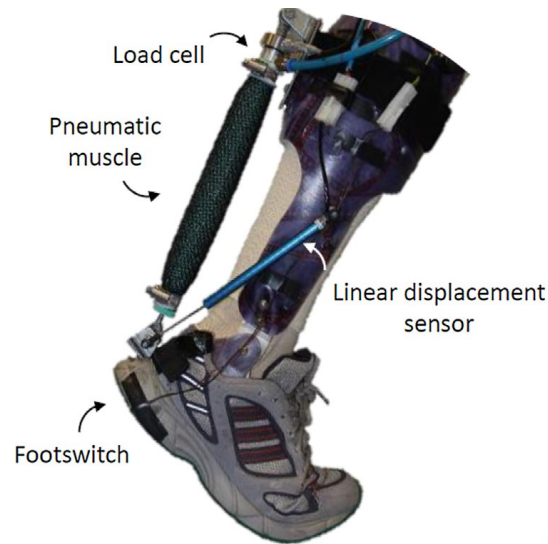
Figure 2-9: Pneumatic artificial muscle used in an ankle exoskeleton [85]

2.2.3.2.3 Electric Motors

Electric motors are the most common type of actuation systems used in robotics applications [86]. Primarily, there are four types of electric motors: brushed Direct Current (DC) motors, Alternating Current (AC) motors, stepper motors and Brushless DC (BLDC) motors [87].

DC motors can be simply run by applying voltage from a DC power supply, while their speed can be controlled by varying the voltage [87]. However, their speed range is limited, therefore, they are adequate for applications where high speed is not required or a major concern such as in gait assistance and rehabilitation exoskeletons [88-90]. Another limitation of DC motors is the need for regular maintenance due to the use of mechanical friction brushes which limits their service life [91].

Stepper motors can move in small steps using an open loop control system [92]. Therefore, they are adequate for positioning applications. The major disadvantages of stepper motors are their low efficiency, relatively big size as well as the difficulty to run at high speeds [93]. In addition, the lack of a closed feedback control in stepper motors does not always guarantee the best performance [94].

AC motors are powered by an alternating current which is used to achieve the commutation of the fields in the rotor and the stator [95]. AC motors are not suitable for autonomous systems because batteries can only produce a direct current.

BLDC motors have the same structure as AC motors, but they create the alternating current from a DC source using special electronics and sensors as well as a control loop [96]. BLDC motors have many advantages over brushed DC motors. They can operate at high speeds while maintaining a relatively high torque, which is an important feature for augmentation exoskeletons. Furthermore, they have a longer service life as well as a higher power density [96]. However, BLDC motors require special drivers for their operation and control which add more complexity and cost. BLDC motors were used in several augmentation exoskeletons [11, 97, 98].

2.2.3.2.4 Series Elastic Actuators

Traditionally, actuators used in industrial robots have a stiff interface which allows a precise position control [99]. Conversely, in human interaction and biomimetic robotics context, a stiff interface with the environment is not desirable and in some cases can be dangerous to the user [100]. A Series Elastic Actuator (SEA), as its name indicates, has an elastic element attached in series with the actuator end [99] (see figures 2-11 and 2-12). This configuration brings many advantages that a stiff interface actuator lacks. In addition to ensuring a compliant safe interface with the environment (a human arm or leg for example), a major asset of SEAs is that precise force control becomes easier [101]. In fact, in a SEA, force control is achieved indirectly through precise positioning of the spring end. Using Hook's Law and knowing the rigidity constant of the spring, the force is deduced by measuring the deformation of the latter [101]. Also, as most actuators have a gearbox, in the presence of shocks, the series elastic element acts as a mechanical filter by absorbing any impacts that could damage the gears [102]. SEAs are more efficient as well since the spring can store and release energy, therefore, reducing the power requirement of the actuator [103].
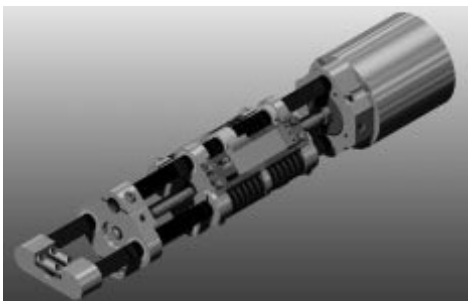
Figure 2-11: SEA used in a walking robot. Copyright © IEEE 1999 [100]
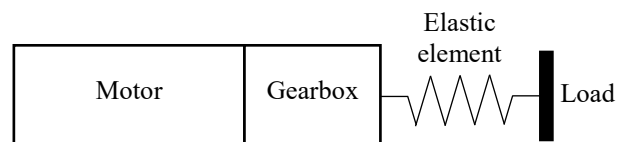
Figure 2-10: Schematic of a SEA

2.2.3.2.5 *Magnetorheological Actuator*

Magneto-Rheological (MR) are a certain category of smart fluids that change their viscosity in the presence of a magnetic field [104]. The viscoelasticity of these fluids can be increased by increasing the magnetic field applied to them.

One application of this interesting property is the MR actuator. An MR actuator is made of an electric motor coupled with an MR clutch which can behave as a brake as well by controlling the magnetic field intensity [105]. When positive power needs to be transmitted, the MR actuator acts as a motor coupled with a clutch, when damping is needed, the MR actuator acts as a brake while the motor is turned off [104]. This feature of switching between a clutch and a brake using one component is an important asset in some applications such as knee assistive devices where both modes are needed. However, one disadvantage of MR actuators is their large size and mass [105]. MR actuators in the context of exoskeletons were used for the knee joint [104, 106], as the torque on this joint has a damping effect on most of the gait cycle [15].

2.2.3.2.6 *Transmission Systems*

The actuation systems that are based on electric motors usually include a transmission system that amplify the torque produced by the motor. These transmission systems include conventional systems such as gear drives, belt drives and Ball screws, and non-conventional systems such as the harmonic drives which have high reduction ratios, near-zero backslash and compact size (see figure 2- 12) [86]. Harmonic drives were used in many robotics applications requiring precision positioning [107]. In the context of exoskeletons, harmonic drives were used for rehabilitation exoskeletons [11, 44] and rarely for augmentation exoskeletons because of the need for relatively high speeds.
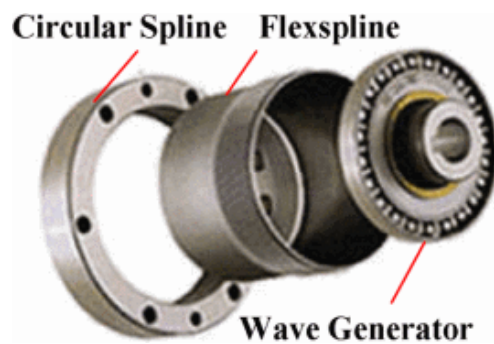
Figure 2-12: Harmonic drive. Copyright © IEEE 2017. [108]

2.2.3.2.7 Selection of the Actuation System

Table 2-1 summarizes the advantages and disadvantages of the types of actuation systems discussed above. The advantages of these actuators are in general complementary. Therefore, selecting one type from another could be a challenging design decision given that the actuation system represents a significant part of an exoskeleton cost and is critical to its performance. For this reason, the design choice needs to be guided by a thorough understanding of the application requirements such as speed and torque as well as size and mass limits. For instance, hydraulic and pneumatic actuators which need compressors for their operation are not suitable for autonomous exoskeletons. Electric motors are the best actuation option for autonomous exoskeletons. Specifically, for an ankle exoskeleton, BLDC motors offer high power density, that is, they provide high power while having low mass and size.

Table 2-1: Actuation systems

Actuation type	Main advantages	Disadvantages
Hydraulic	High power to weight ratio	Need for an external compressor Frequent maintenance
Pneumatic	High power to weight ratio Compliant	Need for an external compressor Frequent maintenance
Brushed DC motors	Simple to operate and control Relatively cheap	Limited service life Limited range of speed
Stepper motors	Position can be controlled with an open loop control	Large size and mass Low efficiency
Brushless DC motors	High power to mass compared to other electric motors Wide range of speed	Require electronic drivers Relatively expensive compared to other electric motors
Series elastic actuators	Allow for safe interaction with the environment Allow for high precision force control	Large size and mass
Magnetorheological actuators	Can operate as a brake and a clutch	Large size and mass

2.2.3.3 Rigid and Soft Physical Interfaces

The physical Human-Robot (pHR) interface of a wearable robot is the set of materials and components used to transfer the mechanical power from the robot to the user [109]. For many years, exoskeletons for augmentation and walking assistance were built using rigid frames as the pHR interface. The frame is commonly made of rigid links and joints attached to the user body at some locations using straps and belts. Rigid physical interfaces have caused substantial issues for exoskeletons including the added inertia of linkage and altering of natural gait as well as misalignment of exoskeleton and biological joints [83]. Recently, a new research direction is being investigated to improve the pHR interface of exoskeletons. It consists of developing exoskeletons called "soft exosuits or soft exoskeletons" [83] which incorporate soft materials such as textiles and webbing to transfer the force to the user (see figure 2-14). The introduction of soft exosuits has alleviated many of the challenges associated with conventional rigid exoskeletons. For instance, the use of textile makes the exosuit transparent to the user, that is to say, the exosuit does not interfere with the natural movements of its wearer [110]. Additionally, exosuits are significantly lighter than conventional exoskeletons. As a result, exosuit can potentially be more efficient because rigid exoskeletons spend a part of their mechanical energy to overcome their own weight and inertia. Actuation in soft exosuit is done through compliant actuators such as McKibben [83] or using cable-based transmission systems [13]. A unique feature of exosuits is the multiarticular actuation, that is to say, the actuation system of the exosuit along with a custom-designed mesh of webbing allows transmission of mechanical power to different joints simultaneously (see figure 2-14 C). Exosuits do have some disadvantages; however, for instance, they don't support compressive loads (such as backpacks) and they are limited in maximum torque and bandwidth [50]. Besides, when the suit is tensioned, there are shear forces between the attachment straps and the user skin [111].
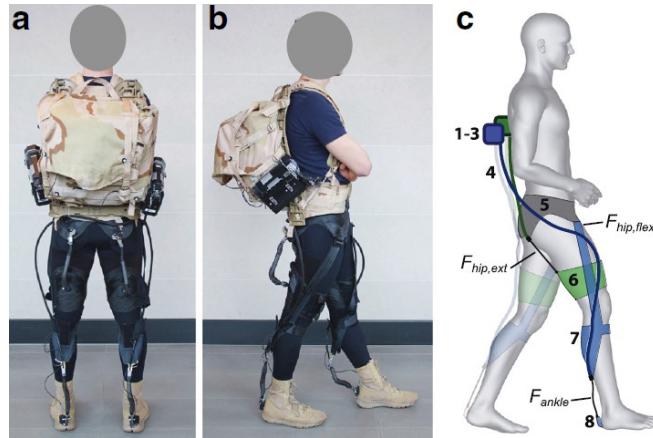
Figure 2-13: Harvard Wyss institute exosuit. ©
Panizzolo et al. 2016 [13]

2.2.3.4 Number of Degrees of Freedom

There are three joints on the human's lower limb: hip, knee and ankle. Early developed augmentation exoskeletons were in most cases made of bilateral frames with a combination of passive and active joints parallel to each of the biological joints with many degrees of freedom (DOF). For example, the Body Extender exoskeleton had 22 actuated DOF [10]. Although this design was adopted for many load-carrying exoskeletons, it has imposed key challenges which resulted in many of these exoskeletons not being able to reduce the energy consumed by the user when walking with the exoskeleton compared to normal walking [16]. Among these challenges, the mass and inertia that these devices add to the user as well as the lack of kinematic compliance between the user limb and the exoskeleton frame [112]. This lack of compliance is featured for example in the misalignment between the biological and exoskeletal joints which can be as large as 10 cm [113]. From a control perspective, a multi-joint exoskeleton requires the control system to handle the coordination of different joints during walking to match the natural gait of the user. Because of all these hurdles, some researchers focused on developing single joint exoskeletons to decrease the complexity and have more control over the design parameters [21, 114]. Moreover, with a single DOF exoskeleton, it is much easier to study the physiological effect of the control and design parameters [115].

Most single DOF walking exoskeletons add positive power on the hip or ankle joints because these joints have a positive average power over the gait cycle [1, 12, 21, 98, 116, 117]. Among hip

exoskeletons that were developed [89, 114, 116], some were able to reduce the metabolic cost of walking [70, 117]. Ankle exoskeletons have more potential to reduce walking energetic cost because during the push up phase, the muscles produce a large peak of power on the ankle joint to lift the body and push it forward (see figure 2-6). Some ankle exoskeletons which supplemented the biological torque during this short phase could reduce the metabolic cost of walking [1, 19, 118]. In the next section, we present and review the design of some of these ankle exoskeletons.

2.2.4 Ankle Exoskeletons for Reducing Metabolic Cost of Walking

Several ankle exoskeletons were developed to reduce the metabolic cost of walking. The ankle joint delivers a high power at the end of the stance phase to push the body forward. For a person with 80 kg weight, the ankle plantar flexion torque can be as high as 96 Nm [22]. For this reason, researchers designed ankle exoskeletons to supplement this biological torque by an artificial torque that could reduce the energy expenditure during walking. In this section, we present some of these ankle exoskeletons and highlight their design characteristics.

2.2.4.1 Unpowered Ankle Exoskeleton from Collins et al.

The exoskeleton developed by Collins et al. is a lightweight unpowered ankle exoskeleton. It was made of a spring attached to a mechanical clutch by a rope [1]. Those components were attached to the back of a lightweight composite structure worn around the shank (see figure 2-15 A), thereby, providing a mechanical behavior similar to that performed by the calf muscles and tendons. During normal walking, soleus and medial gastrocnemius muscles stretch slowly during the single stance phase then recoil rapidly at the end of the late stance allowing the release of mechanical energy stored on the Achilles tendons [119]. This clutch-like behavior of the muscles and spring-like behavior of the Achilles tendons was the motive behind the design of the exoskeleton by Collins et al. [1]. The mechanical clutch placed in parallel to the calf muscle engages the spring placed in parallel to the tendons during the stance phase of the gait cycle to store the energy, then disengages it to release the stored energy at the beginning of the swing phase [1]. Figure 2-15 B shows a CAD model of the clutch mechanism.

Tests were carried out on healthy subjects wearing the exoskeleton on both legs while walking at a speed of 1.25 m s^{-1}. The torque produced by the exoskeleton is similar to the human ankle joint torque but much lower in magnitude. Different values of spring stiffness were tested to examine

its effect on the metabolic cost of gait. The exoskeleton reduced the consumed metabolic energy by 7.2 ± 2.6 % compared to normal walking [1]. This reduction was also associated with a reduction in the soleus muscle activity. In addition, it was shown that a particular value for spring stiffness was optimal, increasing or decreasing this value results in more energy consumption. The main limitation of this unpowered exoskeleton is the inability to provide higher torque due to lack of an active power source. In addition, it is not yet well understood how this approach affects the natural human gait on the short term and long term because this approach relies entirely on the power generated by the biological system.
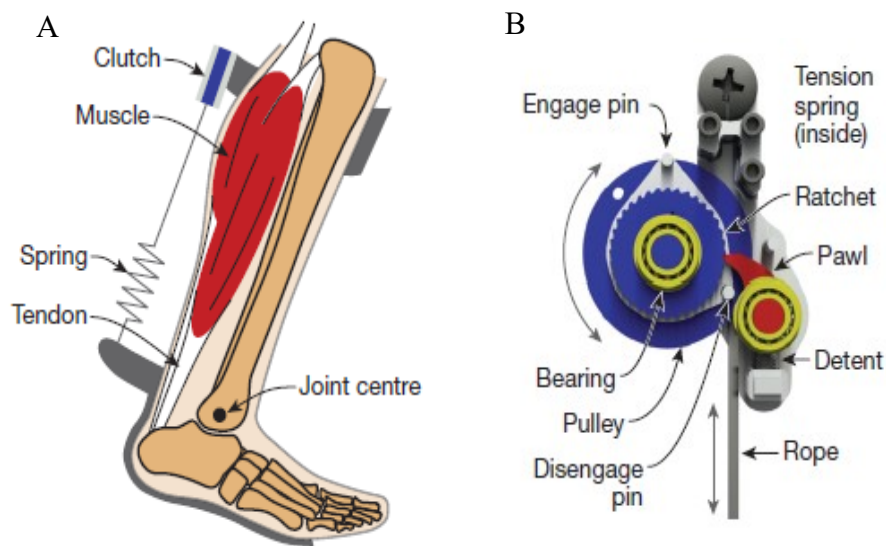
Figure 2-14: (A) a schematic of the unpowered exoskeleton developed by Collins et al. (B) the mechanical clutch [1]

2.2.4.2 Pneumatic Ankle Exoskeleton from Malcolm et al.

Malcolm et al. studied the effect of the actuation onset on the metabolic cost reduction using a powered ankle exoskeleton [19]. This exoskeleton uses a McKibben pneumatic muscle to produce an assistive plantar flexion torque on both legs. This simple lightweight structure adds only 0.67 kg per leg. During the experiments, five actuation onset values were tested: 13, 23, 34, 43 and 54% (percentage of the gait cycle). The actuation offset was set at toe off in all cases.

The experiments were performed on eight typically developed subjects wearing the exoskeleton while walking on a treadmill. The five actuation onset conditions were tested for each participant

in addition to walking with the exoskeleton unpowered which was used as a reference [19]. The highest reduction of metabolic energy was of $6 \pm 2\%$ compared to walking without the exoskeleton. This reduction occurred on the 43% onset condition which is just before heel contact of the other leg [19].

Despite the significance of the result achieved in this study, the tested exoskeleton was tethered to an off-board air compressor. Achieving the same reduction of metabolic rate with an untethered exoskeleton would be more challenging, still, this work gives proof that reducing the metabolic energy consumption is achievable with a powered exoskeleton when the actuation timing is optimal.

2.2.4.3 Achilles Exoskeleton

Achilles is a powered exoskeleton developed to reduce the metabolic cost of walking [20]. The design of Achilles consists of a rigid structure made of two hinged parts: the shank shell and foot shell. A linear actuator was attached from one end to the shank shell and from the other end to a flexible link fixed to the foot shell (see figure 2-16). The set composed of a flexible lever arm and linear actuator form a SEA. Meijneke et al. used a SEA to store and release the negative power provided by the ankle joint during the stance phase, thereby, reducing power requirements of the motor. To further improve the design of the device, an optimization study was conducted with the goal of maximizing the power of the exoskeleton while minimizing its mass by varying the dimensions of the linkage mechanism and stiffness of the lever arm for different motor and gears combinations. The final prototype of the device can output a maximum mechanical power of 80.2W.

The device was tested on seven healthy subjects by collecting kinematic and kinetic data in addition to carbon dioxide consumption in three conditions: waking without the exoskeleton (baseline), walking with the exoskeleton unpowered and walking with the exoskeleton powered on. The maximal assistance torque applied by the exoskeleton during the trials was 0.4 Nm/kg. The experiments showed that the exoskeleton could not reduce the metabolic cost of walking. The authors explained this by a number of reasons related to hardware and control aspects such as the interference of the actuator with the natural gait, particularly during the swing phase and early stance phase. During these phases, no assistive torque is provided. However, the actuator was not completely transparent as it applied a force to match the natural movement of the subject. Other

exoskeletons using unidirectional actuators [1, 12, 19, 21] allow free movement to the user during these non-assistance phases.
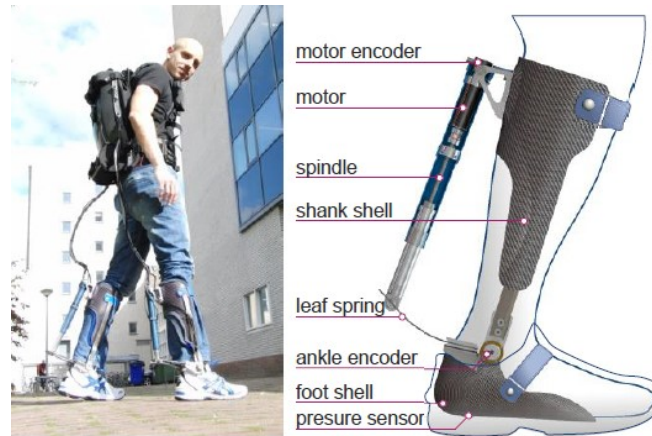
Figure 2-15: The Achilles exoskeleton. Copyright © IEEE 2016 [98]

2.2.4.4 Powered Ankle Exoskeleton from Collins et al.

In an effort to facilitate the understanding of how human adapts and reacts to an exoskeleton, Collins et al. developed an emulator system that includes two end effectors in the form of ankle exoskeletons (Alpha and Beta) tethered through Bowden cables to a powerful off-board electric motor [21] (see figure 2-17). While the main goal of this work was not to develop an autonomous exoskeleton, important improvements were brought to the design of the two exoskeletons to achieve high torque and high bandwidth while keeping their mass at a low level. Both of the exoskeletons had a rigid frame attached to the leg in three points: the shank, the heel and the toe areas. Each frame has a shank and a foot section. The foot section extends posterior to the ankle joint to provide a lever arm. When the Bowden cable is pulled by the motor it compresses the shank section downward and pulls the lever arm upward, thereby, creating a plantar flexion torque. The main difference between the two exoskeletons was the series elastic element (figure 2-17). In the Alpha version, two leaf springs were attached on the lateral and medial sides of the foot frame, thus increasing the envelop of the exoskeleton. In the Beta version, the envelope was reduced by introducing a coil spring.

During walking tests to evaluate the mechanical performance of the two devices, the average torque produced by the Alpha and Beta exoskeletons was 80 Nm and 87 Nm respectively, while the

maximum torque was 119 Nm and 121 Nm. In terms of weight, both exoskeletons were lightweight with a total of 0.835 kg and 0.875 kg for the Alpha and Beta versions respectively.
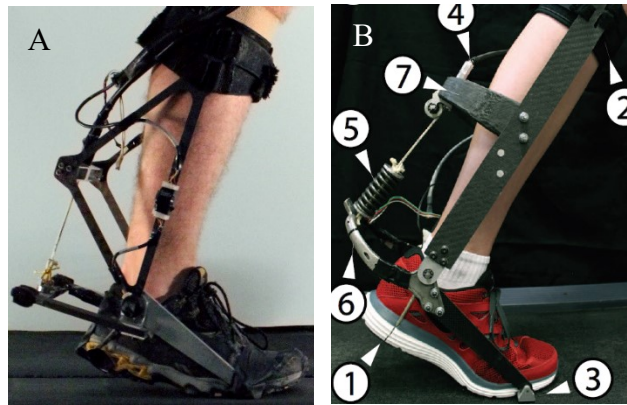
Figure 2-16: (A) Alpha exoskeleton (B) Beta exoskeletons. Copyright © IEEE 2015 [21]

2.2.4.5   Powered Ankle Exoskeleton from Mooney et al.

Mooney et al. developed an exoskeleton capable of providing high positive mechanical power during powered ankle plantar flexion phase [12]. Ankle exoskeletons commonly apply torque by exerting a force in parallel to the leg within a distance behind the ankle joint [1, 21, 98]. This choice limits the lever arm to a short distance as it is impractical to increase the envelope of the exoskeleton far behind the ankle. To overcome this challenge, the exoskeleton built by Mooney et al. applies the force normal to the shank using a winch actuator that pulls two struts attached to the user's boot (see figure 2-18). The struts in this configuration allow for a large lever arm, thus reducing the force requirement of the motor to produce a given torque. In addition, the fiberglass struts reduced significantly the weight of the exoskeleton [12]. Applying force in the normal direction to the leg also reduces the slip of the frame attached to the shank compared to applying tangential forces, therefore, improving user comfort while wearing the exoskeleton [12]. The mass added by the exoskeleton on the foot and shank was 2.12 kg (1.06 kg per leg).

The exoskeleton was tested on healthy participants for both loaded and unloaded walking. On the loaded walking experiment, the subjects wore a 23-kg vest while walking at a speed of 1.5 m/s. On the unloaded test, subjects walked on the treadmill at a speed of 1.4 m/s. The energy consumption measurements on the loaded and unloaded locomotion conditions showed a reduction in metabolic cost of $8 \pm 3\%$ [12] and $10 \pm 3\%$ [97] respectively when walking with the exoskeleton compared

to walking without the exoskeleton. During the two tests, the exoskeleton delivered an average mechanical power per gait cycle of 23 ± 2 W (11.5 per ankle) and 26 ± 1 W (13 per ankle) respectively.

This study marks the importance of concentrating efforts on developing lightweight and powerful exoskeletons that can add substantial mechanical energy without impeding the natural user movement.

Figure 2-17: Mooney et al. exoskeleton. © Mooney and Herr. 2016 [118]

2.2.5 Design Challenges

The variety of design solutions adopted in building exoskeletons is an indication of the different challenges faced by researchers working to improve the performance of these devices. Despite many years of research and development in the field, there are still several challenges in the design of exoskeletons for walking assistance and augmentation. The main design challenges could be summarized as follows:

1. Mass and inertia

   The exoskeletons are generally physically attached to the user in parallel to his limbs, therefore, as the user moves, he perceives the added mass of the device that in most cases makes the movements more difficult and requiring more metabolic energy. To illustrate this, if a mass of 4 kg is attached to the foot, it will increase the metabolic rate of walking at normal speed by nearly 36% [24]. The added mass could be supported by the device actuators; however, this increases power requirement and complexity of the control system.

2. Mechanical Power

   Muscles in the human body can generate very high forces while being compact. For instance, for a male of 79 kg weight and 1.75 m high, the muscles can provide up to 1867 N during ankle plantar flexion [83]. For an exoskeleton to achieve the same levels of force, it needs high power actuators. However, increasing the mechanical power usually also increases the weight and size of the device. Therefore, using actuators with a high power to mass ratio could give the best compromise.

3. Control System

   Naturally, the human body employs the best gait parameters to minimize energy expenditure during walking including the step length [3], joints kinematic [120] and arm swinging movements [121]. For this reason, the exoskeleton control system needs to work in perfect synergy with the biological system. Any disturbance of the normal gait could result in an increase of the metabolic energy. Additionally, for practical use, the exoskeleton needs to adapt to different scenarios such as walking on flat or rough terrain and level or upslope walking. The current control technology used in many exoskeletons relies on a hierarchical architecture that could be decomposed in three control layers [122]. The higher control layer monitors the gait cycle transitions and activity modes of the user. The mid-level layer translates the detected state of the user to a desired input, for example, the input can be a force or position reference signal. The low-layer is the execution layer that uses feedback and feed forward control loops to minimize the error between the desired and the current state.

4. Transparency

   A transparent exoskeleton does not interfere with the natural gait and cadence of the user. In the best scenarios, the exoskeleton must not limit the natural ROM or impede any biological degrees of freedom. Improving the exoskeleton transparency can be achieved both at the mechanical and control levels, for example by reducing the weight and size of the device and implementing biomimetic control strategies.

5. Safety

Although safety does not influence the core functioning of the exoskeleton, it is of vital importance for the user. Moreover, augmentation exoskeletons are usually used by a healthy population, thus, they operate at higher speeds and generate higher mechanical power than other types of exoskeletons. For this reason, user safety must be a core element in the exoskeleton design. Similar to transparency, safety can be achieved by mechanical mechanisms and control software. For example, mechanical stops can be used to limit the movement of the exoskeleton to the maximum ROM of a joint and the control algorithm can contain a safety layer that frequently monitors the state of the device as well as the user to detect any abnormal situations.

6. Autonomy

Unlike tethered exoskeletons where the actuation is provided by an off-board unit, an autonomous exoskeleton carries its own hardware including the actuation system and thus can be used outside the lab. Additionally, for an autonomous exoskeleton, the battery limits the autonomy of the device to a certain duration. Increasing the device autonomy is not only limited by the technological development in batteries because improving the efficiency of the exoskeleton will also increase the autonomy.

CHAPTER 3   RATIONAL OF THE PROJECT

3.1 Summary of the Problem

Powered ankle exoskeletons including those that reduced the metabolic cost of walking add a mass to the user around the ankle joint. This mass that is far from the hip joint requires more metabolic energy from the user to walk when the exoskeleton is not powered on. Therefore, when the exoskeleton is powered on, it loses a part of its mechanical energy to compensate for its added mass. As a result, its benefit to the user in terms of reducing the metabolic expenditure during walking is limited.

3.2 General Objective

The general objective of this project is to develop an ankle exoskeleton with a minimum added distal mass compared to existing autonomous powered ankle exoskeletons providing at least 50 Nm of assistive plantar flexion torque.

3.3 Specific Objectives

The exoskeleton is a biomechatronic device integrating different subsystems. These subsystems guided us in defining the specific objectives for this project as follows:

1. OS1. Develop the mechanical system of the exoskeleton.

   a. Develop a design concept that reduces the distal mass and increases the torque provided by the exoskeleton

   b. Design and assemble the actuation unit

   c. Perform detailed design including optimization studies for the exoskeleton components

2. OS2. Develop the control system of the exoskeleton.

   d. Develop and implement an algorithm for real time detection of gait phases

   e. Build the electronic circuit for the gait detection system

f. Integrate the gait detection system with the motor controller

g. Develop a graphical user interface for the control and monitoring of the device

3. OS3. Assemble and evaluate the exoskeleton

h. Assemble the exoskeleton components and ensure synergic integration of the hardware and the software.

i. Perform mechanical testing for the exoskeleton to determine the mechanical efficiency of the actuation system

j. Perform human walking trials with the exoskeleton to evaluate its effect on the activity of the ankle muscles.

CHAPTER 4   ARTICLE 1: DESIGN AND DEVELOPMENT OF A LIGHTWEIGHT ANKLE EXOSKELETON FOR HUMAN WALKING AUGMENTATION

Yacine Bougrinat, Sofiane Achiche, Maxime Raison.

Abstract

Most of powered ankle exoskeletons add considerable distal mass to the user which limits their capacity in reducing the metabolic energy of walking. The objective of the work presented in this paper is to develop an ankle exoskeleton with a minimum added distal mass compared to existing autonomous powered ankle exoskeletons, while providing at least 50 Nm of assistive plantar flexion torque. The proposed exoskeleton uses Bowden cables to transmit the mechanical force from the actuation unit attached to the waist to the carbon fiber struts fixed on the boot. As the struts are pulled, they create an assistive ankle plantar flexion torque. A 3d-printed brace was attached to the shin to adjust the direction of the cables. A design optimization study was performed to minimize the mass of the struts, thereby limiting the total added distal mass, attached to the shin and foot, to only 348 g. The main result obtained from walking tests was the reduction of the soleus and gastrocnemius muscles activity by a maximum of 37% and 44% respectively when walking with the exoskeleton compared to normal walking. This result shows the potential of the proposed exoskeleton to reduce the metabolic cost of walking and emphasizes the importance of minimizing the distal mass of ankle exoskeletons.

Keywords

Lower limb exoskeleton, human augmentation, ankle exoskeleton, wearable robot

Funding

4.1 Introduction

Walking while carrying heavy loads is a fundamental skill in daily activities of some professions. For example, soldiers are often required to walk while carrying heavy backpacks that weigh more than 50% of their lean body mass [1]. Firefighters also wear protective equipment and breathing apparatus that negatively impact their physical conditions [2]. Several exoskeletons have been developed to reduce the effect of heavy payloads during walking [3, 4]. The design of these exoskeletons varies from full-leg exoskeletons [5-9] to single joint exoskeletons that assist the user at the hip [10, 11] or at the ankle [12-14]. It is important to note that the most commonly used metric to evaluate these exoskeletons is the metabolic cost of walking which is the energy consumed by the human body during walking [4, 15]. Another common metric is the analysis of electromyography (EMG) signals to examine changes in muscle activation [15]. Both of these metrics will be referred to in the rest of the paper.

Among single joint exoskeletons, ankle exoskeletons have shown great potential in reducing the metabolic cost of walking [13, 16, 17]. The power generated on the ankle joint during the push off phase is the largest compared to other joints of the leg [18]. Therefore, adding positive power during this phase on the ankle can have a beneficial effect on the walking energetics. There are different design approaches for ankle exoskeletons in the literature; one of the most distinctive design features is the actuation form as either passive or active, as described in the two next paragraphs, respectively.

Passive exoskeletons are suitable for augmentation on the ankle joint as the power on the ankle has a negative period where energy can be stored in an elastic element and a positive period where the stored energy can be released. Using this approach, Collins et al. developed a lightweight device equipped with a passive clutch mechanism attached to a series spring to augment the ankle torque during push off [19]. Tests performed on healthy typically developed subjects walking with this device showed a reduction in metabolic cost by approximately 7% [13]. The advantage of passive ankle exoskeletons is that they are lightweight and simple; however, the positive power they provide is limited compared to active exoskeletons, due to the lack of actuators.

Pneumatic actuation was used in many ankle foot orthoses for both rehabilitation and gait training purposes [20-23]. Pneumatic actuators have a high specific power [24], and thus they represent a good option for augmentation exoskeletons. Malcolm et al. performed tests on able bodies wearing

a simple bilateral ankle exoskeleton with an artificial muscle behind the shank. By varying the onset actuation timing, the metabolic cost of normal ground level walking was reduced by 6% [17]. Despite the light nature of pneumatic actuators, they require an air compressor which is usually large and heavy and is therefore found off board. This makes pneumatic actuators unsuitable as a solution for autonomous exoskeletons where portability is key. Several research groups used electric motors as actuators instead of pneumatic actuators. For example, Achilles is an autonomous exoskeleton that supports plantar flexion during push-off [12, 25]. The supporting torque is produced by a series elastic actuator composed of an electric motor, a ball screw and a leaf-spring made of carbon fiber. This structure limited the added mass around the ankle to 1.5 kg, while providing 52% of the positive biological plantar flexion power. However, tests on human subjects resulted in an increase in the consumed metabolic energy. This was due to the relatively high weight of the Achilles compared to other active exoskeletons [14, 17] as well as the interference of the actuator with the normal ankle gait during the swing and the early stance, where no support was provided [12]. Walsh et al. developed soft exosuits using textiles that transfer tensile forces in parallel to the muscles, supplementing the hip and ankle biological torques [26-28]. In addition to considerably decreasing the weight of the device, this design has the advantage of not restricting the natural joints movements of the user. Recently, it was demonstrated that an autonomous soft exosuit could reduce the loaded walking energetics by 7.3 ± 5.0 % [29]. Using soft elements to transmit forces is however associated with energy loss due to the compliance in textiles and the interface displacements under shear forces [30, 31]. A non-conventional design for a rigid ankle exoskeleton was proposed by Mooney et al. [32]. It consists of two fiberglass struts that are attached to the boot and that extend backwards from the foot. The two struts are pulled forward during powered plantar flexion by a winch actuator attached on the shin, thereby, augmenting the biological plantar flexion torque. In addition to adding a low distal mass, the struts configuration allowed for a large moment arm, which provides a torque comparable to biological levels. This resulted in a reduction in metabolic cost of loaded walking by 8 ± 3% [14] and normal walking by 10 ± 3% [32] when comparing walking with and without the exoskeleton.

The low added distal mass is the main design characteristic of both powered and passive ankle exoskeletons which demonstrated an improvement on walking efficiency [13, 17, 29, 32]. In an experimental study [33], Browning et al. concluded that distal loads on the leg, compared to

proximal loads, have a larger effect on energy expenditure, particularly around the waist. For powered ankle exoskeletons, reducing the weight is more challenging since the actuation system adds considerable load to the device. However, placing the actuation components near the waist could help significantly reduce the added distal load, compared to placing the components on the shank or foot. For instance, the distal mass per leg reported by Mooney et al. is 1060 g [32]. To our best knowledge, this represents the current lowest distal mass added by an autonomous powered ankle exoskeleton.

The augmentation factor is a model developed by Mooney et al. [14] which allows to estimate the metabolic impact of an exoskeleton considering its mechanical power and mass distribution over the user body. In this model, a mass around the ankle has a negative effect on the metabolic energy that is 4 times higher than the same mass placed around the waist [14]. For instance, reducing the distal mass of an exoskeleton from 1 kg to 0.5 kg (50% reduction) could reduce the metabolic penalty of this mass from 14.8 W to 7.4 W. A mass of 1 kg placed on the waist, however, has a negative effect on the metabolic energy of only 5.6 W.

The objective of this study is to develop an ankle exoskeleton with a minimum added distal mass compared to existing autonomous powered ankle exoskeletons, while providing at least 50 Nm of assistive plantar flexion torque. Quantitatively, the objective of this study consists in reducing the added distal mass by at least 50%, compared to the 1060 g achieved by Mooney et al. [32] which is seen as a reference work. We chose the 50 Nm threshold, as this one represents around 50% of the maximum natural plantar flexion torque generated during the gait cycle for a 75 Kg adult [34].

In this paper, we present the design of the developed device as well as the results of EMG signals analysis of a healthy typically developed subject obtained from walking tests with and without the exoskeleton.

4.2 System Overview

WAXO (Walking Augmentation Ankle Exoskeleton) was the proposed name of the developed ankle exoskeleton for human walking augmentation. Like similar devices, it is characterized by an interaction between different subsystems including the user himself, the mechanical structure and the sensory and control systems. Figure 4-1 shows the main components of the device. Since the main objective was to reduce the distal mass of the exoskeleton, the mechanical structure is

composed of only two struts attached to the left and right sides of the boot. The requirements for our design were inspired by Mooney et al. [14], whom exoskeleton work was significant in reducing the metabolic cost of walking. However, to help further decrease the added distal mass, in our design, the actuation system was attached to the waist instead of to the front of the shank. Two Bowden cables were used to transmit the force from the actuation unit to the tip of each strut. The cables pass through a lightweight custom designed brace attached to the shank which changes their direction from vertical to the actuation direction. The electronics, including the motor driver, were secured into a case attached to the waist. One force sensitive resistor (FSR), placed under the boot insole, was used to monitor the gait cycle. An off-board personal computer (PC) was used to provide a graphical user interface and control the motor.
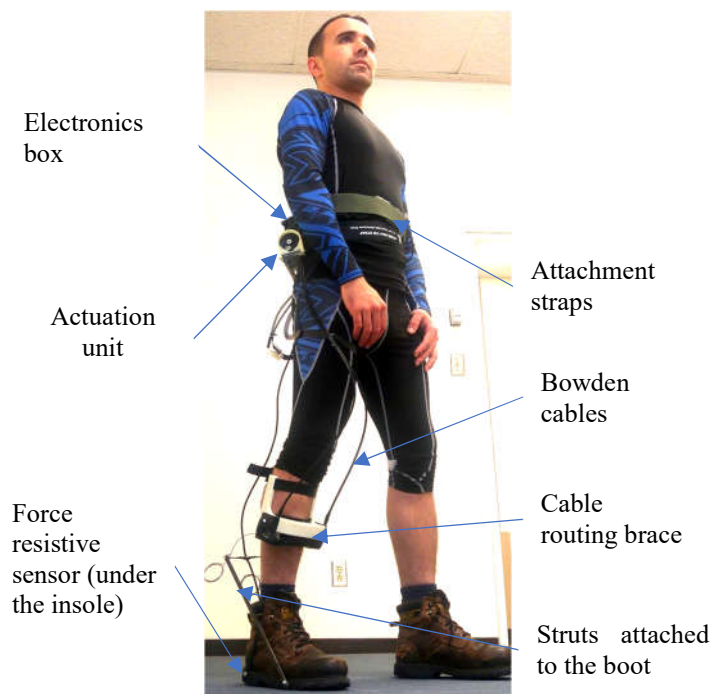
Figure 4-1: Overview of the WAXO exoskeleton. The actuation unit was attached to the waist using straps. Bowden cables were used to transmit the force to the ankle by pulling a struts structure attached to the boot. A 3d-printed brace attached to the shin changed the direction of the cables to pull the struts. An FSR inserted under the insole was used to detect heel strikes. The electronic components were enclosed in a plastic box attached to the waist

4.3 Mechanical Design

4.3.1 Augmentation Principle

Human gait cycle is typically composed of a stance phase where the foot remains in contact with the ground, and a swing phase where the same foot moves in the air [3]. The proposed exoskeleton enables to augment human locomotion by supplementing the ankle joint plantar flexion torque, which is responsible for lifting and propelling the body forward at the end of the stance phase. Although the literature has given evidence that this design choice is valid for walking augmentation exoskeletons, adding minimal mass on the ankle and foot is critical to the energetics of walking; therefore, reducing this mass while providing significant torque levels is the main contradicting objectives of our design. Unlike other ankle exoskeletons where the augmentation force is applied in the vertical direction behind the heel [13, 17, 35], the struts allow the force to be applied normal to the shank [14]. This is more comfortable for the user as vertical forces cause friction between the attachments and the skin [31]. Additionally, using struts, no artificial joint is added in parallel, thus the biological joint itself is used.

The supporting torque is generated by the pulling force of the Bowden cable and the moment arm resulting from the struts configuration. Thus, to increase this torque, those two design parameters should be increased.

Our strategy to lower the distal mass of the exoskeleton is achieved mainly by two elements: first, placing the actuator assembly proximal to the torso, and secondly, optimizing the geometrical layout and mass of the struts assembly.

4.3.2 Design Criteria

The criteria set for the design of WAXO were as follows:

1. It should provide at least 50 Nm of plantar flexion torque. As the maximum plantar flexion torque is around 1.3 Nm/Kg for an adult walking at a normal speed [34], 50 Nm represents around 50% of the maximum plantar flexion torque for a person weighing 75 Kg which, in our judgment, is a significant assistive torque.

2. The distal mass per leg must be at least 50% lower than the current minimum distal mass in the literature. To the best of our knowledge, the minimum added distal mass (on shank and foot)

associated with active rigid ankle exoskeletons that carry their own actuation system was demonstrated by Mooney et al.[32] with a value of 1060 g. Table 4-1 shows a comparison of mass of selected active ankle exoskeletons that were designed for human walking augmentation.

3. It should not impede the natural degrees of freedom of the ankle joint.

Table 4-1: Mass of selected active ankle exoskeletons

Device	Overall mass (g)	Distal mass (shank and foot) on one leg (g)
Mooney et al. 2014 [32]	3600	1060
Kirby et al. (exoskeleton Alpha) 2015 [35]	N/A (tethered)	835
Kirby et al. (exoskeleton Beta) 2015 [35]	N/A (tethered)	875
Van Dijk et al. 2016 [12]	9000	1500

4.3.3 Main Design Components and their Selection

The main components of WAXO are: the actuation unit, force transmission mechanism and the struts attached to the boot. In this section, we give enough details about the design of these components for it to be reproducible by the reader.

4.3.3.1 Actuation Unit

The actuation unit of WAXO is composed of a 200W brushless DC (BLDC) motor (Maxon Motor, Sachseln, Switzerland) coupled with a reduction gearbox of 43:1 ratio (Maxon Motor, Sachseln, Switzerland). Brushless DC motor based actuation was preferred to other actuation options since it offers relatively high power with a compact architecture allowing for portability, as opposed to pneumatic and hydraulic actuators which require an off board compressor. A spool with a 4-cm diameter was attached to the output shaft of the gearbox to pull the two Bowden cables attached to it. Figure 4-2 shows a rendering of the actuation unit.

Although the gearbox adds mass to the actuation unit, it is essential to amplify the torque of the motor and allows for a higher maximum axial load on the shaft. The motor shaft can only withstand 25 N of axial load, which is not sufficient for our application. To ensure user and hardware safety,

the spool diameter, d_s [m] was chosen to maintain the axial load below the maximum permissible load, F_{max}[N]. Using a gearbox with a transmission ratio, γ, and efficiency, η[%], F_{max}[N] is given by:

$$F_{max} = \frac{T_M \, \gamma \, \eta}{\left(\frac{d_s}{2}\right)}$$

(4.1)

where T_M[N] is the torque delivered by the motor. Considering a factor of safety, FoS, the minimum spool diameter is given by:

$$d_s \geq 2 \cdot T_M \cdot \gamma \cdot \eta \cdot \frac{FoS}{F_{max}}$$

(4.2)

The selected gearbox has a ratio of 43 and an efficiency of 72%. The maximum axial load on the gearbox shaft is of 360 N. With a factor of safety, FoS, of 1.5 and a motor torque of 0.15 Nm, the minimum diameter for the spool is 3.9 cm. A 4-cm diameter was therefore chosen.

The actuation unit has the highest weight compared to the other components. Therefore, to reduce its effect on the energy expenditure during walking, the actuator was attached around the waist using straps.
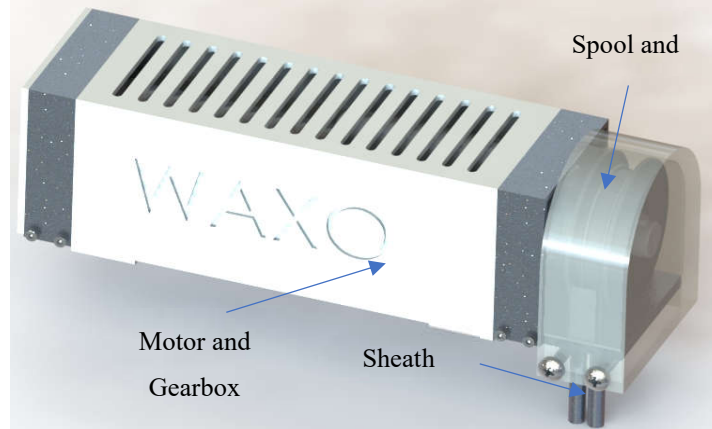
Figure 4-1: WAXO actuation unit. The actuation unit include a geared brushless DC motor and a pulley that guides two Bowden cables

4.3.3.2   Force Transmission Mechanism

The force is transmitted from the actuation unit to the struts on the ankle joint using Bowden cables. Thereby, allowing the actuation unit to be placed near the center of mass of the body. Although using Bowden cables results in loss of mechanical power due to friction, the advantage of this

choice is that it reduces the effect of the actuation unit on the metabolic energy because the actuation unit has the largest weight compared to other main parts of the device.

Two Bowden cables were used to pull the two struts. Each cable was attached to the spool on one end and to one of the two struts on the other end. When the spool rotates, the cables rotate simultaneously in the same direction pulling the two struts forward. A brace was custom-designed, and 3D printed, in such a way as to change the direction of the cables from vertical to the pulling direction (see figure 4-3 A). Two "V brake" noodles were inserted on the left and right sides of the brace to guide the cables (see figure 4-3 B).
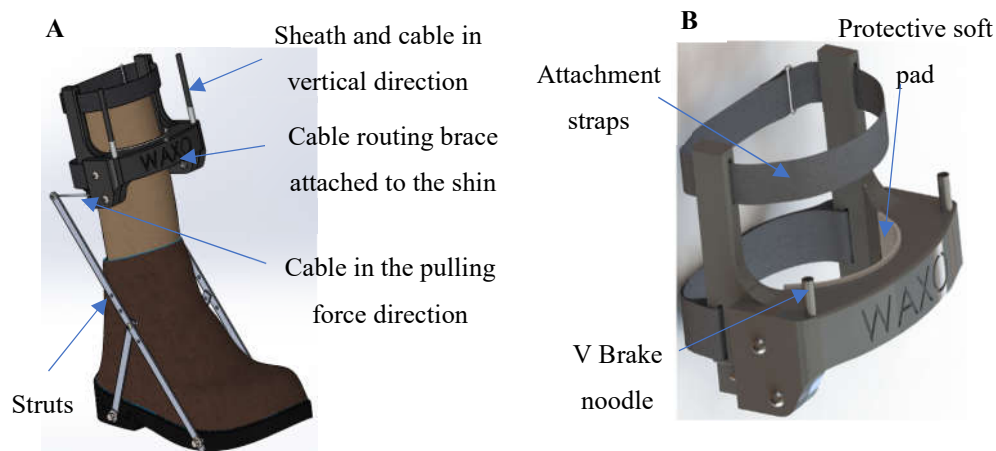
Figure 4-2: (A) The cable routing brace attached to the shin was used to change the direction of the cables (B) a zoomed figure of the cable routing brace

4.3.3.3 Struts

The struts set, which constitutes an exoskeletal foot rigidly attached to the boot, is the physical interface between the exoskeleton and the user and guarantees the transfer of power to the biological joint. The struts were optimized to provide a large moment arm while keeping their mass to a minimum. Details of the optimization are given in the next section. The struts were fixed by bolts to the boot insole on the metatarsophalangeal joint and under the ankle joint. This configuration was chosen to reduce undesired forces and moments on these joints that may alter the natural gait.

4.3.4 Struts Optimization

The struts are the main distal mass added around the ankle joint by the WAXO exoskeleton. Therefore, as our main objective is to reduce the distal mass while providing a high torque, an optimization study of the struts assembly was performed. This optimization was done through two distinct optimization problems. First, the geometrical layout of the struts was optimized to result in a maximum torque lever arm; thus, reducing force requirements of the motor. Then, the thickness and width of the struts were optimized to minimize the mass. In the next subsections, we give details of these two optimization problems.

4.3.4.1 Struts Geometrical Layout Optimization

Optimizing the strut layout is central to reducing the added distal mass while providing high torque comparable to the biological torque. From each side of the foot, the structure consists of two struts attached to each other near the ankle-joint (figure 4-3 A). The longer strut is bolted to the boot insole on the metatarsophalangeal joint on one end and attached to the Bowden cable on the opposite end. The shorter strut is fixed to the previous strut from one end and to the back side of the insole on the other end. The shorter struts help reinforce the bolt in holding the longer struts fixed under the applied cable force, thereby, maximizing the transfer of power from the actuator to the user joint.

Figure 4-4 shows the design variables as well as the different points defining the lines and distances used in the optimization problem below. The point O coincides with the metatarsophalangeal joint representing the origin of the coordinate system. One end of the strut is fixed on the point O and the other end is represented by the point C. C' is the projection of the point C on the x axis. The point B is the location of the posterior extremity of the boot. The point A represents the location of the ankle joint. The point P is the lower tip of the V brake noodle, thus, the line (CP) defines the direction of the force exerted by the cable. The point D in the line (CP) defines the perpendicular distance $\overline{AD}$ between point A and the line (CP). P' is the intersection of the horizontal line passing through the point C and the vertical line passing through the point P.

Design variables.

Three design variables were chosen for this optimization study as shown in Table 4-2.

Table 4-2: Design variables

Variable	Description	Unit
$\overline{OC}$	Length of the strut	[mm]
θ_s	angle between the strut and the line (OB)	[rad]
θ_c	angle between the cable and the line (CP')	[rad]

Design parameters

Design parameters are different from design variables. Unlike the design variables that are changed by the optimization algorithm at each iteration. The design parameters can vary in general but are fixed for each optimization run. Design parameters can be used to examine how their variation affects the final design solution. The design parameters chosen in our optimization problem are given in Table 4-3.

Table 4-3: Design parameters

Parameter	Description	Unit
D_{1max}	Maximum distance behind the strut tip and the back of the insole	[mm]
D_{2min}	Minimum distance between the strut tip and the vertical line passing through the ankle-joint	[mm]
H_{max}	Maximum height of the cable routing brace from the insole	[mm]
L_{max}	Maximum length of the strut	[mm]
θ_{max}	Maximum value for the cable angle θ_c	[rad]
θ_a	Ankle plantar flexion angle defined as the angle between the lines (OC') and (OB)	[rad]
x_A	x coordinate of the ankle-joint (point A)	[mm]
y_A	y coordinate of the ankle-joint (point A)	[mm]
x_P	x coordinate of the point P	[mm]
$\overline{OB}$	Distance between the strut attachment on the insole and the back side of the insole	[mm]

A: ankle joint

C: strut tip

$\overline{OC}$: strut length

θ_s: strut angle

θ_c: cable angle

θ_a: plantarflexion angle

P: lower tip of the V brake noodle

B: posterior point of the boot
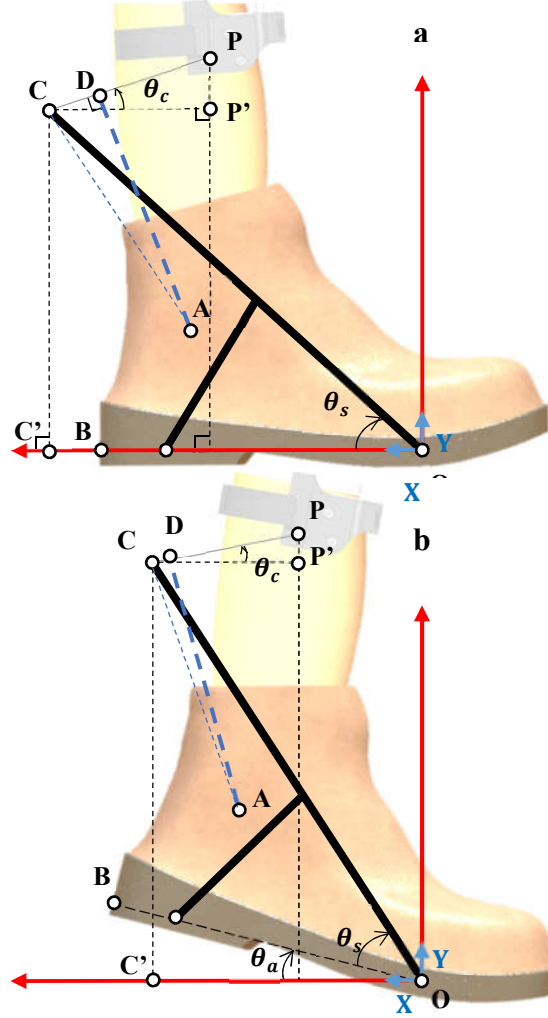
Figure 4-3: Layout of the struts on the foot. (a) configuration of the struts assembly when the foot is on the ground (b) Configuration of the struts assembly when the foot is on maximum plantarflexion during walking

We denote the design variables and parameters by x and p respectively, that is:

$$x = [\overline{OC}, \theta_s, \theta_c]^T$$

$$p = [D_{1max}, D_{2min}, H_{max}, L_{max}, \theta_{max}, \theta_a, x_A, y_A, x_P, \overline{OB}]^T$$

Objective function formulation

This section describes how the objective function is obtained. The main goal of the layout optimization is to maximize the artificial lever arm, $\overline{AD}$[mm], of the augmentation torque. This lever arm is the perpendicular distance between the ankle joint, A, and the line of action of the force exerted by the cable, (CP). Formally, the distance, $\overline{AD}$[mm] is given by:

$$\overline{AD} = \overline{AC}\sin(\overrightarrow{CD}, \overrightarrow{CA}) = \overline{AC}\sin\left(\theta_c + (\overrightarrow{CP'}, \overrightarrow{CO}) + (\overrightarrow{CO}, \overrightarrow{CA})\right) \tag{4.3}$$

When there is a plantar flexion of an angle, θ_a[rad], (see figure 4-4 B), the angle $(\overrightarrow{CP'}, \overrightarrow{CO})$ is given by:

$$(\overrightarrow{CP'}, \overrightarrow{CO}) = \theta_s + \theta_a \tag{4.4}$$

where θ_s, is the angle between the strut (AC) and the horizontal axis.

By substituting (4.4) in (4.3), we get:

$$\overline{AD} = \overline{AC}\sin\left(\theta_c + \theta_s + \theta_a + arcos\left(\frac{\overrightarrow{CO}.\overrightarrow{CA}}{\overline{CO}.\overline{CA}}\right)\right) \tag{4.5}$$

where arcos returns values in the first quadrant.

As:

$$\overrightarrow{CO} = -\overline{OC}\begin{bmatrix} cos(\theta_s + \theta_a) \\ sin(\theta_s + \theta_a) \end{bmatrix} \tag{4.6}$$

$$\overrightarrow{CA} = \begin{bmatrix} x_A - \overline{OC}cos(\theta_s + \theta_a) \\ y_A - \overline{OC}sin(\theta_s + \theta_a) \end{bmatrix} \tag{4.7}$$

By substituting (4.7) in (4.5), we get:

$$\overline{AD}$$

$$= \overline{AC}\sin\left(\theta_c + \theta_s + \theta_a \right.$$

$$+ arcos\left(\frac{cos(\theta_s + \theta_a)(\overline{OC}cos(\theta_s + \theta_a) - x_A) + sin(\theta_s + \theta_a)(\overline{OC}sin(\theta_s + \theta_a) - y_A)}{\sqrt{(\overline{OC}cos(\theta_s + \theta_a) - x_A)^2 + (\overline{OC}sin(\theta_s + \theta_a) - y_A)^2}}\right)\right) \tag{4.8}$$

$\overline{AC}$ can be written in terms of design variables and parameters as follows:

$$\overline{AC} = \sqrt{(\overline{OC}\cos(\theta_s + \theta_a) - x_A)^2 + (\overline{OC}\sin(\theta_s + \theta_a) - y_A)^2} \qquad (4.9)$$

Consequently, by substituting equations (4.9) in (4.8), we obtain the objective function written in terms of design variables and parameters as follows:

$$f(\pmb{x}, \pmb{p}) =$$

$$= \sqrt{(\overline{OC}\cos(\theta_s + \theta_a) - x_A)^2 + (\overline{OC}\sin(\theta_s + \theta_a) - y_A)^2} \; \sin\left(\theta_c + \theta_s + \theta_a \right.$$

$$\qquad (4.10)$$

$$+ \; arcos\left(\frac{\cos(\theta_s + \theta_a)(\overline{OC}\cos(\theta_s + \theta_a) - x_A) + \sin(\theta_s + \theta_a)(\overline{OC}\sin(\theta_s + \theta_a) - y_A)}{\sqrt{(\overline{OC}\cos(\theta_s + \theta_a) - x_A)^2 + (\overline{OC}\sin(\theta_s + \theta_a) - y_A)^2}} \right) \Bigg)$$

Constraints

The constraints associated with the optimization are as follows:

1. When the foot is on the ground ($\theta_a = 0$), the part of the struts behind the foot should not exceed a maximum value D_{1max}[mm] on the horizontal axis. A large strut part behind the foot might make the device impractical or difficult to use in a real setting as the strut or the cable can get stuck to objects from the surrounding environment. This constraint could be expressed in terms of design variables and parameters as follows:

$$g_1(\pmb{x}, \pmb{p}) = \overline{OC}\cos(\theta_s) - \overline{OB} - D_{1max} < 0 \qquad (4.11)$$

2. When maximum plantar flexion is reached (around 15°), the distance on the horizontal axis between the tip of the longer strut (point C in figure 4-4) and the vertical line passing through the ankle joint A must be bigger that D_{2min}. This constraint is necessary for the proper functioning of the cable routing brace and the security of the user.

$$g_2(\pmb{x}, \pmb{p}) = D_{2min} - \overline{OC}\cos(0.26 + \theta_s) + \overline{OA}\cos\left(0.26 + \left(\overrightarrow{OA}, \overrightarrow{OB}\right)\right) < 0 \qquad (4.12)$$

Replacing the angle $\left(\overrightarrow{OA}, \overrightarrow{OB}\right)$ and distance $\overline{OA}$ by their explicit form in terms of design parameters, we obtain:

$$g_2(\boldsymbol{x}, \boldsymbol{p}) = D_{2min} - \overline{OC}\cos(0.26 + \theta_s) + \sqrt{(x_A^2 + y_A^2)}\cos\left(0.26 + \text{atan}\left(\frac{y_A}{x_A}\right)\right) \tag{4.13}$$
$$< 0$$

Here, atan returns values in the first quadrant.

3. When the foot is on the ground ($\theta_a = 0$), the height of the cable routing brace must be lower than H_{max}. This ensures that the brace be placed on the shank area, at a given distance from the knee, making its attachment easy.

The height of the brace, represented by the point P is given by:

$$g_3(\boldsymbol{x}, \boldsymbol{p}) = \overline{OC}\sin(\theta_s) + (\overline{OC}\cos(\theta_s) - x_P)\tan(\theta_c) - H_{max} < 0 \tag{4.14}$$

Where x_P is the x coordinate of the point P.

4. To prevent excessive deflection of the strut when the force is applied to it, the strut length, $\overline{OC}$[mm], was limited to an upper bound, L_{max}[mm]. However, this limit was considered as a design parameter to examine how its variation affects the solution. This bound constraint is given by:

$$\overline{OC} < L_{max} \tag{4.15}$$

5. The cable angle, θ_c[rad], was bounded by zero on the lower bound. A negative angle means that the cable end attached to the strut tip is pulled downward, therefore, the resulting torque will not help the biological plantar flexion torque in lifting the body during push-off. An upper bound for the angle is also necessary to limit the shear forces between the brace attachments and the skin. Those forces increase as the angle increases and could cause user discomfort and brace slippage over the shank. When the cable is horizontal, all the force is applied to the shank at the normal direction. This bound constraint can be expressed as:

$$0 < \theta_c < \theta_{max} \tag{4.16}$$

Consequently, the optimization problem can be written in the negative null form as follows:

$$\min_{x} -f(x, p) =$$

$$= -\sqrt{(\overline{OC}\cos(\theta_s + \theta_a) - x_A)^2 + (\overline{OC}\sin(\theta_s + \theta_a) - y_A)^2} \sin\left(\theta_c + \theta_s + \theta_a\right)$$

$$+ \arccos\left(\frac{\cos(\theta_s + \theta_a)(\overline{OC}\cos(\theta_s + \theta_a) - x_A) + \sin(\theta_s + \theta_a)(\overline{OC}\sin(\theta_s + \theta_a) - y_A)}{\sqrt{(\overline{OC}\cos(\theta_s + \theta_a) - x_A)^2 + (\overline{OC}\sin(\theta_s + \theta_a) - y_A)^2}}\right)\right)$$

subject to:

$$g_1(x, p) = \overline{OC}\cos(\theta_s) - \overline{OB} - D_{1max} < 0$$

$$g_2(x, p) = D_{2min} - \overline{OC}\cos(0.26 + \theta_s) + \sqrt{(x_A^2 + y_A^2)}\cos\left(0.26 + \operatorname{atan}\left(\frac{y_A}{x_A}\right)\right) < 0$$

$$g_3(x, p) = \overline{OC}\sin(\theta_s) + (\overline{OC}\cos(\theta_s) - x_P)\tan(\theta_c) - H_{max} < 0$$

$$\overline{OC} < L_{max}$$

$$0 < \theta_c < \theta_{max}$$

where:

$$x = [\overline{OC}, \theta_s, \theta_c]^T$$

$$p = [D_{1max}, D_{2min}, H_{max}, L_{max}, \theta_{max}, \theta_a, x_A, y_A, x_P, \overline{OB}]^T$$

Results of the geometrical layout optimization

The parameters $(x_A, y_A, x_P, \overline{OB})$ were measured for a typically developed adult wearing the boot on which the struts were attached. Table 4-4 shows the numerical values for the previously mentioned parameters and the chosen values for the other design parameter.

The *fmincon* Matlab function (Mathworks, Natrick, MA, US) was used to solve the optimization problem using the sequential quadratic polynomial algorithm. The obtained results are shown in table 4-5.

Given these values, the maximum obtained lever arm is:

$$\overline{AD} = 179.5 \ mm$$

Table 4-4: Numerical values for parameters

Parameter	Value	Unit
D_{1max}	30	[mm]
D_{2min}	0	[mm]
H_{max}	300	[mm]
L_{max}	330	[mm]
θ_{max}	0.52	[rad]
θ_a	0	[rad]
x_A	130	[mm]
y_A	105	[mm]
x_P	70	[mm]
$\overline{OB}$	195	[mm]

Table 4-5: Obtained results

Variable	Optimal value	Unit
$\overline{OC}$	330	[mm]
θ_s	1.0	[rad]
θ_c	0.2	[rad]

The results show that the second, third and fourth constraints are active. Therefore, a variation in the limit values of these constraints will change the solution, as can be seen in Figure 4-5, which presents isocontours of the objective function and the constraints.
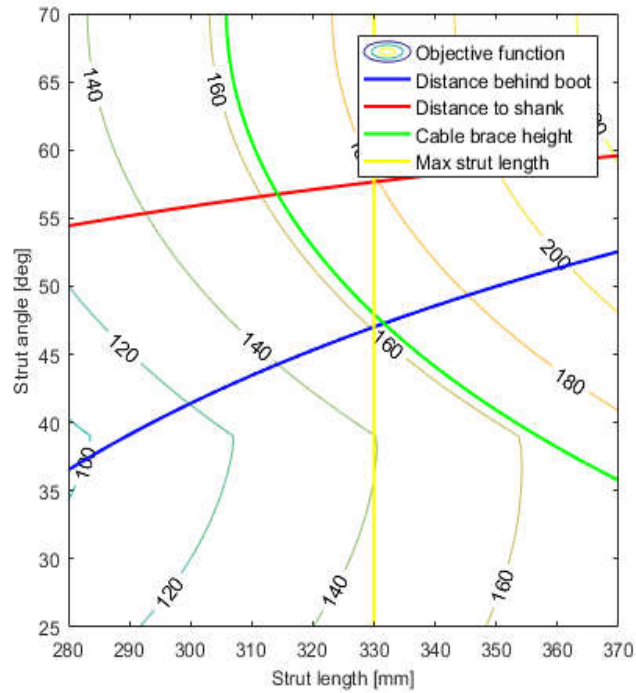
Figure 4-4: Objective function and isocontours of the constraints. The constraints "distance to shank" (red), "cable brace height" (green) and "Max. strut length" (yellow) are active. Changing those constraints will change the solution

The graph presented in figure 4-6 shows how the solution varies when the maximum strut length parameter, L_{max}[mm], is varied. Up to a certain limit, the lever arm length increases linearly with the increase in L_{max}[mm], such that an increase of 1 mm in L_{max}[mm] results in an increase of 1.06 mm in the length of the lever arm. However, because of other constraints, in particular, the maximum height of the cable routing brace, H_{max}[mm], after a certain value of L_{max}[mm] the resulting length of the lever arm remains constant. Specifically, when L_{max}[mm] is above 350 mm, the solution remains near 185 mm.

The H_{max}[mm] parameter exhibits the same general behavior as L_{max}[mm] (see figure 4-7), except that the relationship between the increase in lever arm length and the increase in H_{max}[mm] is nonlinear. Interestingly, this relationship is of particular interest given that H_{max}[mm] can be increased for taller people who might need higher push-off torque.

The obtained results presented in the table 4-5 were used in our design. The obtained lever arm length was sufficient to deliver the required augmentation torque. In fact, to deliver a supportive plantar flexion torque, T[Nm], of 50 Nm, the force, F[N], that needs to be transmitted by the two cables is:

$$F = \frac{T}{AD} = \frac{50}{0.1795} = 278.5 \ N$$

This force is still lower than the 360 N maximum force that the gearbox shaft can support.
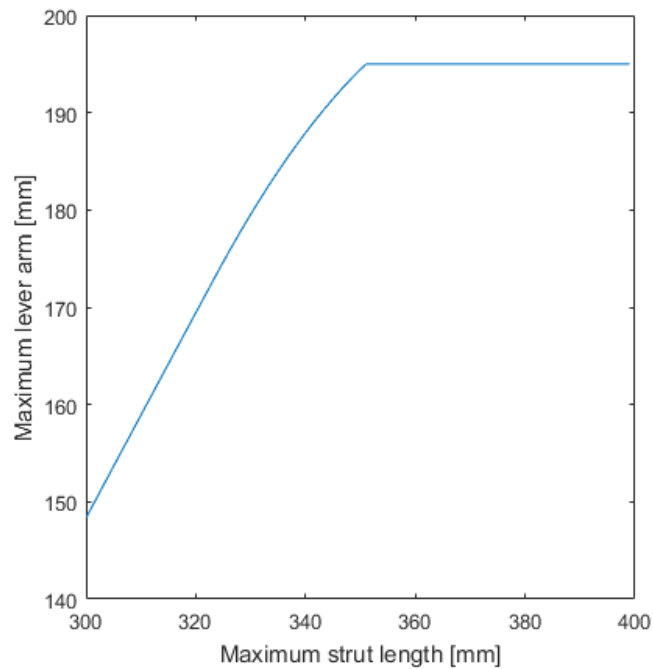
Figure 4-5: Effect of the maximum strut length parameter on the maximum lever arm. In this case, the maximum strut length varied, while the maximum height is fixed at 300 mm
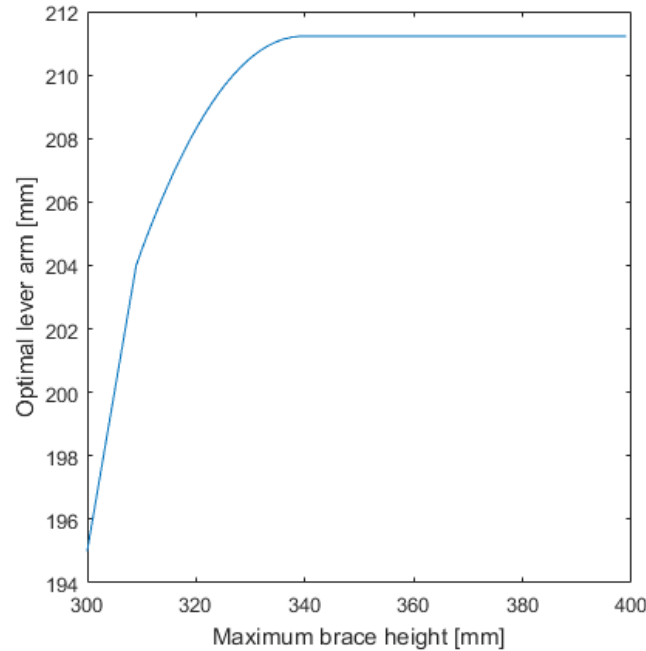
Figure 4-6: Effect of the maximum brace height parameter on the maximum lever arm. In this case, the maximum brace height parameter is varied, while the strut length is fixed to 360 mm in this case

4.3.4.2 Struts Mass Optimization

To ensure a minimal added distal mass, the minimization of the mass of the struts assembly, which is attached to the foot, is necessary. On the other hand, the struts are the only physical interface between the exoskeleton and the user, therefore, their structure must withstand the different loads applied to it.

Design variables and constraints

The selected design variables for this study are: the struts width, w[mm] varying from 10 to 20 mm and the struts thickness, t[mm], varying from 1 to 3 mm (see figure 4-8 A). The chosen material for the struts was the standard carbon fiber as it has high strength and low mass density.

The only constraint set for the mass optimization is the factor of safety that must be greater than 1.5. The factor of safety here is defined as the proportion between the tensile strength of the considered material and the maximum Von-Mises stress resulting from the finite element analysis.

Finite element model

The Finite element analysis tool of Solidworks software (Dassault Systèmes, France) was used to calculate the Von-Mises stress for each combination of the design variables. Figure 4-8 B shows the load and the constraints applied to the struts. A 200N force was applied to the strut tip (point *C*) at an angle of 11° with the horizontal. The two struts were considered rigidly connected and fixed at points *O* and *F*. This configuration is conservative, since in reality, the struts structure can move with the foot under a given load.
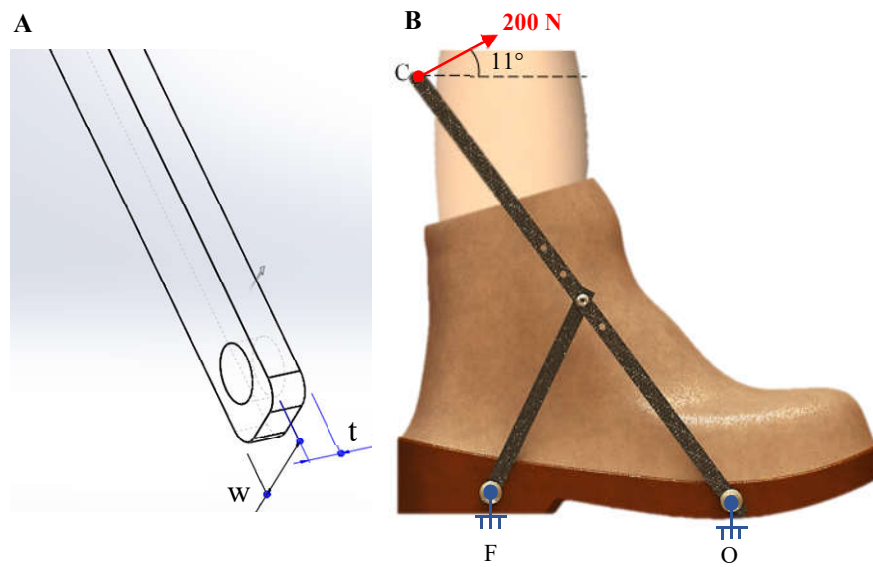
Figure 4-7: (A) The design variables for the mass optimization problem were the thickness, t[mm] and the width, w[mm] of the struts (B) The struts were fixed on the points O and F. A force of 200 N was applied at the point C at an 11° angle with the horizontal

Mass optimization results

The minimization problem was solved using the simulation module of Solidworks. The obtained solution corresponds to 3-mm thick and 10-mm wide struts. The proportion between the width and the thickness of the struts allows to reduce deflection on the direction of the cable pulling force.

4.4 Control System and Electronics

The control system monitors the gait cycle of the user and applies the augmentation torque during ankle plantar flexion on terminal stance. A hierarchic control architecture, composed of a high-level and a low-level controller was used. The high-level controller estimates the gait cycle percentage by dividing the time passed in each cycle by the average walking period measured over 10 cycles. Since the controller assumes that the subject moves at a constant speed (treadmill), 10 cycles are normally enough to estimate the average gait period.

The beginning of each cycle, characterized by a heel strike, was determined by reading the signal of the force sensitive resistor (FSR) (KIT_SENPACK_COM_FSR, Smart Bes, Guangdong, China) inserted under the insole at the heel area. The FSR was used instead of other gait monitoring means, such as inertial measurement units, because the FSR is simple to implement and does not require filtering of the signal, which could introduce some computational delays. At 43% of the gait cycle, a predefined parabolic torque profile was applied. This actuation onset timing was shown to be optimal for reducing the metabolic cost of walking [36].

Figure 4-9 shows a diagram of the electronics and control system. The microcontroller, mbed LPC1768 (NXP Semiconductors, Eindhoven, Netherlands), reads the FSR signal to detect heel strikes and measure the stride period as well as the gait cycle percentage. At the actuation onset timing, the microcontroller communicates to the PC, running a C#.NET program, to transmit the desired current profile to the motor driver. The motor driver, EPOS2 70/10 (Maxon Motor, Sachseln, Switzerland), reads the signal of the encoder (Maxon Motor, Sachseln, Switzerland) and current sensor to apply the torque profile using a PID control loop running at a frequency of 1kHz. The PID parameters were tuned using the EPOS software.

A simple graphical user interface was developed under Visual Studio C#.NET. The interface that was running on the PC allows to turn the exoskeleton on and off and select from different torque profiles. In addition, it gives a visual feedback about the stride duration. The software also allows to select either a manual or an autonomous mode. In the manual mode, the torque profiles could be tested offline. The interface will be used for the tests.
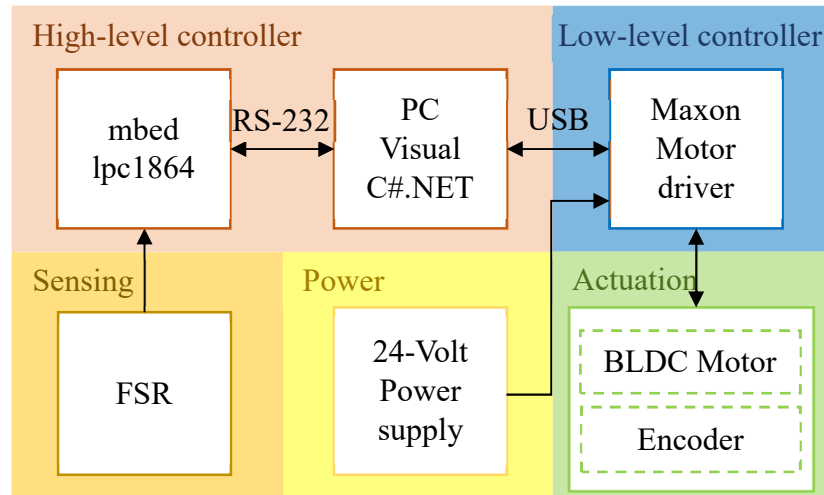
Figure 4-8: Control system architecture. The control system includes an FSR sensor that detects the heel strike. An mbed lpc1864 microcontroller calculates the average gait cycle period, then sends a signal to the PC software at the actuation timing. The PC software sends the desired torque value to the motor driver which uses feedback from the motor encoder and current sensor to regulate the torque using a PID controller

4.5 Experimental Tests

The exoskeleton performance was evaluated by determining the mechanical efficiency of the actuation system as well as the effect of walking with the exoskeleton on muscle activation of a typically developed user.

While performing these tests, the safety of the device and the user were insured by a set of hardware and software measures. For the software, the applied torque was limited by selecting a torque profile with a maximum value lower than 50 Nm. In addition, at any moment, the device can be stopped immediately by pressing a stop button in the graphical user interface.

For the hardware safety measures, mechanical stops were added to the spool and the spool cover to limit the travel distance of the cables.

4.5.1 Mechanical Efficiency

The augmentation torque and power delivered by the actuator on the ankle joint could be measured directly using an inline load cell. However, due to the constrained space between the tips of the struts, where the cable is attached (point C in figure 4-4), and the cable routing brace (point P in figure 4-4), it was preferred to estimate the power on the ankle joint using the transmission efficiency and the measured mechanical power at the motor level. The efficiency of the transmission system (gearbox, spool and cables) was determined experimentally. The mechanical power of the motor was calculated using the velocity and current data obtained from the motor driver. The force applied on the struts was measured by an inline load cell (LFT-13B, Shenzhen Ligent Sensor Tech Co., Ltd, China). The cable velocity was estimated from the motor velocity, the gearbox reduction ratio, and the spool diameter.

A sinusoidal position reference signal of 0.5Hz frequency and 90° amplitude was applied by the motor while the cables were attached to a hanging mass of 2.8 kg. The obtained efficiency was 0.59 ± 0.01 (mean $\pm$ standard deviation).

4.5.2 Human Walking Trials

4.5.2.1 Subject characteristics

The effect of the exoskeleton on the user muscle activity was tested on a healthy typically developed male subject (60 Kg weight, 160 cm height) with no history gait disorders while walking on a treadmill at a speed of 1.2 m/s. This evaluation study was approved by the Research Ethics Board of Centre Hospitalier de Sainte-Justine.

4.5.2.2 Protocol

Three different walking scenarios were experimented: unloaded walking, loaded walking where the subject wore an 11-kg backpack, and inclined loaded walking where the treadmill was inclined by 5 degrees to simulate walking on a slope. The mass of 11 kg was chosen to simulate the mass of the air bottles that firefighters hold on their backs as in [2] for reference purposes.

In each scenario, two conditions were considered: walking without the exoskeleton (NO EXO) and walking with the exoskeleton powered on (EXO ON). The subject walked without the exoskeleton for 5 minutes then rested for 3 minutes before walking with the exoskeleton powered on for 7

minutes. The first 5 minutes of the EXO ON condition were considered as an adaptation phase, the data were recorded on the remaining 2 minutes of walking.

Different human walking tests were performed to evaluate the performance of the exoskeleton and how its control parameters affect its performance. During all these tests, the assistive torque applied by WAXO on the subject ankle joint was a parabolic profile, and only the maximum torque magnitude, actuation duration and onset were changed to examine their effect on muscle activity. The maximum value of the torque profile is attained at the half of the actuation duration. The different tests performed are summarized in table 4-6.

Table 4-6: Human walking trials performed for the exoskeleton evaluation

Trial	Scenario	Maximum torque applied by WAXO on the ankle joint (Nm)	Duration (ms)	Onset (%)
T_1	Unloaded walking	14	150	43
T_2	Unloaded walking	14	200	43
T_3	Unloaded walking	14	200	40
T_4	Unloaded walking	14	200	38
T_5	Unloaded walking	11	200	38
T_6	Unloaded walking	11	200	43
T_7	Loaded walking	14	150	43
T_8	Inclined Loaded walking	14	150	43

4.5.2.3 Data Recording

The EMG signals of the soleus and gastrocnemius (lateralis) muscles were recorded using wireless surface EMG FreeEMG300 system (BTS, Milan, Italy). These muscles were selected because they are directly involved in generating the ankle plantar flexion torque. Self-adhesive pairs of disposable Ag/AgCl surface electrodes with a 10 mm recording diameter (Covidien, Mansfield, MA, USA) were placed following the SENIAM (Surface Electromyography for Non-Invasive Assessment of Muscles) guidelines [37]. The recorded EMG signals were band-pass filtered (10-450 Hz, zero-lag 4th order), full-wave rectified, and smoothed with a low-pass filter (3 Hz, Butterworth zero-lag 2nd order).

Although oxygen consumption was not measured to determine the metabolic cost of walking, it is still accepted that muscle activity induces a large consumption of metabolic energy [13, 38]. Therefore, a significant reduction of muscle activity is an indication of the potential of WAXO to reduce the walking metabolic cost.

The current and the velocity of the motor were recorded using the motor sensors and driver. The recorded data were used to calculate the positive mechanical power delivered by the exoskeleton during walking trials on the EXO ON condition.

4.6 Results and Discussion

4.6.1 Exoskeleton Mass

The total mass of WAXO is 2,045 g. The mass of each component of WAXO is shown in table 4-7. The mass of the parts attached to the waist area accounts for 1050 g for the actuation unit and 647 g for the electronics and motor driver. The distal mass is therefore only 348 g, of which 290 g were on the shin (cable routing brace) and 58 g on the foot (struts assembly and bolts used to fix the struts to the boot). This lightweight structure made the exoskeleton almost transparent to the user and did not restrict any natural degrees of freedom.

Table 4-7: WAXO parts mass

Component	Location	Mass (g)
Actuation Unit	Waist	1050
Electronics box	Waist	647
Cable routing brace	Shin	290
Struts (including bolts)	Foot	58
Total mass (g)		2045

The 348 g of distal mass added by WAXO is 67% lower than the current minimum distal mass added by a powered ankle exoskeleton in the literature [32]. Still, WAXO can provide large mechanical power during powered plantar flexion. In addition, the maximum torque that can be delivered by WAXO is only limited by the maximum axial load of the gearbox shaft. When the motor generates a pulling force of 300 N on the pulley (lower than the 360 N limit of the gearbox

shaft), the torque resulting on the ankle will be 54 Nm as the length of the artificial lever arm is 18 cm. Instead of mounting the pulley directly on the motor shaft, a coupling can be used to connect the two elements, in this manner, the motor can provide large torque while keeping the shaft safe from any damage. This solution was avoided in WAXO design in order to reduce the mass of the actuation unit.

The priority of minimizing the exoskeleton weight is important because it reduces the effort required by the user to move with the device attached to his body, and thus, the power benefit of the exoskeleton is more significant in this case compared to a heavier exoskeleton that provides the same mechanical power. However, in the current design of WAXO, the actuation unit was located on the waist and cables were used to transmit the force. The cables reduce the efficiency of the actuation system and thus, WAXO will draw more electrical energy compared to another exoskeleton with a more efficient transmission system. Still, we adopted this design because increasing the exoskeleton power benefit to the user and reducing its weight are objectives of higher priority in the current state of research in walking augmentation exoskeletons. Additionally, more efficient transmission cables could be used to increase the efficiency of the transmission system.

4.6.2 Human Walking Trials

During the powered plantar flexion phase, the exoskeleton added to the subject ankle joint positive mechanical power of 18 ± 3 W, 19 ± 2 W and 26 ± 5 W during trials T_5 and T_6, T_1 T_7 and T_8, T_2 T_3 and T_4, respectively (see figure 4-10). Figures 4-11 to 4-18 show the results of muscle activity obtained from each trial in both conditions, NO EXO and EXO ON. The activity of the gastrocnemius and soleus muscles was reduced on the EXO ON condition compared to the NO EXO condition in all the trials, with the exception of trials T_7 and T_8 where the gastrocnemius muscle activity increased by 5% and 8% respectively (figures 4-17 and 4-18 respectively), and trial T_1 where the gastrocnemius muscle activity remained nearly unchanged (figure 4-11). The largest reduction of the gastrocnemius muscle activity was 44% and was observed on trial T_4 where the actuation onset was at 38% of the gait cycle with an actuation duration of 200 ms, during which the exoskeleton added 19 ± 2 W of positive mechanical power. The largest reduction in the soleus muscle activity occurred in trial T_4 as well, with a value of 37%. This reduction of muscle activity gives indication of the potential of WAXO in reducing the metabolic cost of walking. For instance,

in the study done by Collins et al. [13], while the exoskeleton reduced the metabolic energy by 7.2 ± 2.6%, the soleus muscle activity during mid-stance was reduced by only 22%.

The effect of the actuation onset on muscle activity can be examined by separately comparing the results of the two trial groups $\{T_2,T_3,T_4\}$ (figures 4-12, 4-13, 4-14) and $\{T_5,T_6\}$ (figures 4-15, 4-16). The mechanical power provided by the exoskeleton was the same (see figure 4-10) for each of the two groups. We found that the reduction in soleus and gastrocnemius activity was significantly larger in the 38% onset condition compared to the 40% and 43% conditions. This could be interpreted by the fact that these muscles are naturally activated early in the gait cycle. Malcolm et al. [17] found that the actuation onset condition of 43% resulted in the largest reduction in metabolic energy. This highlights the need for a study where the implication of the actuation onset condition is examined simultaneously on the metabolic energy consumption and muscle activity; such a study could help in understanding the interaction between the exoskeleton assistive strategy and the metabolic energy consumption on the one hand, and between the metabolic energy and muscle activity during walking on the other hand.

Changing the actuation duration from 150 ms in trial T_1 to 200 ms in trial T_2 decreased the soleus activity reduction between the NO EXO and EXO ON conditions from 17% in trial T_1 to 6% in trial T_2. The powered plantar flexion occurs at 43% of the gait cycle (actuation onset of trials T_1 and T_2) [14], thus since the powered plantar flexion is characterized by a burst of mechanical power that happens in a short time, the 150 ms duration condition was in this case more convenient. The 200 ms duration pushes the actuation torque maximum value forward on the gait cycle compared to the 150 ms duration. This seems to have caused a mismatch between the torque applied by the exoskeleton and the torque of natural ankle plantar flexion.

The effect of the exoskeleton mechanical power and maximum applied exoskeleton torque can be assessed by comparing the results of the trials group $\{T_2,T_6\}$ (figures 4-12,4-16) and $\{T_4,T_5\}$ (figures 4-14, 4-15). As predicted, the muscle activity reduction in trial T_4 was higher than in trial T_5 as the mechanical power generated by the exoskeleton was higher in the former. The soleus activity reduction improved from 6% in trial T_5 to 37% in trial T_4. Results of trials T_2 and T_6 revealed a different trend. The electrical activity reduction of both gastrocnemius and soleus muscles was lower in trial T_2 even though the maximum torque applied by the exoskeleton was higher compared to trial T_6. This difference in the trend of the results between the two trial groups

could be attributed to the actuation onset. In the trials $\{T_2, T_6\}$, the actuation onset was 43%, as discussed earlier, and this actuation onset was less appropriate in our case than the 38% onset; therefore, increasing the torque increases the effect of the disagreement between the exoskeleton torque and natural torque. In addition, even though the mechanical power provided by the exoskeleton was nearly the same in trials T_1 and T_5 (figure 4-10), the reduction of gastrocnemius activity was significantly higher in trial T_5. This emphasizes the importance of finding an optimal combination of actuation onset and amplitude to increase the exoskeleton efficiency and the power benefit it brings to the user.

WAXO did not reduce the activity of the muscles studied in the case of loaded walking (trial T_7, figure 4-17) probably because in this case the muscles produce more work and the torque supplied by the exoskeleton was not sufficient. The same result was observed for inclined loaded walking (T_8, figure 4-18) and this could be attributed to the fact that during inclined walking the kinetics of the joint changes compared to ground level walking [39]. Therefore, the assistive strategy needs to be adapted for inclined walking in terms of control.

The focus of our design was to develop an exoskeleton with minimum distal mass capable of adding mechanical positive power to the ankle joint during the powered plantar flexion phase. While this objective was achieved, there are still some limitations that need to be addressed. In terms of design, the exoskeleton control system used a simple method to monitor gait phases based on detecting the heel strike using a single FSR. In this way, the computational time was reduced, however, the gait detection system becomes not as robust since it is dependent on only one sensor. In future work, other sensors [40] can be incorporated and multi sensor fusion techniques can be used [41]. These techniques can be combined with more advanced methods for torque control [42, 43]. The power density of WAXO can be increased by adding positive mechanical power on the opposite leg. One advantage of our actuation system design is that the same motor used in our current exoskeleton could be used to actuate the second ankle joint without adding another motor. This approach was already demonstrated by Walsh et al. in their exosuit [44]. Our design assumptions were mainly based on the results from the literature, however, modeling [45, 46] and multi-criteria optimization methods [47-49] can be combined to better predict and optimize the exoskeleton performance and interaction with the user. In future work, an extensive evaluation study for WAXO will be performed with a larger group of subjects. This evaluation will include measurement of oxygen consumption to estimate the metabolic expenditure as well as kinematic measurements to compare

the gait of the subjects when walking with and without WAXO. As for now, this is one of the limitations of our work.

Finally, the minimalist design approach we applied here will be extended to other exoskeleton applications targeted to different populations such as those suffering from musculoskeletal diseases and muscular dystrophies [50-52].
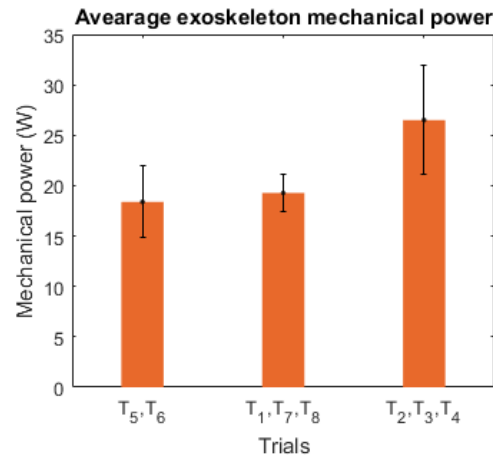
Figure 4-9: Average mechanical power applied by the exoskeleton. WAXO applied 18 ± 3 W, 19 ± 2 W and 26 ± 5 W during trials $\{T_5, T_6\}$, $\{T_1, T_7, T_8\}$ and $\{T_2, T_3, T_4\}$ respectively
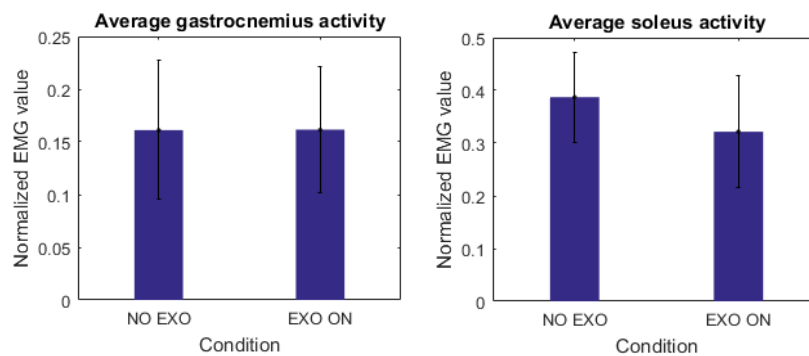
Figure 4-10: Results of trial T_1. The activity of the gastrocnemius muscle remained nearly unchanged in the two conditions, the activity of the soleus muscle was reduced by 17% on the EXO ON condition compared to the NO EXO condition
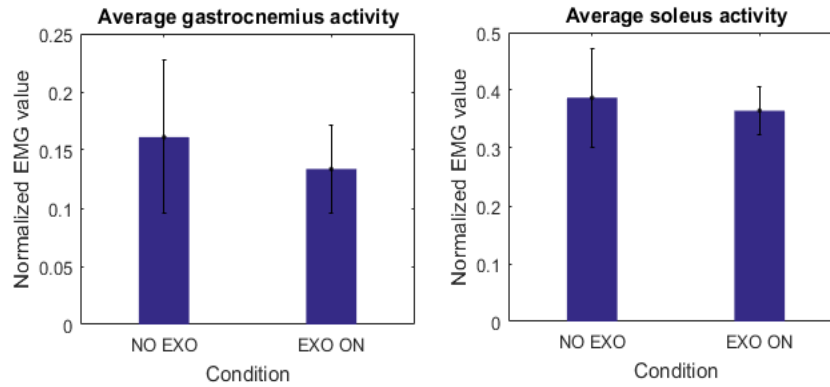
Figure 4-11: Results of trial T_2. The activity of the gastrocnemius and soleus muscles was reduced by 17% and 6% respectively on the EXO ON condition compared to the NO EXO condition
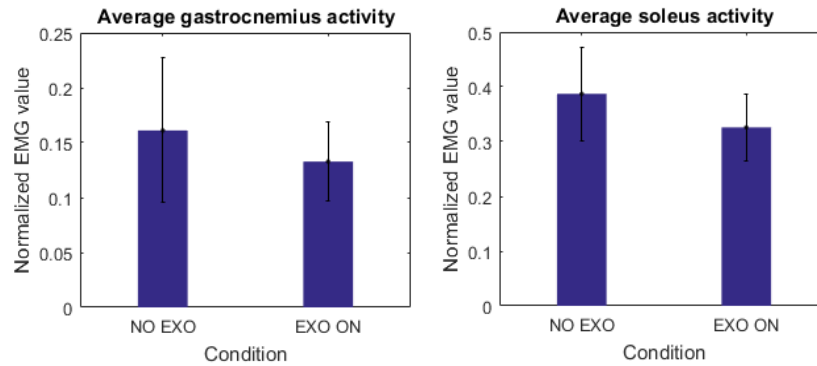
Figure 4-12: Results of trial T_3. The activity of the gastrocnemius and soleus muscles was reduced by 18% and 16% respectively on the EXO ON condition compared to the NO EXO condition
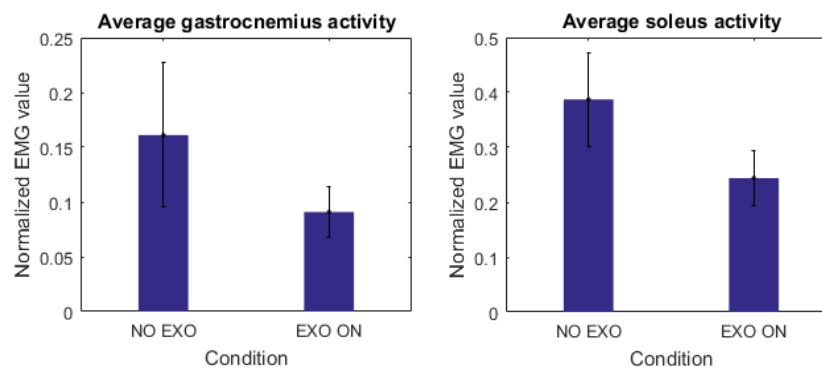
Figure 4-13: Results of trial T_4. The activity of the gastrocnemius and soleus muscles was reduced by 44% and 37% respectively on the EXO ON condition compared to the NO EXO condition
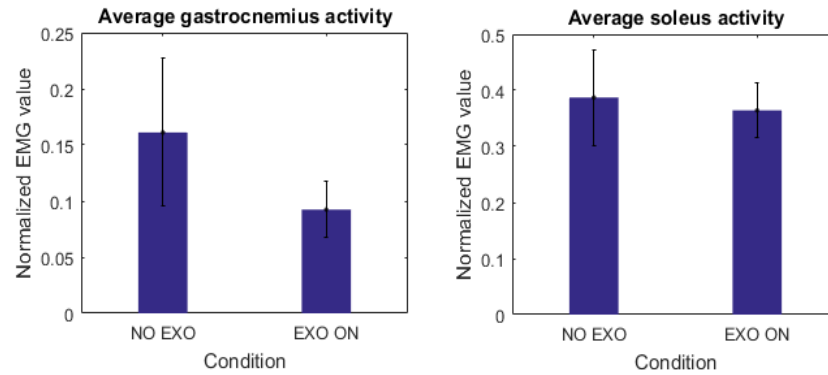
Figure 4-14: Results of trial T_5. The activity of the gastrocnemius and soleus muscles was reduced by 43% and 6% respectively on the EXO ON condition compared to the NO EXO condition
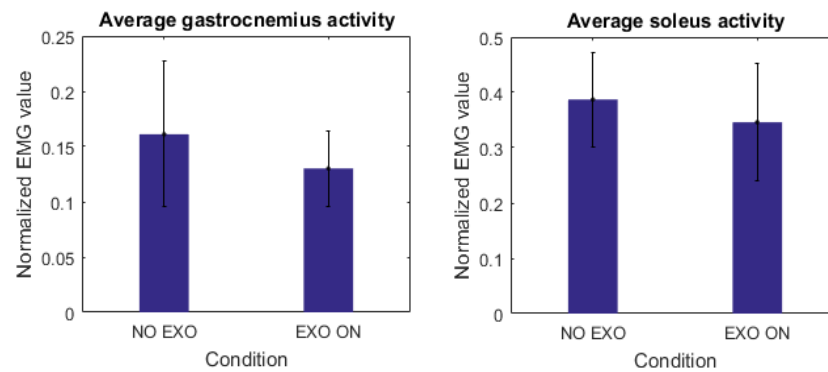
Figure 4-15: Results of trial T_6. The activity of the gastrocnemius and soleus muscles was reduced by 19% and 11% respectively on the EXO ON condition compared to the NO EXO condition
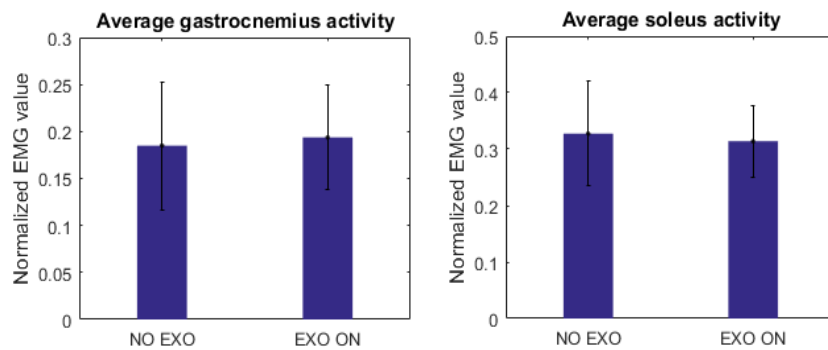
Figure 4-16: Results of trial T_7. The activity of the gastrocnemius muscle increased by 5% and the activity of the soleus muscle decreased by 4% on the EXO ON condition compared to the NO EXO condition
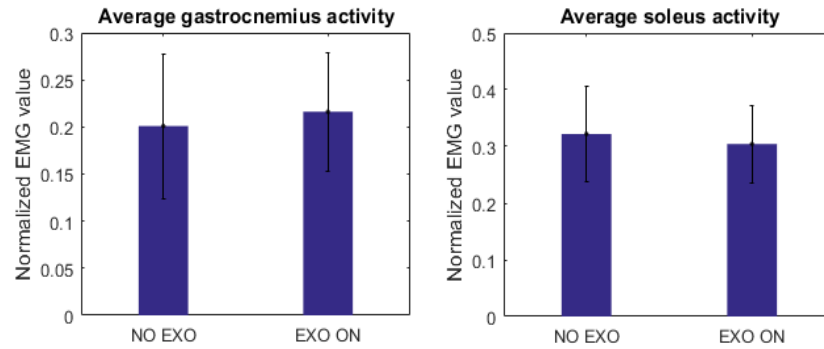
Figure 4-17: Results of trial T_8. The activity of the gastrocnemius increased by 8% and the activity of the soleus muscle decreased by 5% on the EXO ON condition compared to the NO EXO condition

4.7 Conclusion

The objective of this study was to develop an ankle exoskeleton with a minimum added distal mass compared to existing autonomous powered ankle exoskeletons, while providing at least 50 Nm of assistive plantar flexion torque. The optimized design reduced the minimal distal mass to 348 g. This value is the lowest one compared to existing motorized ankle exoskeletons. This shows that it is possible to design powerful exoskeletons with minimal weight, which becomes a feature that should be considered amongst the criteria when designing augmentation exoskeletons.

Tests with a typically developed human subject showed that the gastrocnemius muscle activity was reduced by 44% when walking with the exoskeleton compared to normal walking. This result shows that the proposed exoskeleton has a potential in reducing the energy spent during human walking. The perspective of this work is to develop a bilateral exoskeleton that supports both joints of the ankle using the same design approach will be developed. Additionally, tests on a larger sample of subjects could be performed to examine the effect of this exoskeleton on the metabolic cost during walking.

References

[1]   M. D. Beekley, J. Alt, C. M. Buckley, M. Duffey, and T. A. Crowder, "Effects of heavy load carriage during constant-speed, simulated, road marching," *Military medicine,* vol. 172, pp. 592-595, 2007.

[2]   K. Park, P. Hur, K. S. Rosengren, G. P. Horn, and E. T. Hsiao-Wecksler, "Effect of load carriage on gait due to firefighting air bottle configuration," *Ergonomics,* vol. 53, pp. 882-891, 2010.

[3]   A. M. Dollar and H. Herr, "Lower extremity exoskeletons and active orthoses: challenges and state-of-the-art," *IEEE Transactions on robotics,* vol. 24, pp. 144-158, 2008.

[4]   A. J. Young and D. P. Ferris, "State of the Art and Future Directions for Lower Limb Robotic Exoskeletons," *IEEE Transactions on Neural Systems and Rehabilitation Engineering,* vol. 25, pp. 171-182, 2017.

[5]   A. Chu, H. Kazerooni, and A. Zoss, "On the biomimetic design of the berkeley lower extremity exoskeleton (BLEEX)," in *Robotics and Automation, 2005. ICRA 2005. Proceedings of the 2005 IEEE International Conference on*, 2005, pp. 4345-4352.

[6]   H. Cao, J. Zhu, C. Xia, H. Zhou, X. Chen, and Y. Wang, "Design and Control of a Hydraulic-Actuated Leg Exoskeleton for Load-Carrying Augmentation," in *Intelligent Robotics and Applications: Third International Conference, ICIRA 2010, Shanghai, China, November 10-12, 2010. Proceedings, Part I*, H. Liu, H. Ding, Z. Xiong, and X. Zhu, Eds., ed Berlin, Heidelberg: Springer Berlin Heidelberg, 2010, pp. 590-599.

[7]   S. Marcheschi, F. Salsedo, M. Fontana, and M. Bergamasco, "Body extender: whole body exoskeleton for human power augmentation," in *Robotics and Automation (ICRA), 2011 IEEE International Conference on*, 2011, pp. 611-616.

[8]   S. Yu, H. Lee, S. Lee, W. Kim, J. Han, and C.-S. Han, "Design of an under-actuated exoskeleton system for walking assist while load carrying," *Advanced Robotics,* vol. 26, pp. 561-580, 2012.

[9]   C. J. Walsh, K. Endo, and H. Herr, "A quasi-passive leg exoskeleton for load-carrying augmentation," *International Journal of Humanoid Robotics,* vol. 4, pp. 487-506, 2007.

[10]   K. Seo, J. Lee, Y. Lee, T. Ha, and Y. Shim, "Fully autonomous hip exoskeleton saves metabolic cost of walking," in *Robotics and Automation (ICRA), 2016 IEEE International Conference on*, 2016, pp. 4628-4635.

[11]   Y. Kusuda, "In quest of mobility–Honda to develop walking assist devices," *Industrial Robot: An International Journal,* vol. 36, pp. 537-539, 2009.

[12]   W. van Dijk, C. Meijneke, and H. van der Kooij, "Evaluation of the Achilles Ankle exoskeleton," *IEEE Transactions on Neural Systems and Rehabilitation Engineering,* 2016.

[13]   S. H. Collins, M. B. Wiggin, and G. S. Sawicki, "Reducing the energy cost of human walking using an unpowered exoskeleton," *Nature,* vol. 522, pp. 212-215, 2015.

[14]   L. M. Mooney, E. J. Rouse, and H. M. Herr, "Autonomous exoskeleton reduces metabolic cost of human walking during load carriage," *Journal of neuroengineering and rehabilitation,* vol. 11, p. 80, 2014.

[15]   D. P. Ferris, G. S. Sawicki, and M. A. Daley, "A physiologist's perspective on robotic exoskeletons for human locomotion," *International Journal of Humanoid Robotics,* vol. 4, pp. 507-528, 2007.

[16]   L. M. Mooney and H. M. Herr, "Biomechanical walking mechanisms underlying the metabolic reduction caused by an autonomous exoskeleton," *Journal of neuroengineering and rehabilitation,* vol. 13, p. 4, 2016.

[17]   P. Malcolm, W. Derave, S. Galle, and D. De Clercq, "A simple exoskeleton that assists plantarflexion can reduce the metabolic cost of human walking," *PloS one,* vol. 8, p. e56137, 2013.

[18]   D. Winter, *Biomechanics and motor control of human gait: normal, elderly and pathological*. Waterloo: Waterloo Biomechanics, 1991.

[19]   M. B. Wiggin, G. S. Sawicki, and S. H. Collins, "An exoskeleton using controlled energy storage and release to aid ankle propulsion," in *Rehabilitation Robotics (ICORR), 2011 IEEE International Conference on*, 2011, pp. 1-5.

[20] Y.-L. Park, B.-r. Chen, D. Young, L. Stirling, R. J. Wood, E. Goldfield, *et al.*, "Bio-inspired active soft orthotic device for ankle foot pathologies," in *Intelligent Robots and Systems (IROS), 2011 IEEE/RSJ International Conference on*, 2011, pp. 4488-4495.

[21] K. E. Gordon, G. S. Sawicki, and D. P. Ferris, "Mechanical performance of artificial pneumatic muscles to power an ankle–foot orthosis," *Journal of biomechanics,* vol. 39, pp. 1832-1841, 2006.

[22] G. S. Sawicki and D. P. Ferris, "A pneumatically powered knee-ankle-foot orthosis (KAFO) with myoelectric activation and inhibition," *Journal of neuroengineering and rehabilitation,* vol. 6, p. 23, 2009.

[23] D. P. Ferris, J. M. Czerniecki, and B. Hannaford, "An ankle-foot orthosis powered by artificial pneumatic muscles," *Journal of applied biomechanics,* vol. 21, pp. 189-197, 2005.

[24] A. J. Veale and S. Q. Xie, "Towards compliant and wearable robotic orthoses: A review of current and emerging actuator technologies," *Medical engineering & physics,* vol. 38, pp. 317-325, 2016.

[25] C. Meijneke, W. van Dijk, and H. van der Kooij, "Achilles: an autonomous lightweight ankle exoskeleton to provide push-off power," in *Biomedical Robotics and Biomechatronics (2014 5th IEEE RAS & EMBS International Conference on*, 2014, pp. 918-923.

[26] A. T. Asbeck, R. J. Dyer, A. F. Larusson, and C. J. Walsh, "Biologically-inspired soft exosuit," in *Rehabilitation robotics (ICORR), 2013 IEEE international conference on*, 2013, pp. 1-8.

[27] A. T. Asbeck, S. M. De Rossi, K. G. Holt, and C. J. Walsh, "A biologically inspired soft exosuit for walking assistance," *The International Journal of Robotics Research,* vol. 34, pp. 744-762, 2015.

[28] A. T. Asbeck, S. M. De Rossi, I. Galiana, Y. Ding, and C. J. Walsh, "Stronger, smarter, softer: next-generation wearable robots," *IEEE Robotics & Automation Magazine,* vol. 21, pp. 22-33, 2014.

[29] F. A. Panizzolo, I. Galiana, A. T. Asbeck, C. Siviy, K. Schmidt, K. G. Holt*, et al.*, "A biologically-inspired multi-joint soft exosuit that can reduce the energy cost of loaded walking," *Journal of neuroengineering and rehabilitation,* vol. 13, p. 43, 2016.

[30] M. B. Yandell, D. Popov, B. T. Quinlivan, C. Walsh, K. O'Donnell, and K. E. Zelik, "Systematic evaluation of human-exosuit physical interfaces."

[31] M. B. Yandell, B. T. Quinlivan, D. Popov, C. Walsh, and K. E. Zelik, "Physical interface dynamics alter how robotic exosuits augment human movement: implications for optimizing wearable assistive devices," *Journal of NeuroEngineering and Rehabilitation,* vol. 14, p. 40, 2017.

[32] L. M. Mooney, E. J. Rouse, and H. M. Herr, "Autonomous exoskeleton reduces metabolic cost of human walking," *Journal of neuroengineering and rehabilitation,* vol. 11, p. 151, 2014.

[33] R. C. Browning, J. R. Modica, R. Kram, and A. Goswami, "The effects of adding mass to the legs on the energetics and biomechanics of walking," *Medicine and science in sports and exercise,* vol. 39, p. 515, 2007.

[34] G. Bovi, M. Rabuffetti, P. Mazzoleni, and M. Ferrarin, "A multiple-task gait analysis approach: kinematic, kinetic and EMG reference data for healthy young and adult subjects," *Gait & posture,* vol. 33, pp. 6-13, 2011.

[35] K. A. Witte, J. Zhang, R. W. Jackson, and S. H. Collins, "Design of two lightweight, high-bandwidth torque-controlled ankle exoskeletons," in *Robotics and Automation (ICRA), 2015 IEEE International Conference on*, 2015, pp. 1223-1228.

[36] S. Galle, P. Malcolm, S. H. Collins, and D. De Clercq, "Reducing the metabolic cost of walking with an ankle exoskeleton: interaction between actuation timing and power," *Journal of NeuroEngineering and Rehabilitation,* vol. 14, p. 35, 2017.

[37] H. J. Hermens, B. Freriks, R. Merletti, D. Stegeman, J. Blok, G. Rau*, et al.*, "European recommendations for surface electromyography," *Roessingh research and development,* vol. 8, pp. 13-54, 1999.

[38] O. M. Blake and J. M. Wakeling, "Estimating changes in metabolic power from EMG," *SpringerPlus,* vol. 2, p. 229, 2013.

[39]   A. S. McIntosh, K. T. Beatty, L. N. Dwan, and D. R. Vickers, "Gait dynamics on an inclined walkway," *Journal of biomechanics,* vol. 39, pp. 2491-2502, 2006.

[40]   C. Zizoua, M. Raison, S. Boukhenous, M. Attari, and S. Achiche, "Detecting muscle contractions using strain gauges," *Electronics Letters,* vol. 52, pp. 1836-1838, 2016.

[41]   A. Duivenvoorden, K. Lee, M. Raison, and S. Achiche, "Sensor fusion in upper limb area networks: A survey," in *Global Information Infrastructure and Networking Symposium (GIIS), 2017*, 2017, pp. 56-63.

[42]   P. Geoffroy, O. Bordron, N. Mansard, M. Raison, O. Stasse, and T. Bretl, "A two-stage suboptimal approximation for variable compliance and torque control," in *Control Conference (ECC), 2014 European*, 2014, pp. 1151-1157.

[43]   P. Geoffroy, N. Mansard, M. Raison, S. Achiche, and E. Todorov, "From inverse kinematics to optimal control," in *Advances in Robot Kinematics*, ed: Springer, 2014, pp. 409-418.

[44]   A. T. Asbeck, K. Schmidt, I. Galiana, D. Wagner, and C. J. Walsh, "Multi-joint soft exosuit for gait assistance," in *Robotics and Automation (ICRA), 2015 IEEE International Conference on*, 2015, pp. 6197-6204.

[45]   M. Raison, "On the quantification of joint and muscle efforts in the human body during motion," UCL-Université Catholique de Louvain, 2009.

[46]   S. Hernandez, M. Raison, L. Baron, and S. Achiche, "Refinement of exoskeleton design using multibody modeling: an overview," in *CCToMM Mechanisms, Machines, and Mechatronics Symposium*, 2015, p. 110.

[47]   M. Leroux, S. Achiche, D. Beaini, and M. Raison, "Design guidelines for shoulder design of an anthropomorphic robotic arm," in *DS 87-4 Proceedings of the 21st International Conference on Engineering Design (ICED 17) Vol 4: Design Methods and Tools, Vancouver, Canada, 21-25.08. 2017*, 2017.

[48]   A. Mohebbi, L. Baron, S. Achiche, and L. Birglen, "Trends in concurrent, multi-criteria and optimal design of mechatronic systems: A review," in *Innovative Design and Manufacturing (ICIDM), Proceedings of the 2014 International Conference on*, 2014, pp. 88-93.

[49]   A. Mohebbi, S. Achiche, and L. Baron, "Mechatronic multicriteria profile (MMP) for conceptual design of a robotic visual servoing system," in *ASME 2014 12th Biennial Conference on Engineering Systems Design and Analysis*, 2014, pp. V003T15A015-V003T15A015.

[50]   B. Samadi, S. Achiche, A. Parent, L. Ballaz, U. Chouinard, and M. Raison, "Custom sizing of lower limb exoskeleton actuators using gait dynamic modelling of children with cerebral palsy," *Computer methods in biomechanics and biomedical engineering,* vol. 19, pp. 1519-1524, 2016.

[51]   M. Yazji, M. Raison, C.-É. Aubin, H. Labelle, C. Detrembleur, P. Mahaudens*, et al.*, "Are the mediolateral joint forces in the lower limbs different between scoliotic and healthy subjects during gait?," *Scoliosis,* vol. 10, p. S3, 2015.

[52]   R. Hart, L. Ballaz, M. Robert, A. Pouliot, S. D'Arcy, M. Raison*, et al.*, "Impact of exercise-induced fatigue on the strength, postural control, and gait of children with a neuromuscular disease," *American Journal of Physical Medicine & Rehabilitation,* vol. 93, pp. 649-655, 2014.

CHAPTER 5   ADDITIONAL DETAILS ON METHODS AND RESULTS

The article presented in chapter 4 included important information related to the methodology and the results; however, due to page limits, some details were not presented in the article. In this chapter, we present additional details concerning the methodology. Specifically, this chapter starts by highlighting the main tasks accomplished in this project; then, additional details about the design and testing of the exoskeleton are presented.

5.1 Summary of the Accomplished Work

The main milestones accomplished during this project could be summarized in the following points. The numbering of these points does not necessarily refer to their chronological order because most of these tasks were accomplished with a concurrent design approach due to the complexity and interdependency of the exoskeleton subsystems.

1. **Literature review:** a detailed literature review was performed to examine the state of the art of research in wearable robots in general. A more focused review was done for human augmentation exoskeletons to identify their design specifications and challenges faced by researchers to improve the performance of these exoskeletons. The main conclusions from this review helped in defining the scope of this project.

2. **Concept development:** some design concepts were developed and sketched before selecting the best one for the detailed design. These concepts incorporated mechanisms that reduce the number of components of the exoskeleton and allow adding power to multiple biological joints using the same motor (underactuated systems).

3. **Gait detection system development:** one important layer of the control system for an exoskeleton is the gait detection system. This detection system allows monitoring the gait cycle of the user in real time. This way, the actuation onset can be fixed at a specific percent of the gait cycle.

4. **Motor control and control system integration:** the low-level layer of the control system consisted of a PID controller that applies the desired torque profile. The controller was implemented using the Maxon EPOS2 70/10 driver that comes with built-in functions allowing speed control as well as position and current control.

5. **Graphical user interface development:** a GUI was developed to facilitate the use and control of the exoskeleton. The GUI allows the user to execute different functions to operate the exoskeleton as well as facilitating debugging for the developer in case of errors.

6. **Motor selection and actuation unit design:** the actuation system components, including the motor, gearbox and pulley were selected based on torque and speed requirements of the ankle joint.

7. **Mechanical design optimization:** design optimization methods were applied on the struts geometry and mass to minimize their weight while increasing the lever arm they create to deliver a higher augmentation torque for a given force.

8. **Technical drawing:** the detailed CAD of the exoskeleton components were performed in SolidWorks as well as technical drawing for the parts that needed to be machined such as the struts and the actuation unit housing. These drawings are shown on appendix A.

9. **Device assembly and system integration:** the different hardware parts of the exoskeleton were assembled and software units were carefully integrated to ensure a robust control for the exoskeleton.

10. **Mechanical evaluation:** the objective of the mechanical testing of the exoskeleton is to determine its actuation unit transmission efficiency. The mechanical efficiency is essential to estimate the mechanical power added by the exoskeleton to the user ankle joint without using sensors such as a load cell during walking trials.

11. **Human walking trials:** the final step in the project consisted in evaluating the exoskeleton on a human subject. The goal is to determine how the exoskeleton affects the activity of the user's muscles during walking with the exoskeleton compared to walking without it.

5.2 Control System

Monitoring the gait cycle of the user in real time can be achieved using different methods. For example, inertial measurement units (IMUs) can be attached to specific locations on the leg and foot to constantly calculate the angle of each joint. Knowing the value of each joint, it is possible to determine the gait cycle phase in real time. This method was avoided because IMUs data requires filtering in order to get precise angles. Also, attaching sensors to the user could reduce the

practicality of the device. Instead of IMUs, we used a force resistive sensor (FSR) placed under the insole on the heel area. An FSR is a sensor that changes its resistance when pressure is applied on it in such a way that when a threshold is specified, the FSR could be used to trigger a desired output. The flow diagram of the developed algorithm that uses the FSR to monitor the gait cycle is shown on appendix B. On each new gait cycle the heel strike is detected, the gait period was defined as time measured between two consecutive strikes. The measured period is then used to estimate the percentage of the gait cycle in real time. The major drawback of this approach, however, is that the speed of the user needs to be constant after measuring the period. For the WAXO prototype, this was not a critical problem as the trials were done on a treadmill allowing the control of the walking speed.

The second block of the algorithm detects when the user arrives on the actuation onset and sends a signal to the motor driver to apply the desired torque profile. The flow diagram of this algorithm is shown on appendix C.

The microcontroller mbed NXP LPC181764 was used to implement the two algorithms above. This microcontroller is based on the 32-bit ARM Cortex-M3 processor running at 96 MHz. It is programed in C using an online platform offering existing libraries that facilitate the development. The schematic of the electronic circuit board is shown on figure 5-1.

The low-level layer of the control system uses a PID controller to reduce the error between the desired torque and the actual torque. This controller was implemented using the Maxon motor controller EPOS 2 70/10 that comes with built-in control functions as well as a software to tune the PID controller parameters.
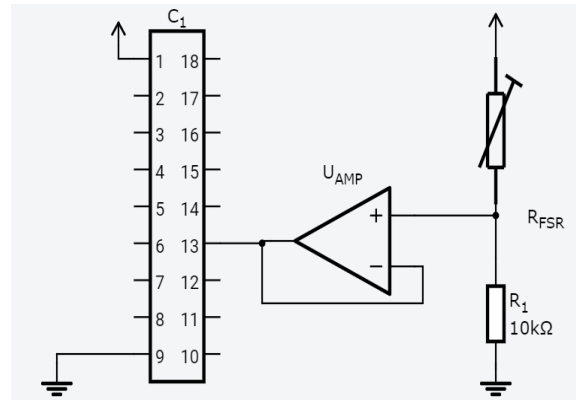
Figure 5-1: schematic of the electronic circuit. The FSR connects to the microcontroller C_1 using a pull-down resistor R_1 and an operational amplifier U_{AMP}

5.3 Graphical User Interface

The GUI was developed in Visual Studio using C#.NET and was running on a laptop. The custom functionalities of the GUI were mainly targeted to help both the user to operate the device and the developer to debug errors more quickly. The main functionalities of the GUI are:

- Connect to the motor driver and the microcontroller.

- Give instructions to users such as: "you can start walking".

- Give visual feedback in real time while walking, such as the number of steps and gait period.

- Test different torque profiles offline, i.e. without the user walking with the device.

- Enable the autonomous mode. In this mode, the motor delivers the mechanical power at the specified actuation onset of each gait cycle.

- Apply the position sinusoidal reference signal of the mechanical test.

- Save data of motor speed and current. These data were used to calculate the mechanical power of the motor.

- Stop the motor immediately in case of abnormal functioning or when the user wants to.

A screenshot of the GUI is shown of figure 5-2.
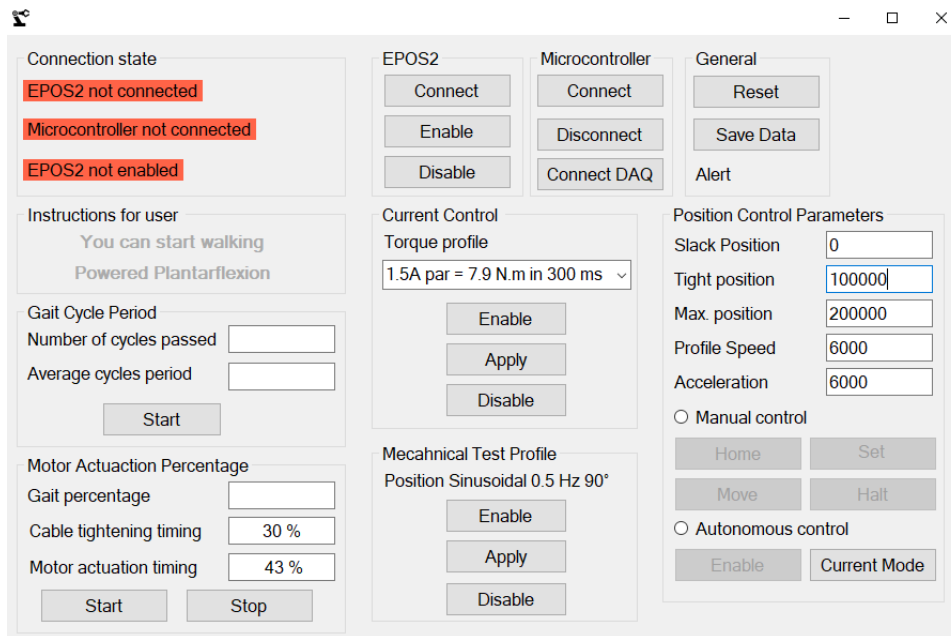
Figure 5-2: Screenshot of the GUI

5.4 Mechanical Test

A test setup was prepared in order to determine the efficiency of the actuation system of the exoskeleton. Figure 5-3 shows the components used to perform the mechanical test. A mass of 3.8 kg was attached to the two Bowden cables coming from the actuation unit. An inline load cell was inserted between the mass and the two cables to measure the pulling force applied on the mass. An Arduino board was used for load cell data acquisition. The data measured by the Arduino during the test were sent to the PC with a frequency of 100 Hz via serial communication. The software running on the laptop collects the motor current and speed from the motor driver with a frequency of 100 Hz. The synchronization between the data coming from the Arduino and the motor driver was insured by the software using timers and serial interrupts.

A sinusoidal reference signal of 0.5 Hz frequency and 90° amplitude was applied by the motor on the hanged mass. The power applied on the mass was calculated from the force measured by the load cell and the estimated cable speed. The mechanical power provided by the motor was calculated from the current and speed measurements provided by the motor driver. The test was repeated 3 times resulting in a mechanical efficiency of 0.59 ± 0.01 (mean ± standard deviation).
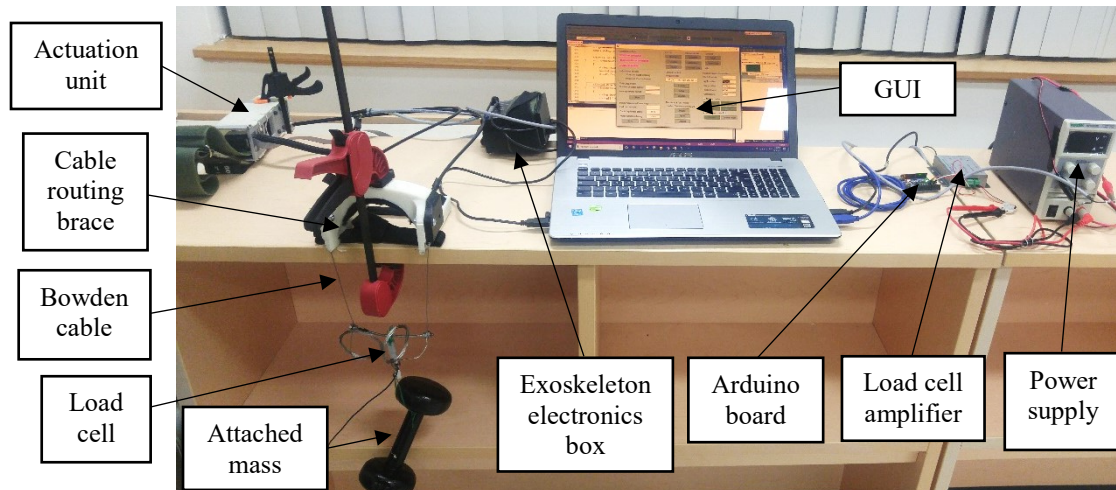
Figure 5-3: Mechanical test setup

5.5 Human Walking Tests

The human walking tests protocol and data recording were explained in the article. In this section, we give other details that were not mentioned in the article.

5.5.1 Hardware Testing

The walking tests were performed on a treadmill (Woodway, Wisconsin, USA) (figure 5-4) at the Centre de Réadaptation Marie-Enfant de l'Hôpital Sainte-Justine. The treadmill allows the control of the walking speed and inclination. The EMG signals of the gastrocnemius and soleus muscles were recorded using the BTS FreeEMG300 wireless system. Figure 5-5 shows the placement of the electrodes on the subject.

The motor data (current and speed) were recorded using the motor driver EPOS2 70/10. These data were used to estimate the mechanical power delivered by the exoskeleton to the subject during gait. The GUI of the exoskeleton software was used in each test to select the maximum torque to be applied by the exoskeleton, measure the average gait cycle period, start and stop the exoskeleton as well as storing the motor data.

Figure 5-4: The subject walking with the exoskeleton on the treadmill
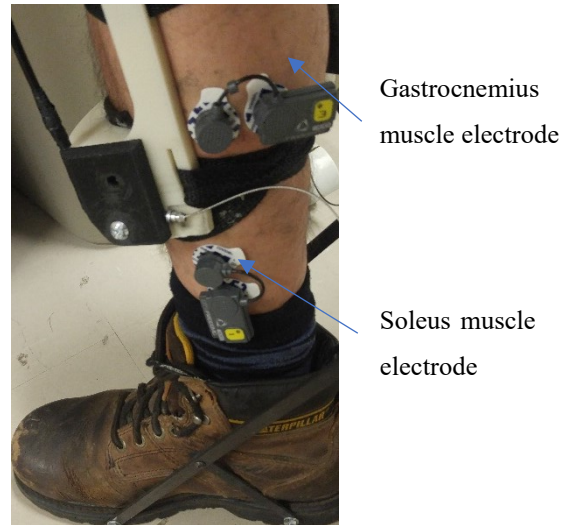
Figure 5-5: Placement of the EMG electrodes on the subject

5.5.2 Data Processing

The raw data obtained from each test were processed in MATLAB following these steps:

1. Band-filtering (10-450 Hz, zero-lag 4th order).

2. Full-wave rectification.

3. Low-pass filtering (3 Hz, Butterworth zero-lag 2nd order).

4. Normalization of the signal by the maximum value obtained during the NO EXO condition (walking without the exoskeleton).

The obtained signal (after step 4) includes all the data recorded during the walking duration of the test. A MATLAB function was written to split this signal into signals representing all the gait cycles included in this signal. Then, the maximum EMG value in each gait cycle was identified. The average of the maximum EMG values obtained in each of these gait cycles represents the average maximum EMG value over the gait cycle for a given walking trial.

CHAPTER 6   GENERAL DISCUSSION

The design of human augmentation exoskeletons has transitioned from developing bulky rigid devices to focusing on lightweight powerful devices. This transition was guided by the results and conclusions learned from assessing the effect of an exoskeleton weight on the metabolic cost of walking. Despite the efforts made in reducing the weight of exoskeletons, powered exoskeletons still add considerable mass to the user due to the presence of motors and rigid frames. Our goal in this work was to develop an ankle exoskeleton with a minimum added distal mass compared to existing autonomous powered ankle exoskeletons, while providing at least 50 Nm of assistive plantar flexion torque. In this chapter, we first summarize the key elements of the discussion presented in the article on chapter 4. Then we present the main limitations of the project and suggestions for future work.

6.1 Summary of the Article's Discussion

We showed in the article presented in chapter 4, that WAXO exoskeleton has only 348 g of added distal mass, that is, 67% lower than the current minimum distal mass added by a powered ankle exoskeleton in the literature [97]. The actuation system in our exoskeleton can provide up to 54 Nm of assistive plantar flexion torque representing around 50% of natural plantar flexion torque for an adult with 70 kg weight. The torque limit can be increased by mounting the pulley on a separate shaft and connecting the latter with the motor shaft using a coupling. Our mechanical test result showed that only 60% of the mechanical power provided by the motor is transmitted to the ankle joint during powered plantar flexion phase. The rest of the energy is lost due to cables friction. This loss can be limited using more efficient cables.

The different human walking trials allowed us to examine the effect of our exoskeleton on the activity of gastrocnemius and soleus muscles which are the principal muscles involved in ankle plantar flexion. The trials combined different conditions of actuation onset and duration as well as maximum torque magnitude. The maximum reduction in the muscles activity was recorded when the exoskeleton applied 19 ± 2 W of mechanical power with an actuation onset at 38% of the gait cycle along with an actuation duration of 200 ms. These test conditions resulted in a reduction of 44% and 37% in the activity of the gastrocnemius and soleus muscles respectively. These results were achieved when the actuation onset was fixed at 38% of the gait cycle giving an indication that

this actuation onset is optimal for reducing the activity of soleus and gastrocnemius muscles. However, this result needs to be validated with other subjects.

In general, our results show that the powered assistance parameters (actuation onset, duration and magnitude) affect the activity of the muscles. In addition, even if the mechanical power provided is the same but with different torque magnitude and actuation duration conditions, the obtained results are not the same. The results of different actuation duration conditions show that the latter depend on the actuation onset. For instance, for the 38% and 43% actuation onset conditions, better results were obtained on the 200 ms and 150 ms respectively. This is because the natural powered plantar flexion phase ends at the toe off around 63% of the gait cycle. For this reason, instead of using a fixed actuation duration, gait events such as toes off can be used to determine the actuation offset.

6.2 Limits and Perspectives of the Project

The general objective and specific objectives (OS1, OS2 and OS3) presented in chapter 3 were achieved in this thesis. Still, the present project has several limitations that can be addressed in future work. These limitations span the different aspects of the exoskeleton design. Specifically, the mechanical design, the control system as well as the evaluation of the exoskeleton. The main opportunities of improvements in each of these aspects are presented in this subsection.

6.2.1 Mechanical Design

The mechanical structure constitutes the physical interface between the exoskeleton and the human, therefore, it has to be both strong to transfer the power and comfortable to extend its use. In our actuation system, we choose to use Bowden cables as means of transmitting power. Although this choice helped reduce the distal weight of the exoskeleton, Bowden cables have introduced some problems. For instance, in many instances, the cables were jamming or sliding out from their place in the pulley. When these issues occur multiple times, it could damage the cable. These problems were caused mainly by the slack of the cable on the pulley after the actuation phase. One solution to prevent these problems is by introducing a mechanism that keeps the cable on the pulley tight in all cases. Also, a metal grooved pulley can be used to reduce the sliding of the cables on the pulley.

Although the mechanical power that can be provided by our exoskeleton is relatively high. It can be increased using a coupling to transfer the power from the motor shaft to the pulley. This way, the maximum linear force on the cable will not be limited by the maximum allowed force of the motor shaft. Instead, the shaft of the pulley can be custom designed to allow higher linear force, therefore, higher augmentation torque and power. However, these additional elements on the actuation unit will increase its weight, therefore, a minimalistic design approach needs to be always adopted. The exoskeleton mechanical power added to the ankle joint can also be increased by increasing the struts length. We introduced a constraint in our struts optimization study to limit the maximum length of the struts, however, the limit value of this constraint can be changed to allow higher struts length. This constraint can be replaced by another constraint that limits the deflection magnitude of the struts to a maximum value.

Our exoskeleton adds power on only one ankle joint. This design decision was taken considering the time limit of the project. However, for future work, it is very important to add power on the other ankle joint as well. This can be achieved by adding another motor but can also be achieved with a single motor i.e. using the same actuation unit of the current exoskeleton. In this case, the control system needs to be carefully designed so that the motor switch actuation from one joint to another accurately and rapidly. Using a single motor to add power on the two joints will significantly increase the specific power of the exoskeleton, and thus, increase its potential in reducing the metabolic cost of walking. Also, series elastic elements can be added to the actuation system instead of using only rigid cables. These elastic elements will help increase the efficiency of the device and improve the force control.

6.2.2 Control System

One of the major limitations of our control system hardware is the use of a laptop that limits the autonomy of the exoskeleton. An embedded PC can be used to replace both the microcontroller and the laptop. This embedded PC can be a low-cost board such as a Raspberry PI or preferably a more sophisticated one such as a PC/104 computer board. A laptop or a desktop PC can be added only for visualization and data storage when doing tests in the lab.

As stated earlier, the gait detection system of our exoskeleton only relies on one FSR sensor. In addition, the control algorithm assumes that the user will not change his walking speed once the average gait period is calculated. Although this scenario is acceptable in the lab, it is not suitable

for real applications. Also, a system that can handle different walking scenarios will allow a more realistic evaluation for the exoskeleton. In order to take speed change into account, the algorithm can update the average speed continuously during walking after each given number of gait cycles. Additionally, IMUs can be used to increase the accuracy of the gait detection system. IMUs can be particularly useful in detecting abnormal situations or activity change such as when the user stops walking or falls.

6.2.3 Exoskeleton Evaluation

The principal objective of our project is the design and development of the exoskeleton. The evaluation of the exoskeleton with a human subject was performed only to obtain an initial information of how the exoskeleton affects the user. A complete evaluation of the exoskeleton will require other tests and additional experimental instruments. For instance, the oxygen consumption is the main standard method used in the literature to evaluate augmentation exoskeleton because it allows the calculation of the metabolic cost of walking. In addition, a complete evaluation of the exoskeleton will require examining how the exoskeleton affects the normal gait kinematics. In order to do that, kinematic data need to be recorded while a subject is walking with the exoskeleton and without it, then this data can be used to compare the user kinematics in the two situations.

Another major limitation in our human walking trials is the use of a conventional treadmill instead of an instrumented treadmill which is the standard used treadmills for exoskeleton evaluation. Using an instrumented treadmill, additional information can be recorded such as the ground reaction force.

CHAPTER 7   CONCLUSION AND RECOMMENDATIONS

The objective of this thesis was to develop an ankle exoskeleton with a minimum added distal mass compared to existing autonomous powered ankle exoskeletons, while providing at least 50 Nm of assistive plantar flexion torque. This objective was achieved using two main strategies. First, by distributing the mass of the exoskeleton on the user body in such a way that the negative effect of the added mass on the metabolic cost of walking will be minimal. And secondly, by performing optimization studies of the mechanical structure both in terms of geometry and mass. The mechanical system of the exoskeleton included an actuation unit attached to the waist area and a pair of carbon fiber struts bolted to the user's boot. Two Bowden cables were used to transmit the force from the actuation unit to the struts. These two cables pass through a lightweight custom designed brace attached to the shin in order to adjust the orientation of the cables. The control system of the exoskeleton adopted a hierarchical architecture composed of a high-level and low-level control layers. The high-level layer monitors the gait cycle of the user in real time to continuously detect the phases of the gait cycle. When the user arrives at the actuation onset instant, the high-level controller sends a signal to the low-level controller along with the desired torque profile. The low-level controller uses a PID controller to apply the desired torque profile. The main assistance parameters such as torque magnitude, actuation onset and duration can be varied using a custom developed graphical user interface.

Our exoskeleton has a total mass of 2045 g with only 348 g of distal mass. The walking trials showed that our exoskeleton has a significant potential in reducing the metabolic cost of walking. A 40% of reduction in the activity of soleus and gastrocnemius muscles was recorded during the walking trials. These trials also showed that an actuation onset of 38% was the best to reduce the electrical activity of the soleus and gastrocnemius muscles during walking.

As perspective of this project, the actuation could be extended to the other ankle joint. Then, an extensive evaluation study of the exoskeleton that including metabolic, kinematic and dynamic data could be performed with a significant number of subjects. During this evaluation study, different assistive strategies could be applied to determine which assistance parameters are the best for reducing the metabolic cost of walking. This way, the developed exoskeleton would also serve as a test platform to validate the scientific hypotheses and help answer fundamental questions related to human biomechanics.

BIBLIOGRAPHY

[1]   S. H. Collins, M. B. Wiggin, and G. S. Sawicki, "Reducing the energy cost of human walking using an unpowered exoskeleton," *Nature,* vol. 522, pp. 212-215, 2015.

[2]   K. R. Westerterp, "Physical activity and physical activity induced energy expenditure in humans: measurement, determinants, and effects," *Frontiers in physiology,* vol. 4, p. 90, 2013.

[3]   M. Zarrugh, F. Todd, and H. Ralston, "Optimization of energy expenditure during level walking," *European journal of applied physiology and occupational physiology,* vol. 33, pp. 293-306, 1974.

[4]   M. D. Beekley, J. Alt, C. M. Buckley, M. Duffey, and T. A. Crowder, "Effects of heavy load carriage during constant-speed, simulated, road marching," *Military medicine,* vol. 172, pp. 592-595, 2007.

[5]   K. Park, K. S. Rosengren, G. P. Horn, D. L. Smith, and E. T. Hsiao-Wecksler, "Assessing gait changes in firefighters due to fatigue and protective clothing," *Safety science,* vol. 49, pp. 719-726, 2011.

[6]   N. Yagn, "Apparatus for facilitating walking," ed: Google Patents, 1890.

[7]   A. B. Zoss, H. Kazerooni, and A. Chu, "Biomechanical design of the Berkeley lower extremity exoskeleton (BLEEX)," *IEEE/ASME Transactions On Mechatronics,* vol. 11, pp. 128-138, 2006.

[8]   H. Cao, J. Zhu, C. Xia, H. Zhou, X. Chen, and Y. Wang, "Design and Control of a Hydraulic-Actuated Leg Exoskeleton for Load-Carrying Augmentation," in *Intelligent Robotics and Applications: Third International Conference, ICIRA 2010, Shanghai, China, November 10-12, 2010. Proceedings, Part I*, H. Liu, H. Ding, Z. Xiong, and X. Zhu, Eds., ed Berlin, Heidelberg: Springer Berlin Heidelberg, 2010, pp. 590-599.

[9]   S. Yu, H. Lee, S. Lee, W. Kim, J. Han, and C.-S. Han, "Design of an under-actuated exoskeleton system for walking assist while load carrying," *Advanced Robotics,* vol. 26, pp. 561-580, 2012.

[10]   S. Marcheschi, F. Salsedo, M. Fontana, and M. Bergamasco, "Body extender: whole body exoskeleton for human power augmentation," in *Robotics and Automation (ICRA), 2011 IEEE International Conference on*, 2011, pp. 611-616.

[11]   D. Lim, W. Kim, H. Lee, K. Hojun, S. Kyoosik, P. Taejoon*, et al.*, "Development of a lower extremity Exoskeleton Robot with a quasi-anthropomorphic design approach for load carriage," in *2015 IEEE/RSJ International Conference on Intelligent Robots and Systems (IROS)*, 2015, pp. 5345-5350.

[12]   L. M. Mooney, E. J. Rouse, and H. M. Herr, "Autonomous exoskeleton reduces metabolic cost of human walking during load carriage," *Journal of neuroengineering and rehabilitation,* vol. 11, p. 80, 2014.

[13]   F. A. Panizzolo, I. Galiana, A. T. Asbeck, C. Siviy, K. Schmidt, K. G. Holt*, et al.*, "A biologically-inspired multi-joint soft exosuit that can reduce the energy cost of loaded walking," *Journal of neuroengineering and rehabilitation,* vol. 13, p. 43, 2016.

[14] H. Kazerooni and R. Steger, "The Berkeley lower extremity exoskeleton," *Journal of dynamic systems, measurement, and control,* vol. 128, pp. 14-25, 2006.

[15] A. M. Dollar and H. Herr, "Lower extremity exoskeletons and active orthoses: challenges and state-of-the-art," *IEEE Transactions on robotics,* vol. 24, pp. 144-158, 2008.

[16] A. J. Young and D. P. Ferris, "State of the Art and Future Directions for Lower Limb Robotic Exoskeletons," *IEEE Transactions on Neural Systems and Rehabilitation Engineering,* vol. 25, pp. 171-182, 2017.

[17] J. E. Pratt, B. T. Krupp, C. J. Morse, and S. H. Collins, "The RoboKnee: an exoskeleton for enhancing strength and endurance during walking," in *Robotics and Automation, 2004. Proceedings. ICRA'04. 2004 IEEE International Conference on*, 2004, pp. 2430-2435.

[18] Y. Kusuda, "In quest of mobility–Honda to develop walking assist devices," *Industrial Robot: An International Journal,* vol. 36, pp. 537-539, 2009.

[19] P. Malcolm, W. Derave, S. Galle, and D. De Clercq, "A simple exoskeleton that assists plantarflexion can reduce the metabolic cost of human walking," *PloS one,* vol. 8, p. e56137, 2013.

[20] C. Meijneke, W. van Dijk, and H. van der Kooij, "Achilles: an autonomous lightweight ankle exoskeleton to provide push-off power," in *Biomedical Robotics and Biomechatronics (2014 5th IEEE RAS & EMBS International Conference on*, 2014, pp. 918-923.

[21] K. A. Witte, J. Zhang, R. W. Jackson, and S. H. Collins, "Design of two lightweight, high-bandwidth torque-controlled ankle exoskeletons," in *Robotics and Automation (ICRA), 2015 IEEE International Conference on*, 2015, pp. 1223-1228.

[22] G. Bovi, M. Rabuffetti, P. Mazzoleni, and M. Ferrarin, "A multiple-task gait analysis approach: kinematic, kinetic and EMG reference data for healthy young and adult subjects," *Gait & posture,* vol. 33, pp. 6-13, 2011.

[23] C. J. Walsh, K. Endo, and H. Herr, "A quasi-passive leg exoskeleton for load-carrying augmentation," *International Journal of Humanoid Robotics,* vol. 4, pp. 487-506, 2007.

[24] R. C. Browning, J. R. Modica, R. Kram, and A. Goswami, "The effects of adding mass to the legs on the energetics and biomechanics of walking," *Medicine and science in sports and exercise,* vol. 39, p. 515, 2007.

[25] J. Perry and J. R. Davids, "Gait analysis: normal and pathological function," *Journal of Pediatric Orthopaedics,* vol. 12, p. 815, 1992.

[26] D. Winter, *Biomechanics and motor control of human gait: normal, elderly and pathological*. Waterloo: Waterloo Biomechanics, 1991.

[27] D. Richfield, "Medical gallery of David Richfield," ed: WikiJournal of Medicine, 2014.

[28] Y. Muramatsu, H. Kobayashi, Y. Sato, H. Jiaou, T. Hashimoto, and H. Kobayashi, "Quantitative Performance Analysis of Exoskeleton Augmenting Devices–Muscle Suit–for Manual Worker," *International Journal of Automation Technology,* vol. 5, pp. 559-567, 2011.

[29] K. E. Gordon and D. P. Ferris, "Learning to walk with a robotic ankle exoskeleton," *Journal of biomechanics,* vol. 40, pp. 2636-2644, 2007.

[30] J.-M. Belda-Lois, S. Mena-del Horno, I. Bermejo-Bosch, J. C. Moreno, J. L. Pons, D. Farina*, et al.*, "Rehabilitation of gait after stroke: a review towards a top-down approach," *Journal of NeuroEngineering and Rehabilitation,* vol. 8, p. 66, December 13 2011.

[31] A. Esquenazi, M. Talaty, A. Packel, and M. Saulino, "The ReWalk powered exoskeleton to restore ambulatory function to individuals with thoracic-level motor-complete spinal cord injury," *American journal of physical medicine & rehabilitation,* vol. 91, pp. 911-921, 2012.

[32] S. Murray and M. Goldfarb, "Towards the use of a lower limb exoskeleton for locomotion assistance in individuals with neuromuscular locomotor deficits," in *Engineering in Medicine and Biology Society (EMBC), 2012 Annual International Conference of the IEEE,* 2012, pp. 1912-1915.

[33] K. A. Strausser, T. A. Swift, A. B. Zoss, H. Kazerooni, and B. C. Bennett, "Mobile exoskeleton for spinal cord injury: Development and testing," in *Proceeding of ASME Dynamic Systems and Controls Conference,* 2011, pp. 419-425.

[34] G. S. Sawicki and D. P. Ferris, "A pneumatically powered knee-ankle-foot orthosis (KAFO) with myoelectric activation and inhibition," *Journal of neuroengineering and rehabilitation,* vol. 6, p. 23, 2009.

[35] D. P. Ferris, J. M. Czerniecki, and B. Hannaford, "An ankle-foot orthosis powered by artificial pneumatic muscles," *Journal of applied biomechanics,* vol. 21, pp. 189-197, 2005.

[36] J. A. Blaya and H. Herr, "Adaptive control of a variable-impedance ankle-foot orthosis to assist drop-foot gait," *IEEE Transactions on neural systems and rehabilitation engineering,* vol. 12, pp. 24-31, 2004.

[37] P. Beyl, J. Naudet, R. Van Ham, and D. Lefeber, "Mechanical design of an active knee orthosis for gait rehabilitation," in *Rehabilitation Robotics, 2007. ICORR 2007. IEEE 10th International Conference on,* 2007, pp. 100-105.

[38] J. Nikitczuk, B. Weinberg, P. K. Canavan, and C. Mavroidis, "Active knee rehabilitation orthotic device with variable damping characteristics implemented via an electrorheological fluid," *IEEE/ASME transactions on Mechatronics,* vol. 15, pp. 952-960, 2010.

[39] B. Weinberg, J. Nikitczuk, S. Patel, B. Patritti, C. Mavroidis, P. Bonato*, et al.*, "Design, control and human testing of an active knee rehabilitation orthotic device," in *Robotics and Automation, 2007 IEEE International Conference on,* 2007, pp. 4126-4133.

[40] A. Esquenazi, "New bipedal locomotion option for individuals with thoracic level motor complete spinal cord injury," *J. Spinal Res. Found,* vol. 8, pp. 26-28, 2013.

[41] P. Lawrenson, "Stepping Motors: a Guide to Modern Theory and Practice," *Electronics and Power,* vol. 29, p. 659, 1983.

[42] C. Hartigan, C. Kandilakis, S. Dalley, M. Clausen, E. Wilson, S. Morrison*, et al.*, "Mobility outcomes following five training sessions with a powered exoskeleton," *Topics in spinal cord injury rehabilitation,* vol. 21, pp. 93-99, 2015.

[43]   P. R. Geigle and M. Kallins, "Exoskeleton-Assisted Walking for People With Spinal Cord Injury," *Archives of Physical Medicine and Rehabilitation,* vol. 98, pp. 1493-1495, 2017.

[44]   H. Kawamoto, S. Kanbe, and Y. Sankai, "Power assist method for HAL-3 estimating operator's intention based on motion information," in *Robot and human interactive communication, 2003. proceedings. ROMAN 2003. The 12th IEEE international workshop on*, 2003, pp. 67-72.

[45]   K. A. Strausser and H. Kazerooni, "The development and testing of a human machine interface for a mobile medical exoskeleton," in *Intelligent Robots and Systems (IROS), 2011 IEEE/RSJ International Conference on*, 2011, pp. 4911-4916.

[46]   P. D. Neuhaus, J. H. Noorden, T. J. Craig, T. Torres, J. Kirschbaum, and J. E. Pratt, "Design and evaluation of Mina: A robotic orthosis for paraplegics," in *Rehabilitation Robotics (ICORR), 2011 IEEE International Conference on*, 2011, pp. 1-8.

[47]   R. J. Farris, H. A. Quintero, and M. Goldfarb, "Preliminary evaluation of a powered lower limb orthosis to aid walking in paraplegic individuals," *IEEE Transactions on Neural Systems and Rehabilitation Engineering,* vol. 19, pp. 652-659, 2011.

[48]   A. Nilsson, K. S. Vreede, V. Häglund, H. Kawamoto, Y. Sankai, and J. Borg, "Gait training early after stroke with a new exoskeleton – the hybrid assistive limb: a study of safety and feasibility," *Journal of NeuroEngineering and Rehabilitation,* vol. 11, p. 92, June 02 2014.

[49]   M. Bortole, A. Venkatakrishnan, F. Zhu, J. C. Moreno, G. E. Francisco, J. L. Pons*, et al.*, "The H2 robotic exoskeleton for gait rehabilitation after stroke: early findings from a clinical study," *Journal of NeuroEngineering and Rehabilitation,* vol. 12, p. 54, June 17 2015.

[50]   A. T. Asbeck, S. M. De Rossi, I. Galiana, Y. Ding, and C. J. Walsh, "Stronger, smarter, softer: next-generation wearable robots," *IEEE Robotics & Automation Magazine,* vol. 21, pp. 22-33, 2014.

[51]   G. Colombo, M. Wirz, and V. Dietz, "Driven gait orthosis for improvement of locomotor training in paraplegic patients," *Spinal cord,* vol. 39, pp. 252-255, 2001.

[52]   J. F. Veneman, R. Kruidhof, E. E. Hekman, R. Ekkelenkamp, E. H. Van Asseldonk, and H. Van Der Kooij, "Design and evaluation of the LOPES exoskeleton robot for interactive gait rehabilitation," *IEEE Transactions on Neural Systems and Rehabilitation Engineering,* vol. 15, pp. 379-386, 2007.

[53]   C. Werner, S. Von Frankenberg, T. Treig, M. Konrad, and S. Hesse, "Treadmill training with partial body weight support and an electromechanical gait trainer for restoration of gait in subacute stroke patients," *Stroke,* vol. 33, pp. 2895-2901, 2002.

[54]   R. W. Horst, "A bio-robotic leg orthosis for rehabilitation and mobility enhancement," in *Engineering in Medicine and Biology Society, 2009. EMBC 2009. Annual International Conference of the IEEE*, 2009, pp. 5030-5033.

[55]   K.-H. Seo and J.-J. Lee, "The development of two mobile gait rehabilitation systems," *IEEE transactions on neural systems and rehabilitation engineering,* vol. 17, pp. 156-166, 2009.

[56] M. P. de Looze, T. Bosch, F. Krause, K. S. Stadler, and L. W. O'Sullivan, "Exoskeletons for industrial application and their potential effects on physical work load," *Ergonomics,* vol. 59, pp. 671-681, 2016/05/03 2016.

[57] V. G. Parent-Thirion Agnès, van Houten Gijs, Lyly-Yrjänäinen Maija, Biletta, Isabella Cabrita Jorge, "Fifth European Working Conditions Survey," 05 June 2012.

[58] M. Abdoli-e, M. J. Agnew, and J. M. Stevenson, "An on-body personal lift augmentation device (PLAD) reduces EMG amplitude of erector spinae during lifting tasks," *Clinical Biomechanics,* vol. 21, pp. 456-465, 2006.

[59] H. Kobayashi and H. Nozaki, "Development of muscle suit for supporting manual worker," in *Intelligent Robots and Systems, 2007. IROS 2007. IEEE/RSJ International Conference on*, 2007, pp. 1769-1774.

[60] B. L. Ulrey and F. A. Fathallah, "Subject-specific, whole-body models of the stooped posture with a personal weight transfer device," *Journal of Electromyography and Kinesiology,* vol. 23, pp. 206-215, 2013/02/01/ 2013.

[61] Z. Luo and Y. Yu, "Wearable stooping-assist device in reducing risk of low back disorders during stooped work," in *Mechatronics and Automation (ICMA), 2013 IEEE International Conference on*, 2013, pp. 230-236.

[62] R. Y. M. Li and D. P. L. Ng, "Wearable Robotics, Industrial Robots and Construction Worker's Safety and Health," Cham, 2018, pp. 31-36.

[63] J. Knapik, E. Harman, and K. Reynolds, "Load carriage using packs: A review of physiological, biomechanical and medical aspects," *Applied Ergonomics,* vol. 27, pp. 207-216, 1996/06/01/ 1996.

[64] S. J. Zaroodny, "BUMPUSHER-A POWERED AID TO LOCOMOTION," BALLISTIC RESEARCH LABS ABERDEEN PROVING GROUND MD1963.

[65] K. Gilbert, "Exoskeleton prototype project: Final report on phase I," *General Electric Company, Schenectady, NY, GE Tech. Rep. S-67-1011,* 1967.

[66] E. Garcia, J. M. Sater, and J. Main, "Exoskeletons for human performance augmentation (EHPA): A program summary," *Journal of the Robotics Society of Japan,* vol. 20, pp. 822-826, 2002.

[67] C. J. Walsh, K. Pasch, and H. Herr, "An autonomous, underactuated exoskeleton for load-carrying augmentation," in *Intelligent Robots and Systems, 2006 IEEE/RSJ International Conference on*, 2006, pp. 1410-1415.

[68] E. Guizzo and H. Goldstein, "The rise of the body bots [robotic exoskeletons]," *IEEE spectrum,* vol. 42, pp. 50-56, 2005.

[69] K. H. Low, X. Liu, C. H. Goh, and H. Yu, "Locomotive Control of a Wearable Lower Exoskeleton for Walking Enhancement," *Journal of Vibration and Control,* vol. 12, pp. 1311-1336, 2006/12/01 2006.

[70] K. Seo, J. Lee, Y. Lee, T. Ha, and Y. Shim, "Fully autonomous hip exoskeleton saves metabolic cost of walking," in *Robotics and Automation (ICRA), 2016 IEEE International Conference on*, 2016, pp. 4628-4635.

[71]   W. van Dijk and H. Van der Kooij, "XPED2: A passive exoskeleton with artificial tendons," *IEEE Robotics & Automation Magazine,* vol. 21, pp. 56-61, 2014.

[72]   Y. Hasegawa and K. Ogura, "First report on passive exoskeleton for easy running: PEXER IV," in *Micro-NanoMechatronics and Human Science (MHS), 2013 International Symposium on*, 2013, pp. 1-6.

[73]   M. B. Wiggin, G. S. Sawicki, and S. H. Collins, "An exoskeleton using controlled energy storage and release to aid ankle propulsion," in *Rehabilitation Robotics (ICORR), 2011 IEEE International Conference on*, 2011, pp. 1-5.

[74]   G. Elliott, A. Marecki, and H. Herr, "Design of a Clutch–Spring Knee Exoskeleton for Running," *Journal of Medical Devices,* vol. 8, pp. 031002-031002-11, 2014.

[75]   S. Diller, C. Majidi, and S. H. Collins, "A lightweight, low-power electroadhesive clutch and spring for exoskeleton actuation," in *Robotics and Automation (ICRA), 2016 IEEE International Conference on*, 2016, pp. 682-689.

[76]   I. W. Hunter, J. M. Hollerbach, and J. Ballantyne, "A comparative analysis of actuator technologies for robotics," *Robotics Review,* vol. 2, pp. 299-342, 1991.

[77]   S. Habibi, R. Richards, and A. Goldenberg, "Hydraulic actuator analysis for industrial robot multivariable control," in *American Control Conference, 1994*, 1994, pp. 1003-1007.

[78]   E. Richer and Y. Hurmuzlu, "A high performance pneumatic force actuator system: Part I-Nonlinear mathematical model," *Transactions-American Society of Mechanical Engineers Journal of Dynamic Systems Measurement and Control,* vol. 122, pp. 416-425, 2000.

[79]   R. B. Van Varseveld and G. M. Bone, "Accurate position control of a pneumatic actuator using on/off solenoid valves," *IEEE/ASME Transactions on mechatronics,* vol. 2, pp. 195-204, 1997.

[80]   B. Tondu and P. Lopez, "Modeling and control of McKibben artificial muscle robot actuators," *IEEE control systems,* vol. 20, pp. 15-38, 2000.

[81]   P. Beyl, M. e. Van Damme, R. Van Ham, B. Vanderborght, and D. Lefeber, "Pleated pneumatic artificial muscle-based actuator system as a torque source for compliant lower limb exoskeletons," *IEEE/ASME Transactions on Mechatronics,* vol. 19, pp. 1046-1056, 2014.

[82]   N. Costa and D. G. Caldwell, "Control of a biomimetic" soft-actuated" 10dof lower body exoskeleton," in *Biomedical Robotics and Biomechatronics, 2006. BioRob 2006. The First IEEE/RAS-EMBS International Conference on*, 2006, pp. 495-501.

[83]   M. Wehner, B. Quinlivan, P. M. Aubin, E. Martinez-Villalpando, M. Baumann, L. Stirling*, et al.*, "A lightweight soft exosuit for gait assistance," in *Robotics and Automation (ICRA), 2013 IEEE International Conference on*, 2013, pp. 3362-3369.

[84]   Y.-L. Park, B.-r. Chen, N. O. Pérez-Arancibia, D. Young, L. Stirling, R. J. Wood*, et al.*, "Design and control of a bio-inspired soft wearable robotic device for ankle–foot rehabilitation," *Bioinspiration & biomimetics,* vol. 9, p. 016007, 2014.

[85]   S. Galle, W. Derave, F. Bossuyt, P. Calders, P. Malcolm, and D. Clercq, "Exoskeleton plantarflexion assistance for elderly," *Gait Posture,* vol. 52, 2017.

[86] B. Siciliano and O. Khatib, *Springer handbook of robotics*: Springer Science & Business Media, 2008.

[87] R. H. Bishop, *Mechatronic systems, sensors, and actuators: fundamentals and modeling*: CRC press, 2007.

[88] J.-f. Zhang, Y.-m. Dong, C.-j. Yang, Y. Geng, Y. Chen, and Y. Yang, "5-Link model based gait trajectory adaption control strategies of the gait rehabilitation exoskeleton for post-stroke patients," *Mechatronics,* vol. 20, pp. 368-376, 2010.

[89] R. Baud, A. Ortlieb, J. Olivier, M. Bouri, and H. Bleuler, "HiBSO hip exoskeleton: Toward a wearable and autonomous design," in *International Workshop on Medical and Service Robots*, 2016, pp. 185-195.

[90] U. Keller and R. Riener, "Design of the pediatric arm rehabilitation robot ChARMin," in *Biomedical Robotics and Biomechatronics (2014 5th IEEE RAS & EMBS International Conference on*, 2014, pp. 530-535.

[91] T. Wilson and P. Trickey, "DC machine with solid-state commutation," *Electrical Engineering,* vol. 81, pp. 879-884, 1962.

[92] L. ENGINEERING. *Design Accuracy Comparison 0.9° vs. 1.8°*. Available: https://www.linengineering.com/resources/white-papers/design-accuracy-comparison-0-9-vs-1-8/

[93] V. Athani, *Stepper motors: fundamentals, applications and design*: New Age International, 1997.

[94] M. Zribi and J. Chiasson, "Position control of a PM stepper motor by exact linearization," *IEEE Transactions on Automatic Control,* vol. 36, pp. 620-625, 1991.

[95] A. Hughes and W. Drury, *Electric motors and drives: fundamentals, types and applications*: Newnes, 2013.

[96] P. Yedamale, "Brushless DC (BLDC) motor fundamentals," *Microchip Technology Inc,* vol. 20, pp. 3-15, 2003.

[97] L. M. Mooney, E. J. Rouse, and H. M. Herr, "Autonomous exoskeleton reduces metabolic cost of human walking," *Journal of neuroengineering and rehabilitation,* vol. 11, p. 151, 2014.

[98] W. van Dijk, C. Meijneke, and H. van der Kooij, "Evaluation of the Achilles Ankle exoskeleton," *IEEE Transactions on Neural Systems and Rehabilitation Engineering,* 2016.

[99] G. A. Pratt and M. M. Williamson, "Series elastic actuators," in *Intelligent Robots and Systems 95.'Human Robot Interaction and Cooperative Robots', Proceedings. 1995 IEEE/RSJ International Conference on*, 1995, pp. 399-406.

[100] D. W. Robinson, J. E. Pratt, D. J. Paluska, and G. A. Pratt, "Series elastic actuator development for a biomimetic walking robot," in *Advanced Intelligent Mechatronics, 1999. Proceedings. 1999 IEEE/ASME International Conference on*, 1999, pp. 561-568.

[101] J. Pratt, B. Krupp, and C. Morse, "Series elastic actuators for high fidelity force control," *Industrial Robot: An International Journal,* vol. 29, pp. 234-241, 2002.

[102] A. Edsinger-Gonzales and J. Weber, "Domo: A force sensing humanoid robot for manipulation research," in *Humanoid Robots, 2004 4th IEEE/RAS International Conference on*, 2004, pp. 273-291.

[103] K. W. Hollander, R. Ilg, T. G. Sugar, and D. Herring, "An efficient robotic tendon for gait assistance," *Journal of biomechanical engineering,* vol. 128, pp. 788-791, 2006.

[104] J. Chen and W. Liao, "Design, testing and control of a magnetorheological actuator for assistive knee braces," *Smart Materials and Structures,* vol. 19, p. 035029, 2010.

[105] J. Carlson, "6.6 Magnetorheological Fluid Actuators," *Adaptronics and Smart Structures: Basics, Materials, Design, and Applications,* p. 1808, 2013.

[106] F. Ahmadkhanlou, J. L. Zite, and G. N. Washington, "A magnetorheological fluid-based controllable active knee brace," in *Proc. SPIE*, 2007, p. 65270O.

[107] T. D. Tuttle and W. P. Seering, "A nonlinear model of a harmonic drive gear transmission," *IEEE Transactions on Robotics and Automation,* vol. 12, pp. 368-374, 1996.

[108] X. Zhang, G. Jiang, C. Zou, and S. Wang, "Modeling of compliance and hysteresis with erasure property in harmonic drive by active loading," in *Cybernetics and Intelligent Systems (CIS) and IEEE Conference on Robotics, Automation and Mechatronics (RAM), 2017 IEEE International Conference on*, 2017, pp. 439-445.

[109] J. L. Pons, *Wearable robots: biomechatronic exoskeletons*: John Wiley & Sons, 2008.

[110] A. T. Asbeck, R. J. Dyer, A. F. Larusson, and C. J. Walsh, "Biologically-inspired soft exosuit," in *Rehabilitation robotics (ICORR), 2013 IEEE international conference on*, 2013, pp. 1-8.

[111] M. B. Yandell, D. Popov, B. T. Quinlivan, C. Walsh, K. O'Donnell, and K. E. Zelik, "Systematic evaluation of human-exosuit physical interfaces."

[112] M. Cenciarini and A. M. Dollar, "Biomechanical considerations in the design of lower limb exoskeletons," in *Rehabilitation Robotics (ICORR), 2011 IEEE International Conference on*, 2011, pp. 1-6.

[113] A. Schiele and F. C. van der Helm, "Influence of attachment pressure and kinematic configuration on pHRI with wearable robots," *Applied Bionics and Biomechanics,* vol. 6, pp. 157-173, 2009.

[114] A. J. Young, H. Gannon, and D. P. Ferris, "a Biomechanical comparison of Proportional electromyography control to Biological Torque control Using a Powered hip exoskeleton," *Frontiers in bioengineering and biotechnology,* vol. 5, 2017.

[115] B. Quinlivan, S. Lee, P. Malcolm, D. Rossi, M. Grimmer, C. Siviy*, et al.*, "Assistance magnitude versus metabolic cost reductions for a tethered multiarticular soft exosuit," *Science Robotics,* vol. 2, p. eaah4416, 2017.

[116] C. Buesing, G. Fisch, M. O'Donnell, I. Shahidi, L. Thomas, C. K. Mummidisetty*, et al.*, "Effects of a wearable exoskeleton stride management assist system (SMA®) on spatiotemporal gait characteristics in individuals after stroke: a randomized controlled trial," *Journal of neuroengineering and rehabilitation,* vol. 12, p. 69, 2015.

[117]   G. Lee, J. Kim, F. Panizzolo, Y. Zhou, L. Baker, I. Galiana*, et al.*, "Reducing the metabolic cost of running with a tethered soft exosuit," *Science Robotics,* vol. 2, p. eaan6708, 2017.

[118]   L. M. Mooney and H. M. Herr, "Biomechanical walking mechanisms underlying the metabolic reduction caused by an autonomous exoskeleton," *Journal of neuroengineering and rehabilitation,* vol. 13, p. 4, 2016.

[119]   M. Ishikawa, P. V. Komi, M. J. Grey, V. Lepola, and G.-P. Bruggemann, "Muscle-tendon interaction and elastic energy usage in human walking," *Journal of applied physiology,* vol. 99, pp. 603-608, 2005.

[120]   L. Bianchi, D. Angelini, G. Orani, and F. Lacquaniti, "Kinematic coordination in human gait: relation to mechanical energy cost," *Journal of neurophysiology,* vol. 79, pp. 2155-2170, 1998.

[121]   S. H. Collins, P. G. Adamczyk, and A. D. Kuo, "Dynamic arm swinging in human walking," *Proceedings of the Royal Society of London B: Biological Sciences,* vol. 276, pp. 3679-3688, 2009.

[122]   M. R. Tucker, J. Olivier, A. Pagel, H. Bleuler, M. Bouri, O. Lambercy*, et al.*, "Control strategies for active lower extremity prosthetics and orthotics: a review," *Journal of neuroengineering and rehabilitation,* vol. 12, p. 1, 2015.

[123]   K. Park, P. Hur, K. S. Rosengren, G. P. Horn, and E. T. Hsiao-Wecksler, "Effect of load carriage on gait due to firefighting air bottle configuration," *Ergonomics,* vol. 53, pp. 882-891, 2010.

[124]   A. Chu, H. Kazerooni, and A. Zoss, "On the biomimetic design of the berkeley lower extremity exoskeleton (BLEEX)," in *Robotics and Automation, 2005. ICRA 2005. Proceedings of the 2005 IEEE International Conference on*, 2005, pp. 4345-4352.

[125]   D. P. Ferris, G. S. Sawicki, and M. A. Daley, "A physiologist's perspective on robotic exoskeletons for human locomotion," *International Journal of Humanoid Robotics,* vol. 4, pp. 507-528, 2007.

[126]   Y.-L. Park, B.-r. Chen, D. Young, L. Stirling, R. J. Wood, E. Goldfield*, et al.*, "Bio-inspired active soft orthotic device for ankle foot pathologies," in *Intelligent Robots and Systems (IROS), 2011 IEEE/RSJ International Conference on*, 2011, pp. 4488-4495.

[127]   K. E. Gordon, G. S. Sawicki, and D. P. Ferris, "Mechanical performance of artificial pneumatic muscles to power an ankle–foot orthosis," *Journal of biomechanics,* vol. 39, pp. 1832-1841, 2006.

[128]   A. J. Veale and S. Q. Xie, "Towards compliant and wearable robotic orthoses: A review of current and emerging actuator technologies," *Medical engineering & physics,* vol. 38, pp. 317-325, 2016.

[129]   A. T. Asbeck, S. M. De Rossi, K. G. Holt, and C. J. Walsh, "A biologically inspired soft exosuit for walking assistance," *The International Journal of Robotics Research,* vol. 34, pp. 744-762, 2015.

[130]   M. B. Yandell, B. T. Quinlivan, D. Popov, C. Walsh, and K. E. Zelik, "Physical interface dynamics alter how robotic exosuits augment human movement: implications for

optimizing wearable assistive devices," *Journal of NeuroEngineering and Rehabilitation,* vol. 14, p. 40, 2017.

[131]   S. Galle, P. Malcolm, S. H. Collins, and D. De Clercq, "Reducing the metabolic cost of walking with an ankle exoskeleton: interaction between actuation timing and power," *Journal of NeuroEngineering and Rehabilitation,* vol. 14, p. 35, 2017.

[132]   H. J. Hermens, B. Freriks, R. Merletti, D. Stegeman, J. Blok, G. Rau*, et al.*, "European recommendations for surface electromyography," *Roessingh research and development,* vol. 8, pp. 13-54, 1999.

[133]   O. M. Blake and J. M. Wakeling, "Estimating changes in metabolic power from EMG," *SpringerPlus,* vol. 2, p. 229, 2013.

[134]   !!! INVALID CITATION !!! {}.

[135]   A. S. McIntosh, K. T. Beatty, L. N. Dwan, and D. R. Vickers, "Gait dynamics on an inclined walkway," *Journal of biomechanics,* vol. 39, pp. 2491-2502, 2006.

[136]   C. Zizoua, M. Raison, S. Boukhenous, M. Attari, and S. Achiche, "Detecting muscle contractions using strain gauges," *Electronics Letters,* vol. 52, pp. 1836-1838, 2016.

[137]   A. Duivenvoorden, K. Lee, M. Raison, and S. Achiche, "Sensor fusion in upper limb area networks: A survey," in *Global Information Infrastructure and Networking Symposium (GIIS), 2017*, 2017, pp. 56-63.

[138]   P. Geoffroy, O. Bordron, N. Mansard, M. Raison, O. Stasse, and T. Bretl, "A two-stage suboptimal approximation for variable compliance and torque control," in *Control Conference (ECC), 2014 European*, 2014, pp. 1151-1157.

[139]   P. Geoffroy, N. Mansard, M. Raison, S. Achiche, and E. Todorov, "From inverse kinematics to optimal control," in *Advances in Robot Kinematics*, ed: Springer, 2014, pp. 409-418.

[140]   A. T. Asbeck, K. Schmidt, I. Galiana, D. Wagner, and C. J. Walsh, "Multi-joint soft exosuit for gait assistance," in *Robotics and Automation (ICRA), 2015 IEEE International Conference on*, 2015, pp. 6197-6204.

[141]   M. Raison, "On the quantification of joint and muscle efforts in the human body during motion," UCL-Université Catholique de Louvain, 2009.

[142]   S. Hernandez, M. Raison, L. Baron, and S. Achiche, "Refinement of exoskeleton design using multibody modeling: an overview," in *CCToMM Mechanisms, Machines, and Mechatronics Symposium*, 2015, p. 110.

[143]   M. Leroux, S. Achiche, D. Beaini, and M. Raison, "Design guidelines for shoulder design of an anthropomorphic robotic arm," in *DS 87-4 Proceedings of the 21st International Conference on Engineering Design (ICED 17) Vol 4: Design Methods and Tools, Vancouver, Canada, 21-25.08. 2017*, 2017.

[144]   A. Mohebbi, L. Baron, S. Achiche, and L. Birglen, "Trends in concurrent, multi-criteria and optimal design of mechatronic systems: A review," in *Innovative Design and Manufacturing (ICIDM), Proceedings of the 2014 International Conference on*, 2014, pp. 88-93.

[145] A. Mohebbi, S. Achiche, and L. Baron, "Mechatronic multicriteria profile (MMP) for conceptual design of a robotic visual servoing system," in *ASME 2014 12th Biennial Conference on Engineering Systems Design and Analysis*, 2014, pp. V003T15A015-V003T15A015.

[146] B. Samadi, S. Achiche, A. Parent, L. Ballaz, U. Chouinard, and M. Raison, "Custom sizing of lower limb exoskeleton actuators using gait dynamic modelling of children with cerebral palsy," *Computer methods in biomechanics and biomedical engineering,* vol. 19, pp. 1519-1524, 2016.

[147] M. Yazji, M. Raison, C.-É. Aubin, H. Labelle, C. Detrembleur, P. Mahaudens*, et al.*, "Are the mediolateral joint forces in the lower limbs different between scoliotic and healthy subjects during gait?," *Scoliosis,* vol. 10, p. S3, 2015.

[148] R. Hart, L. Ballaz, M. Robert, A. Pouliot, S. D'Arcy, M. Raison*, et al.*, "Impact of exercise-induced fatigue on the strength, postural control, and gait of children with a neuromuscular disease," *American Journal of Physical Medicine & Rehabilitation,* vol. 93, pp. 649-655, 2014.

APPENDIX A – TECHNICAL DRAWINGS

4   3   2   1

F   F

E

6

11.50

4 x Ø 3.30 ∇ 4
M4 - 6H ∇ 3

Ø5.30

5
5

26

8

E

D

Ø2.50

3.60

41.50

33

32

48

80   19

2

4 x Ø 1.60 ∇ 6
M2 - 6H ∇ 6

D

C

2.50

9
28

3
9

4

188

C

B   B

	NAME	SIGNATURE	DATE			TITLE:		
DRAWN	Yacine Bougrinat		03/05/2017					
QTY	1					Housing bottom plate		
APPV'D								
MFG								
			MATERIAL: Al 6061			DWG NO.		A4
			WEIGHT:			SCALE:1:2	SHEET 1 OF 1	

A   A

4   3   2   1

4   3   2   1

F

E

45

5   5

4

∅28.50 THRU

17.50

6

22.50

4 x ∅ 3.30 ⊼ 3
M4 - 6H ⊼ 3

3

48

53

33

12

4 x ∅ 3.30 ⊼ 3
M4 - 6H ⊼ 3

26

6

UNLESS OTHERWISE SPECIFIED:
DIMENSIONS ARE IN MILLIMETERS
SURFACE FINISH:
TOLERANCES:
  LINEAR:
  ANGULAR:
	FINISH:			DEBURR AND
				BREAK SHARP
				EDGES
					DO NOT SCALE DRAWING		REVISION

	NAME	SIGNATURE	DATE			TITLE:	
DRAWN	Yacine Bougrinat		17/05/2017				
QTY	1					**Motor bracket**	
APPV'D							
MFG							
Q.A			MATERIAL: Al6061-T4		DWG NO.		A4
			WEIGHT:		SCALE:1:1	SHEET 1 OF 1	

4   3   2   1

Ø 1.60 ▽ 12.20
M2 - 6H ▽ 12.20

5.25

10.50
13.50

2.25

4

7.80

R6

Ø 50

2 × Ø 1.60 ▽ 2.50
M2 - 6H ▽ 4

2

1.50

5

4.50

1.50

2.50   2.50

UNLESS OTHERWISE SPECIFIED:
DIMENSIONS ARE IN MILLIMETERS
SURFACE FINISH:
TOLERANCES:
  LINEAR:
  ANGULAR:
	FINISH:			DEBURR AND
				BREAK SHARP
				EDGES
					DO NOT SCALE DRAWING		REVISION	

	NAME	SIGNATURE	DATE		TITLE:			
DRAWN	Yacine Bougrinat		08/09/2017					
QTY	1					Cable Pulley		
APPV'D								
MFG								

MATERIAL:
POM Acetal

DWG NO.

A4

WEIGHT: SCALE:1:1   SHEET 1 OF 1

Technical drawing — Bottom Lateral Bar

Dimensions: 2, 15, 5°, 2, 15 (left view); 10, 5, 7.50, 130, 7.50 (front view)

Ø 4 THRU

Ø 6.40 THRU

	NAME	SIGNATURE	DATE			TITLE:		
DRAWN	Yacine Bougrinat		09/05/2017			**Bottom Lateral Bar**		
QTY	2							
APPV'D								
MFG								
Q.A				MATERIAL:		DWG NO.		A4
				E-Fiberglass				
				WEIGHT:		SCALE:1:1	SHEET 1 OF 1	

UNLESS OTHERWISE SPECIFIED:
DIMENSIONS ARE IN MILLIMETERS
SURFACE FINISH:
TOLERANCES:
  LINEAR:
  ANGULAR:

FINISH:

DEBURR AND BREAK SHARP EDGES

DO NOT SCALE DRAWING

REVISION

4   3   2   1

F

340

E

3

Ø 4 THRU

5

7

133

D

∅ 4 THRU   ∅ 6.40 THRU

R5   R5

10

C

B

UNLESS OTHERWISE SPECIFIED: DIMENSIONS ARE IN MILLIMETERS SURFACE FINISH: TOLERANCES: LINEAR: ANGULAR:	FINISH:		DEBURR AND BREAK SHARP EDGES	DO NOT SCALE DRAWING	REVISION

	NAME	DATE			TITLE:
DRAWN	Yacine Bougrinat	03/11/17			
Qty	2				**Torque strut**
APPV'D					
MFG					
Q.A			MATERIAL: Standard Carbon Fiber	DWG NO.	A4

WEIGHT: SCALE:1:5   SHEET 1 OF 1

4   3   2   1

⌀ 3.30 ▽ 8
M4 - 6H ▽ 8

⌀ 4

4.50

9

5

1

9

1

20

2

4

	NAME	SIGNATURE	DATE			TITLE:		
DRAWN	Yacine Bougrinat		04/05/2017			**Load cell mount**		
QTY	1							
APPV'D								
MFG								
Q.A				MATERIAL: Al 6061-T4		DWG NO.		A4

UNLESS OTHERWISE SPECIFIED:
DIMENSIONS ARE IN MILLIMETERS
SURFACE FINISH:
TOLERANCES:
 LINEAR:
 ANGULAR:

FINISH:

DEBURR AND
BREAK SHARP
EDGES

DO NOT SCALE DRAWING

REVISION

WEIGHT:

SCALE:2:1

SHEET 1 OF 1

Ø 3.30 ⬎ 6
M4 - 6H ⬎ 6

9

6

Ø 3.30 THRU ALL
M4 - 6H THRU ALL

UNLESS OTHERWISE SPECIFIED:
DIMENSIONS ARE IN MILLIMETERS
SURFACE FINISH:
TOLERANCES:
  LINEAR:
  ANGULAR:
	FINISH:			DEBURR AND
				BREAK SHARP
				EDGES
					DO NOT SCALE DRAWING		REVISION	

|	NAME	SIGNATURE	DATE			TITLE:		
DRAWN	Yacine Bougrinat		05/05/2017					
QTY	1					load cell-cable interface		
APPV'D								
MFG								
				MATERIAL: Al 6061-T4	DWG NO.			A4
				WEIGHT:	SCALE:5:1		SHEET 1 OF 1	

APPENDIX B – FLOW DIAGRAM OF THE GAIT DETECTION ALGORITHM
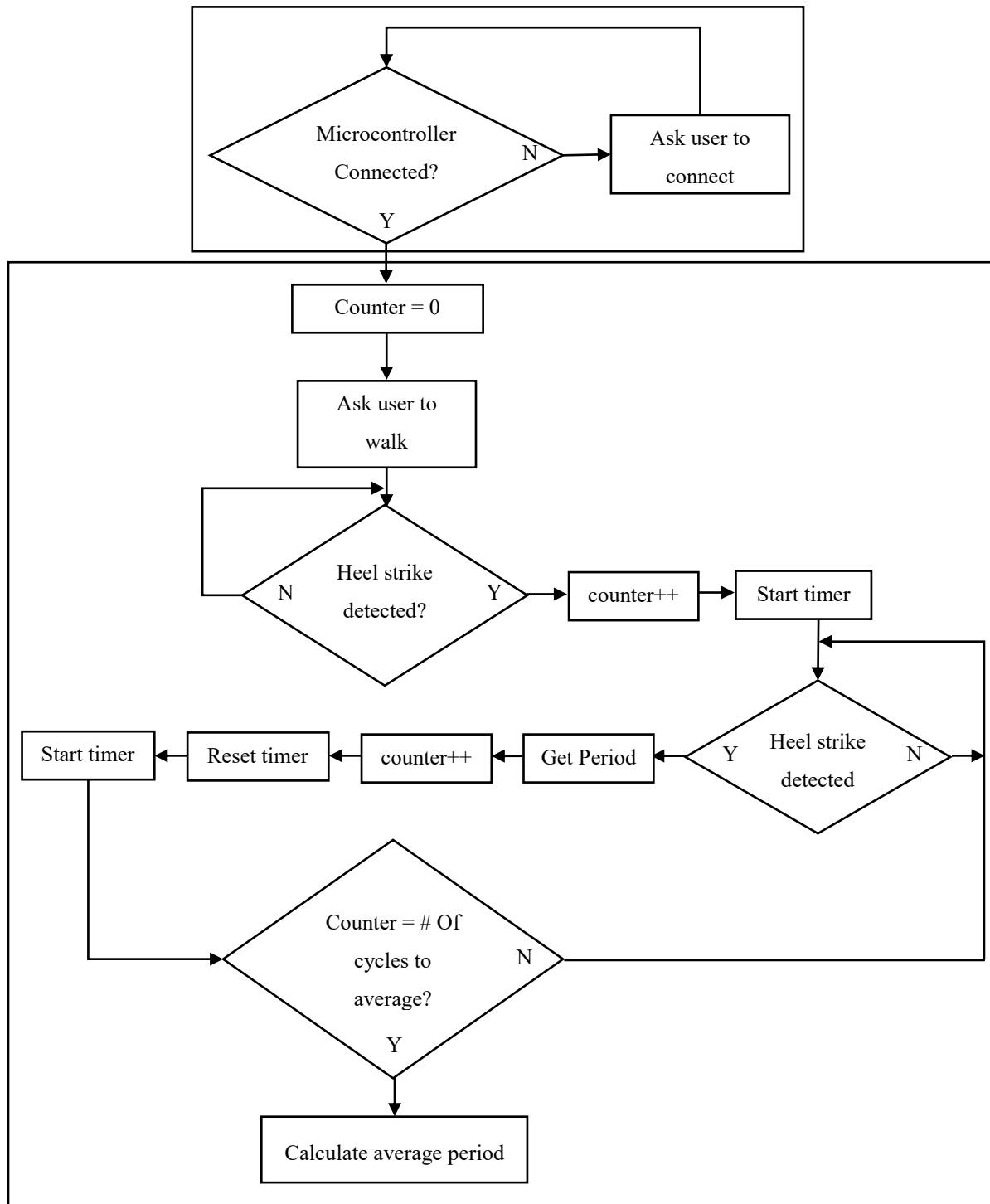
APPENDIX C – FLOW DIAGRAM OF THE ACTUATION ALGORITHM